THE JOURNAL
OF
CHEMICAL PHYSICS

VOLUME 4 FEBRUARY, 1936 NUMBER 2

Effects of Isomerism on Infrared Absorption Spectra

WALTER GORDY AND DUDLEY WILLIAMS, *Department of Physics, University of North Carolina*

(Received November 7, 1935)

The absorption spectra of four organic cyanides, two organic thiocyanates, and the corresponding isomers have been studied in the region from 1.0μ to 6.5μ. The intense band appearing near 4.4μ in the normal cyanides appears at a longer wave-length and with doubled intensity in the isocyanides, the variation in wave-length and intensity being nearly constant for all compounds. In the case of the thiocyanates the variation in wave-length of the 4.6μ band for the two configurations is less than in the cyanides, whereas the intensity differences are greater. No other bands in these organic compounds were appreciably affected by isomerism. In the absorption spectrum of aqueous solutions of hydrocyanic gas there appears an intense band at 4.75μ and also a less intense band at 4.95μ. The band at 4.95μ can be attributed to a small amount of the isomer HNC.

COBLENTZ[1] in his studies of the infrared absorption of isomeric organic compounds found that differences in the structure of the molecules are accompanied by differences in spectra, the effects being more pronounced in the region of longer wave-lengths. In many cases the spectra of isomers are identical up to about 6 μ, at which point marked shifts begin to appear. Other studies[2] made by Weniger on alcohols, acids, and esters show that the greater the difference in structure between isomers, the greater the difference in their spectra.

Recently the authors have investigated the absorption spectra of thirteen cyanides and thiocyanates.[3] For each of these compounds a well-defined band was observed in the region between 4.4 μ and 4.9 μ, the exact position of the band being different for different compounds. The absorption in this region was attributed to fundamental frequencies of the cyanide and thiocyanate molecules in which a CN vibration is active. It was the purpose of the present investigation to ascertain the effects of isomerism on this characteristic vibration. The isocyanides are different from isomers previously studied in that the carbon is divalent in the isocyanides and tetravalent in the normal cyanides.

The experimental method was the same as that used in the previous investigation.[3] A Hilger spectrometer with a fluorite prism was used for the entire region from 1.0 μ to 6.5 μ. Cell windows were of fluorite, and the thickness of the absorbing layer was 0.03 mm for all materials studied unless otherwise specified.

Absorption curves for four cyanides and the corresponding isocyanides are shown in Fig. 1. The solid lines represent the percent transmission of the cyanides; the broken lines, that of the isocyanides. The band in the region of 3.25 μ is characteristic of the group associated with the cyanide group and is found in other methyl, ethyl, butyl, and phenyl compounds.[2, 4] Within the limits of experimental error the position and

[1] W. W. Coblentz, *Investigations of Infrared Spectra* 1–2, (Carnegie Institution of Washington, 35, 1905), pp. 101–102.

[2] W. Weniger, Phys. Rev. **31**, 388 (1910).

[3] W. Gordy and D. Williams, J. Chem. Phys. **3**, 664 (1935).

[4] E. K. Plyler and T. Burdine, Phys. Rev **35**, 605. (1930).

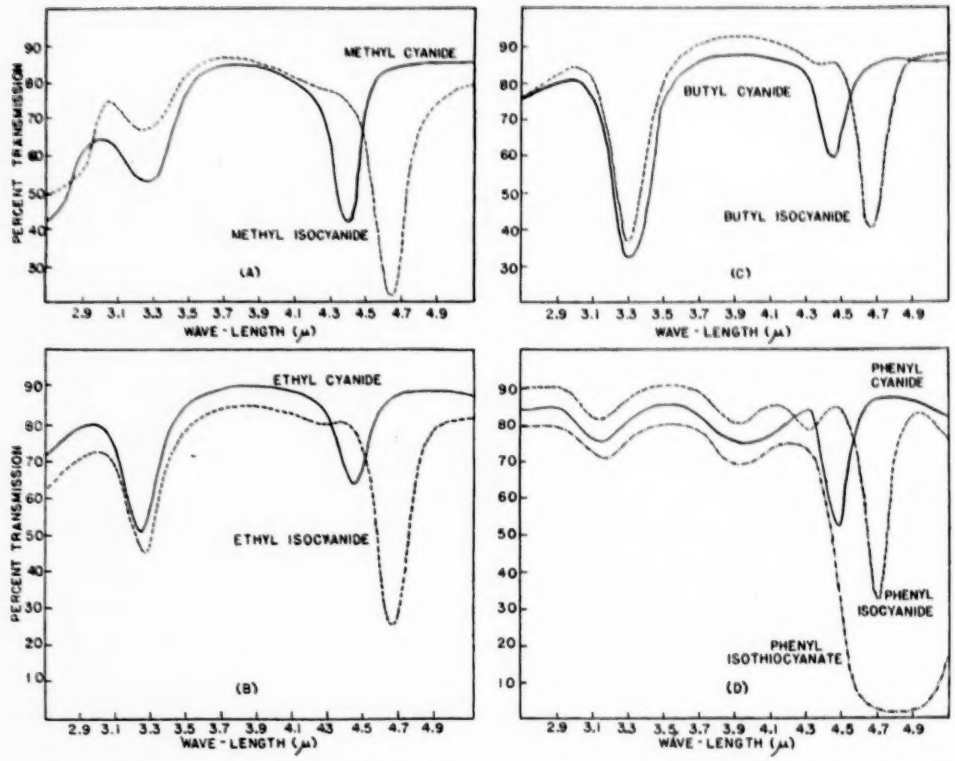

FIG. 1. (a) Transmission of methyl cyanide and methyl isocyanide. (b) Transmission of ethyl cyanide and isocyanide. (c) Transmission of butyl cyanide and isocyanide. (d) Transmission of phenyl cyanide, phenyl isocyanide, and phenyl thiocyanate 2.7μ to 5.1μ.

intensity of this band are the same for both isomeric forms, the band arising from the methyl group being a possible exception. The characteristic cyanide band in the region of 4.6 μ is shifted to the longer wave-lengths by about 0.2 μ and its intensity is approximately doubled in the isocyanides. Furthermore, these variations in wave-length and intensity are approximately constant for all the compounds studied. The shift in wave-length is in agreement with the chemical data which indicate divalent carbon in the isocyanides and hence weaker binding forces. Table I gives a numerical comparison of band positions and intensities for corresponding compounds.

TABLE I.

	Band Positions		Variation in Wave-Length	Ratio of Band Intensity
	Cyanide	*Isocyanide*	$\Delta\lambda$	*Isocyanide to Cyanide*
Methyl	3.25μ	3.25μ	0.00μ	0.7
	4.38	4.58	0.20	2.0
Ethyl	3.22	3.25	0.03	1.0
	4.43	4.63	0.20	2.0
Butyl	3.30	3.30	0.00	1.0
	4.45	4.65	0.20	2.0
Phenyl	3.16	3.14	−0.02	1.0
	4.48	4.71	0.23	1.9
	Thiocyanate	*Isothiocyanate*		
Methyl	3.32	3.32	0.00	1.3
	4.64	4.70	0.06	3.8
Ethyl	3.28	3.29	0.01	1.0
	4.63	4.75	0.12	3.9

The earlier work of Coblentz[1] on two thiocyanates and the corresponding mustard oils was repeated for purposes of intensity comparison and for more accurate determination of band position. The absorption curves for methyl and ethyl thiocyanates and their isomers are given in Fig. 2. As may be seen from the figure, the shifts due to isomerism are different for the two and in both cases are less than the corresponding shift for the cyanides. On the other hand, the intensity variation is much greater than in the case of the cyanides. As before there is no apparent shift in the

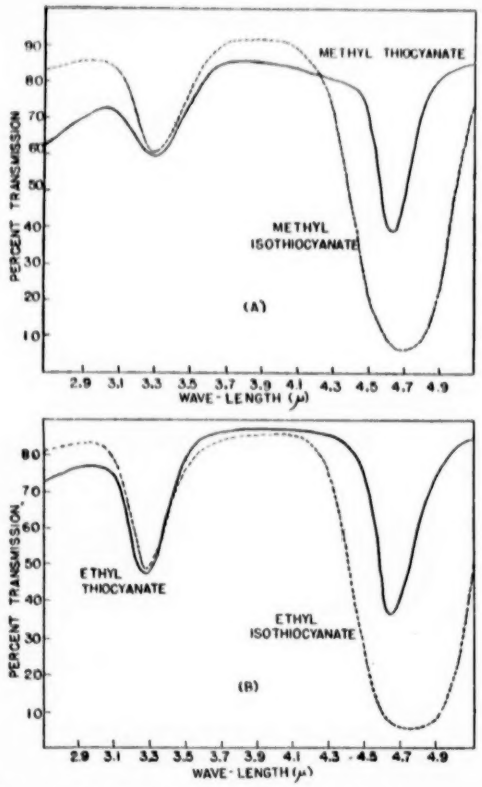

FIG. 2. (a) Transmission of methyl thiocyanate and isothiocyanate. (b) Transmission of ethyl thiocyanate and isothiocyanate. Region: 2.7μ to 5.1μ.

band characteristic of the associated methyl and ethyl groups. The absorption of phenyl thiocyanate was measured and is given in Fig. 1 with the other phenyl compounds.

The fact that the band in the 4.6 μ region varies while the 3.25 μ band remains constant indicates that both these bands depend primarily on the structure of certain groups rather than upon the structure of the molecule as a whole. Although a survey was made of the whole region from 1.0 μ to 6.5 μ, no bands were observed which could be classified either as harmonics of the 4.6 μ band or as combinations involving this characteristic frequency. This is further indication of a simple type of binding between the carbon and nitrogen atoms, which is only slightly modified by associated groups in the molecule.

Nef[5] has proposed the two configurations, HCN and HNC, for hydrocyanic gas. If both configurations be present in a given sample, it should be possible to observe two bands in the region of 4.7 μ. In the previous investigations,

[5] J. V. Nef, J. Am. Chem. Soc. **26**, 1549 (1904).

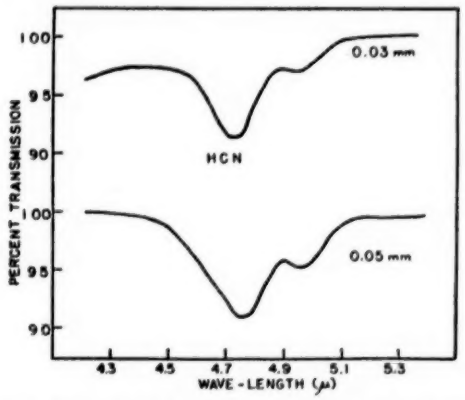

FIG. 3. The ratio of the transmission of hydrocyanic acid solution to that of an equal thickness of water for two cell thicknesses. Region: 4.1μ to 5.5μ.

the authors obtained an absorption curve showing a band at 4.75 μ characteristic of HCN in aqueous solution. In this absorption curve there is also a slight depression at 4.95 μ. For greater cell thickness this depression becomes deeper and can be interpreted as arising from the isomer HNC. In Fig. 3 are given the transmission curves of hydrocyanic acid for two cell thicknesses. On account of the different absorption coefficients for CN and NC compounds it is impossible to ascertain very accurately the relative abundance of the isomers, but it is evident from the figure that the amount of HNC present is very small, as is to be expected from chemical theory.[6] Assuming the absorption coefficient of HNC to be twice that of HCN, as is the case for the other isomers studied, we estimate the concentration of HNC to be from two to four percent that of HCN.

Barker[7] and Choi and Barker[8] have studied the absorption of gaseous HCN, but have reported no absorption in the region of 4.9 μ. This region may have been beyond the range of their investigation, as their published curves for this part of the spectrum extend only from 4.68 μ to 4.86 μ. A second possibility is that the isomer HNC may be more abundant in aqueous solution than in the gas.

The authors wish to express their thanks to Professor E. K. Plyler for his helpful discussion of the manuscript and to Mr. G. C. Kyker of the Chemistry Department, who prepared the chemicals and offered valuable suggestions.

[6] J. Schmidt, *Text Book of Organic Chemistry*, (D. Van Nostrand Co., 1932), p. 323.
[7] E. F. Barker, Phys. Rev. **23**, 200 (1924).
[8] K. N. Choi and E. F. Barker, Phys. Rev. **42**, 777 (1932).

Raman Spectrum of Crystalline Ammonium Chloride*

F. T. HOLMES, *Rouss Physical Laboratory, University of Virginia*

(Received September 9, 1935)

Crystalline NH_4Cl was studied in its room temperature and high temperature forms. Cylindrical crystals were grown by sublimation in a special furnace. At room temperature vibrational frequencies were observed at 3146, 3041, 2824, 2010, 1768, 1709, 1407 and subsidiary frequencies at 3300, 3232 cm^{-1}. In the high temperature modification vibrational frequencies were observed at 3102, 2801, 1931, 1655, 1400 cm^{-1}.

CRYSTALLINE ammonium salts have many curious physical properties,[1] some of which are ascribable to characteristics of the ammonium radical not yet fully understood. This work was undertaken in the hope that light would be thrown on some of these characteristics by more complete observations of the Raman effect in NH_4Cl.

The data obtained have been combined with the infrared observations of previous workers and interpreted with the help of two reasonable assumptions. Probably the most important result is the indication that the NH_4 group in crystalline NH_4Cl either has not the geometrical structure of a tetrahedron of cubic symmetry or else has this structure but is strongly perturbed in a nongeometrical sense.

Growing Crystals by Sublimation

A major difficulty was encountered in preparing a relatively pure and optically clear crystal of suitable size in the room temperature modification of this substance. Many attempts to grow crystals in the high temperature form and cool them through the 184°C transition[1a] produced merely mediocre crystals. However, it was found that an optically clear cylindrical crystal 3 cm long could be grown by sublimation, at a temperature below[2] 184°C, in about a month.

The essentials of the glass-walled furnace constructed for this purpose are shown in Fig. 1. The heating wire was wound directly on tube 1,

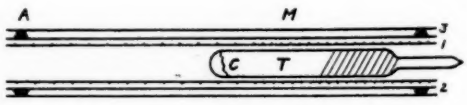

FIG. 1.

this assembly being separated from tube 2 by a coarse winding of asbestos string. Annular windings of asbestos, as at A, separated tubes 2 and 3. Heating current was obtained from a commercial power line, the voltage fluctuations being sufficiently reduced by the use of "ballast tubes."

The tube T was half filled with NH_4Cl (previously sublimed several times in vacuum), evacuated, heated for some time, and sealed off. It was inserted in the furnace as shown and moved toward the left. After the rounded end of T had passed M, the region of maximum temperature, a crystal C started to form. The rate of motion was then determined by the appearance of the surface of C, minute facets indicating dangerously fast growth.

For high temperature observations a similar furnace was inserted in the arc chamber. Essential modifications consisted in replacing 2 by a tube of Corning Red Ultra glass[3] and sealing a flat window on the end of T. Crystals were grown and then maintained at temperatures well above 184°C during exposures.

Room Temperature Results

Spectra of the room temperature modification were obtained by using Hilger constant deviation type instruments fitted with extra-dense flint prisms and long and short focus cameras. Commercial mercury and helium arcs were used

* Portion of a dissertation presented for the degree of Doctor of Philosophy at Yale University.

[1] Most of the peculiarities of the ammonium halides are mentioned by A. C. Menzies and H. R. Mills, Proc. Roy. Soc. **A148**, 407 (1935).

[1a] *International Critical Tables*, Vol. 4, p. 7.

[2] R. Pohlman, Zeits. f. Physik **79**, 394 (1932).

[3] L. J. Buttolph, Rev. Sci. Inst. **1**, 650 (1930).

with standard filters in the arc chamber described by Buttolph.[3]

The vibrational frequencies in cm^{-1}, with estimated relative visual intensities, are: 3146, *15*; 3041, *20*; 2824, *7*; 2010, *2*; 1768, *2*; 1709, *5*; 1407, *2* (average deviation 4 cm^{-1} or less). The first three are inherently of intermediate width, the next two are broad[4] and without cores, 1709 is sharp, and 1407 is sharp on its low wave-length side, as is the wider line 2824 (and possibly 3146).

The infrared absorption frequencies observed by Wilberg[5] at approximately 2350 and 2250 cm^{-1} were not found, although 2350 (He 3888A), if present, might have been masked by an observed Raman line assigned to 2824 (He 3819A).

Considering the widths of most lines, these results agree satisfactorily with the less complete results of Schaefer, Matossi, and Aderhold,[6] Kastler,[7] and Menzies and Mills,[4] and, except for 2824 and 1407, with weighted means of the infrared results of Wilberg[5] and Pohlman.[2] One should note, however, that 1709 is inactive in infrared absorption at room temperature.

Subsidiary frequencies were observed at 3300 ± 6 and 3232 ± 5 cm^{-1}. These may correspond to fine-structure lines observed by Pohlman at $-80°C$.

High Temperature Results

The spectrum of the high temperature modification was obtained only at low dispersion with helium excitation.

Observed frequencies in cm^{-1} are: 3102, *30*; 2801, *4*; 1931, *2*; 1655, *2*; 1400, *2* (average deviation 6 cm^{-1} or less). The first, a very wide line, corresponds to one or both components of the high frequency pair which are well resolved in crystals at room temperature with this dispersion. On the basis of their intensities and widths 1931 and 1655 correspond to 2010 and 1768. Apparently the room temperature 1709 cm^{-1} frequency is much weaker or has shifted in the direction of shorter wave-lengths to an unobservable position. No asymmetries were observed.

Discussion

The 1407 cm^{-1} frequency seems to be an unresolved doublet.[2, 5] This view is supported by the fact that the corresponding NH_4Br frequency is definitely double at low temperature.[2] Thus ten vibrational frequencies can be said to have been observed at room temperature in crystalline NH_4Cl.

Two assumptions will be applied throughout the rest of this paper: (1) That of most authors, namely, that all frequencies in this spectral region are produced by NH_4^+; (2) that no NH_4^+ frequency in crystalline NH_4Cl lies below[8] 1407 cm^{-1}. These assumptions necessitate regarding at least one of the observed frequencies as due to a harmonic, a combination, or a perturbation. Consideration of all relevant data indicates that in NH_4Cl 2824 may be the harmonic of 1407 and 3146 may be a combination frequency, possibly due to 1407 plus 1709.

The structure usually assumed for NH_4^+ is that of a tetrahedron of cubic symmetry. Using this model Hettich[9] and Menzies and Mills[4] have presented explanations of the complex macroscopic phenomena in ammonium halide crystals. Also, Pohlman[2] has deduced from observed fine structure (without allowing for the possibility of vibration-rotation interaction[10]) a value for the N−H distance which agrees with that calculated by Laschkarew and Usyskin[11] from electron diffraction patterns. However, this structure is spectroscopically unsatisfactory unless seriously perturbed in a nongeometrical sense, since without such a perturbation only four fundamental vibrational frequencies could be observed.[12] Unfortunately the available spec-

[4] Compare A. C. Menzies and H. R. Mills, Proc. Roy. Soc. **A148**, 407 (1935).

[5] L. Wilberg, Zeits. f. Physik **64**, 304 (1930). See also O. Reinkober, ibid. **5**, 192 (1921).

[6] C. Schaefer, F. Matossi, and H. Aderhold, Zeits. f. Physik **65**, 289 (1930).

[7] A. Kastler, Proc.-verb. soc. sciences phys. natur. Bordeaux (1931–1932).

NH_4F	2830 m	3070 m	
NH_4Cl	2820 w	3050 s	3150 m
NH_4Br	2810 w	3030 s	3130 m

w weak; m medium; s strong

[8] See, however, A. da Silveira, Comptes rendus **195**, 521 (1932) and Wilberg, reference 5.

[9] A. Hettich, Zeits. f. physik. Chemie **A168**, 353 (1934).

[10] D. M. Dennison and M. Johnston, Phys. Rev. **47**, 93 (1935), E. Teller and L. Tisza, Zeits. f. Physik **73**, 791 (1932).

[11] W. E. Laschkarew and I. D. Usyskin, Zeits. f. Physik **85**, 618 (1933).

[12] D. M. Dennison, Rev. Mod. Phys. **3**, 280 (1931).

troscopic data do not strongly indicate the correctness of any particular geometrical configuration.

Comparison of the Raman spectra of the room temperature and high temperature forms of NH_4Cl suggests various possibilities. Of these, the simplest are that the frequencies occurring at room temperature at 2010 and 1768 cm^{-1} originate in similar types of vibration and that the properties of NH_4^+ undergo only minor changes at the high temperature transition point.

The author is indebted to the physics departments at Lehigh University and the University of Virginia for laboratory facilities, and wishes to thank Dr. J. E. Rosenthal of Columbia University for discussions, and Professor W. W. Watson of Yale University for his interest and advice.

FEBRUARY, 1936 JOURNAL OF CHEMICAL PHYSICS VOLUME 4

The Reaction Rates of Propionic and Acetic Propionic Anhydrides

E. S. BARR AND E. K. PLYLER, *Department of Physics, University of North Carolina*

(Received October 4, 1935)

The infrared absorption spectra of mixtures of water and acetic propionic and of propionic anhydrides have been measured in the region from 5μ to 6.4μ. The intensity of the bands was found to decrease with time. By using the relative intensity of the anhydride band the reaction rate was calculated for three concentrations. The reactions were unimolecular but the value of the reaction constant was different for each concentration, its value being approximately proportional to the concentration of the water. The value of the reaction constant of acetic propionic anhydride was about twice the value of the constant for propionic anhydride. A table is given of the values of the reaction constants for the different concentrations.

THE reaction velocity of acetic anhydride has been measured[1] recently by means of its infrared absorption spectra. The results showed that the reaction constant increased with temperature and that the value of the constant decreased in a given set of observations. The latter result may have been produced by the method of calculation. In order to study further the effect of concentration the work has been extended to propionic and acetic propionic anhydrides. Before the absorption spectra of different concentrations were measured the region from 5 μ to 6.5 μ was studied. It was found that the absorption spectra of acetic and of propionic acid were similar in this region and that the bands, which were at about 5.7 μ, varied in position by about 0.03 μ. The propionic and acetic propionic anhydrides were studied and it was found that there were two absorption bands at 5.48 μ and 5.66 μ, and 5.50 μ and 5.68 μ, respectively. When cells of about 0.01 mm in thickness were used, the two bands could be separated by the fluorite prism. The two anhydrides have similar spectra, as can be seen by the absorption curves shown in Fig. 1. The fact that the 5.50 μ band can be separated from the other anhydride band at 5.68 μ and the acid bands at 5.7 μ made it suitable for the study of reaction rates.

In the study of the reaction velocity, cells were made of three concentrations. The first solution had equivalent amounts of water and anyhdride, the second two equivalent parts of water to one of anhydride, and the third three of water and one of anhydride. The actual concentrations of water and anhydride are given in Table I. The same concentrations were used for each anhydride. The reactions were allowed to progress in the absorption cell. After preliminary trials it was found that the reactions were slow and that the absorption curves should be measured at time intervals of from one to two hours. In this way six to eight sets of observations were obtained for each concentration. In Fig. 2 are shown the curves for the three concentrations of propionic anhydride. The bands in the section on the left are for equivalent amounts and the time of observation

[1] Plyler and Barr, J. Chem. Phys. **3**, 679 (1935).

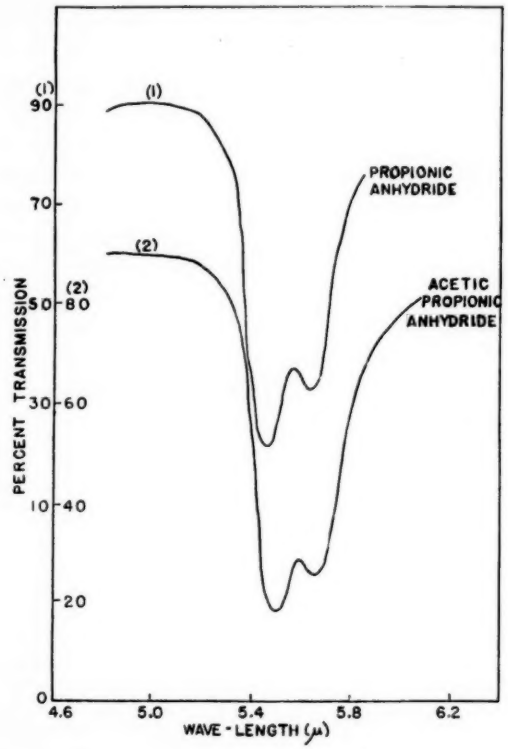

FIG. 1. The absorption spectra of propionic and acetic propionic anhydrides in the region from 4.8μ to 6.1μ. The cell thickness was 0.01 mm.

is given beside each curve. The fourth curve in the first group was placed inaccurately on the drawing. It should be shifted 0.06 μ to the shorter wave-lengths. The middle set of observations are for two parts water and one part anhydride. The lowest curve in each set is for the shortest interval of time after mixing, and shows the 5.48 μ band with the greatest intensity. These curves show that in any concentration the absorption in the region of 5.5 μ decreases with time. Also this decrease in intensity with time is greater when the concentration of the anhydride is smaller. Three sets of observations were also made for the acetic propionic anhydride. The absorption spectra were similar to those shown in Fig. 2.

It was found by considering the reaction as unimolecular, that approximately consistent values were obtained for the reaction constant. In order to find the concentration of the anhydride at any time, it was necessary to know the relative intensity of the band at the beginning of the reaction and also the relative intensity at the time of

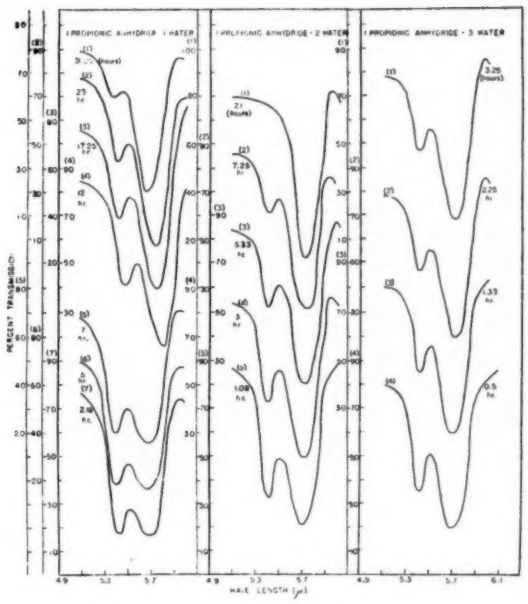

FIG. 2. The absorption of propionic anhydride and water after different intervals of time. The different sets of curves represent mixtures of 1, 2 and 3 parts water to one part anhydride.

TABLE I. *The reaction constants of propionic and acetic propionic anhydrides at 27°C, for different concentrations.*

SUBSTANCE	CONCENTRATION (mole/l) H_2O	ANHYDRIDE	TIME (sec.)	$k \times 10^4$
Propionic anhydride	6.85	6.85	7800	0.32
			18000	0.26
			25200	0.27
			43200	0.25
	12.2	6.1	3900	0.52
			10800	0.47
			19200	0.41
			26100	0.41
	16.5	5.5	1800	1.6
			4800	1.1
			8100	1.0
			11700	1.0
Acetic propionic anhydride	7.65	7.65	6600	0.67
			10800	0.65
			16200	0.65
			23400	0.53
			30600	0.45
	13.58	6.74	2400	1.3
			4500	1.1
			7200	1.0
			9900	0.95
			13800	1.1
			17400	1.1
	18.00	6.00	1800	3.0
			3600	2.7
			5400	3.0
			7200	2.8

the observation. The relative intensity of the bands for different times of observation was found by determining the area under the absorption curve. The relative intensity at zero time was found by extrapolation.[2]

In Table I the values of the reaction constant are given for the reaction rate of propionic and acetic propionic anhydrides.

The constant for acetic propionic anhydride is roughly twice that of propionic anhydride for each concentration. For a given concentration the values of k tend to decrease with time. However, this effect is not so great as found in the case of acetic anhydride. The change in the value of the constant may not be a real property of the reaction. The method of measurement and calculation may produce the change. All measurements were made at 27°C.

When the concentration of water in the solution was increased the reaction rate increased. It was found that the value of k for the different concentrations was approximately proportional to the equivalent amounts of water in the mixture.

On account of the anhydride band being less overlapped by the acid band, it is believed that the accuracy is greater than in the previous study of acetic anhydride. The percent error in the results are probably between 5 and 10 percent.

[2] A more complete description of the method of calculation can be found in the paper of reference 1.

FEBRUARY, 1936 JOURNAL OF CHEMICAL PHYSICS VOLUME 4

The Near Infrared Absorption Spectra of Acid and Basic Solutions

E. S. BARR AND E. K. PLYLER, *Physics Department, University of North Carolina*

The infrared absorption spectra of H_2O and aqueous solutions of HCl, HBr, NaOH, KOH, $ZnBr_2$, $ZnCl_2$ and Na_2CO_3 have been measured from 1.5μ to 2.8μ. Bands were observed at 2.30μ and 2.45μ in hydroxides, at 2.30μ and 2.55μ in acids, and at 2.30μ, 2.45μ and 2.55μ in hydrolyzing salts. The band at 2.30μ is produced by hydration and 2.45μ band by the OH ion.

STUDIES[1] have already been made on the infrared absorption of acid and basic solutions from 1μ to 7μ. In the study on acid solutions a broad band was observed at 2.4μ and in the hydroxide solutions at 2.3μ. When the hydrolyzing salts were studied, the two bands could not be separated. With greater resolution it would be possible to separate the bands in the 2.4μ region.

A large type Hilger infrared spectrometer, with a quartz prism, was used for the resolving instrument. The deflections were increased by using a Moll thermorelay. The effective slit width at 2.5μ was 0.015μ. The percent absorption of water was first determined in order that a comparison could be made with the absorption curves of the solutions, the thickness of all cells being 0.1 mm. The absorption spectra for some of the solutions which were studied are shown in Fig. 1. It can be seen that the absorption of all the solutions in the region of 2.4μ is greater than that of water. Aqueous solutions of KOH, NaOH, $ZnBr_2$, and $ZnCl_2$ of 5 and 10 N concentrations, 5 N Na_2CO_3, 18 and 36 percent HCl, and 17 and 34 percent HBr were studied. The ratio of the percent absorption of the solutions to that of water was plotted and the results are shown in Fig. 2. The water content of the solution cells was less than in the water cell and the transmission is greater than 100 percent at some wave-lengths. Also, because of the shift of the 1.95μ water band to longer wave-lengths in some of the solutions, a minimum appears at about 2μ, but this is not an actual band.

[1] E. K. Plyler and E. S. Barr, J. Chem. Phys. **2**, 306 (1934); E. K. Plyler and W. Gordy, J. Chem. Phys. **2**, 470 (1934).

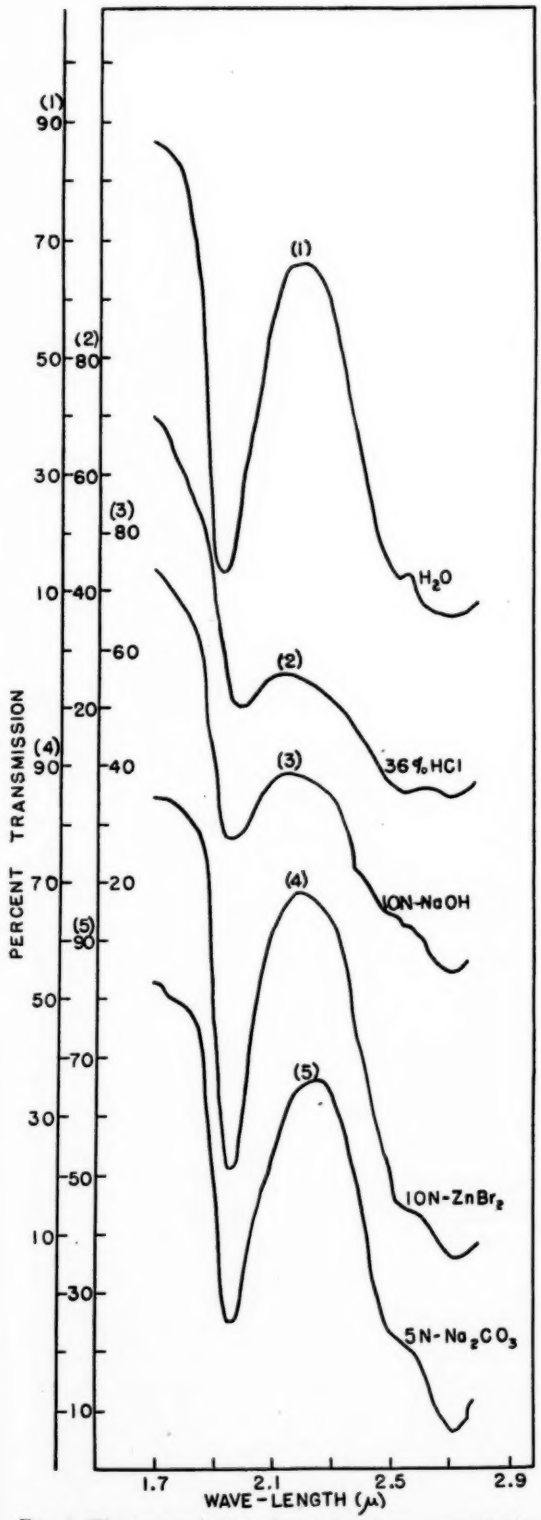

FIG. 1. The transmission of water and aqueous solutions of HCl, NaOH, $ZnBr_2$ and Na_2CO_3 in the region from 1.7μ to 2.8μ. The scale that applies to a curve has the same number.

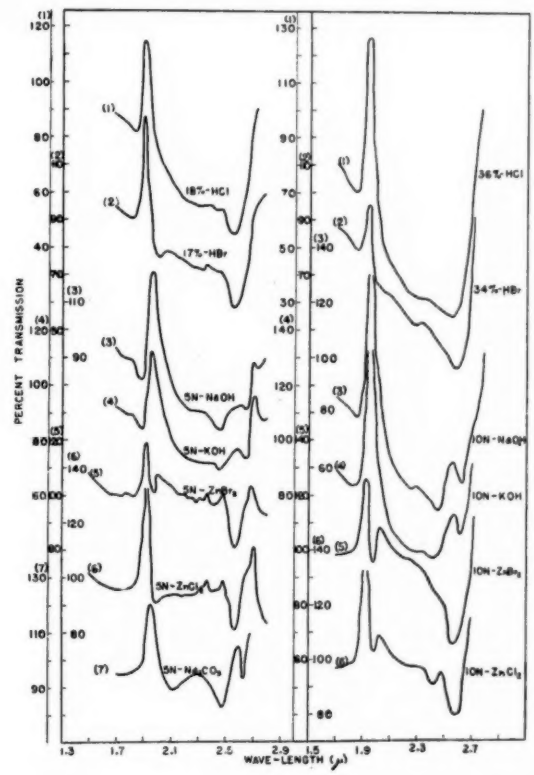

FIG. 2. The ratio of the percent transmission of the solutions to that of water for equal cell thickness (0.1 mm). The scale that applies to a curve has the same number.

The HCl and HBr solutions have bands at 2.30μ and 2.55μ and the NaOH and KOH solutions at 2.30μ and 2.45μ. The hydrolyzing salts have bands at 2.30μ, 2.45μ and 2.55μ. The absorption spectra for the more concentrated solutions are shown in the second part of Fig. 2. The same bands are present with greater intensity. The absorption band at 2.30μ is present in all the solutions and is probably due to hydration. A comparison of the intensity of the 2.45μ band in the different hydrolyzing salts shows that the absorption is due to the OH ion. The nature of the absorption at 2.55μ in the acids cannot be determined from the hydrolyzing salts.

All of the solutions studied in this work have intense bands in the region of 1.85μ. This band is sharp in the hydroxide and acid solutions, but much broader in the case of the hydrolyzing salts. These bands are due to combinations of the fundamental frequencies at longer wave-lengths and have been classified in a previous study.[1]

Sodium Resonance Radiation and the Polymerization of Ethylene

JOSEPH C. JUNGERS AND HUGH S. TAYLOR, *Frick Chemical Laboratory, Princeton University*

(Received November 17, 1935)

Ethylene has been found to quench the resonance radiation of sodium between 130 and 250°C. No measurable polymerization of ethylene results as a consequence of quenching, in contrast to previous results with excited mercury and cadmium. A catalytic polymerization of ethylene at sodium surfaces occurs above 250°C with an activation energy of 20 kcal. The inefficiency of the energy of sodium resonance radiation in producing polymerization is ascribed to unfavorable localization of the energy received by ethylene in the quenching process.

IT is known that the polymerization of ethylene can be accelerated by both excited mercury[1] and cadmium[2] by using the resonance radiation of these elements as exciting radiation. With mercury this occurs at room temperature; with cadmium around 200°C. Thermally, polymerization may be secured at temperatures in the neighborhood of 350–400°C with an observed activation energy of 35–42 kcal.[3, 4] Quite recently the subject of ethylene polymerization has acquired a new interest by reason of the demonstration that it is a chain reaction that can be brought about by the production in the ethylene system, at temperatures of 200–300°C, of free radicals; for example by thermal decomposition of metal alkyls[5] and azomethane,[6] or by photo production of free radicals.[7] It was, therefore, of interest to test the effect of the resonance radiation of sodium as exciting agent, in an ethylene system containing sodium vapor. The choice of this source of energy derives its interest from the magnitude of the energy quantum involved ($\lambda = 5897$A; $E = 48$ kcal.) since this energy is greater than the necessary thermal activation energy but too small of itself or even with the accompanying formation of sodium hydride ($Q_{NaH} = 12.1$ kcal.) to effect the breaking of a carbon-hydrogen linkage thus producing a free radical.

We have, accordingly, studied the effect of ethylene on the quenching of sodium resonance radiation, the rate of polymerization of ethylene in presence and absence of such radiation and also a polymerization which occurs in somewhat higher ranges of temperature due to the presence of sodium surfaces or vapor in such reaction systems.

[1] Olson and Myers, J. Am. Chem. Soc. **48**, 389 (1926); Bates and Taylor, ibid. **49**, 2438 (1927).
[2] Bates and Taylor, J. Am. Chem. Soc. **50**, 771 (1928).
[3] Pease, J. Am. Chem. Soc. **53**, 613 (1931).
[4] Storch, J. Am. Chem. Soc. **56**, 374 (1934).
[5] Taylor and Jones, J. Am. Chem. Soc. **52**, 1111 (1930).
[6] O. K. Rice and Sickman, J. Am. Chem. Soc. **57**, 1374 (1935).
[7] Taylor and Emeleus, J. Am. Chem. Soc. **53**, 562 (1931).

EXPERIMENTAL

Light source

As source of resonance radiation we have used the commercial Zeiss sodium lamp of the standard type used in polarimetric and other optical work. The lamp operates on a 110-volt a.c. circuit with suitable external resistance, at 1.3 amperes. We have used such lamps for illumination periods of many hours with good satisfaction. While we have made no quantitative measurements of light intensity, visual observation showed a reasonable constancy of this light source.

Reaction system

We have used a Pyrex reaction system, the actual reaction vessel a cylinder 10 cm long by 2 cm diameter, fitted with suitable manometric device and pump system for evacuation. Into the reaction vessel, after a standard high temperature exhaustion, the sodium metal was introduced by distillation and formed on the walls of the vessel a bright metallic mirror. Large amounts of the metal were always present. The temperature of the reaction system was controlled by means of suitable vapor baths in Pyrex tubes surrounding the reaction space. The ethylene used was obtained from cylinders, passed through a carbon dioxide-ether trap and purified before use by several fractional condensations in liquid air with removal of permanent gases by evacuation. In all cases the gas

was condensed onto bright metallic sodium before introduction into the reaction system, in order to minimize still further the possible oxygen concentration.

Quenching of resonance radiation by ethylene

Upon illumination of the heated reaction tube containing sodium and its vapor alone with the light from the resonance lamp the whole vessel became suffused with the characteristic yellow glow of the resonance radiation. This glow was especially striking in the temperature region of 150–200°C. At the temperature of boiling diphenyl (255°C) the concentration of sodium vapor is already sufficiently high that complete absorption occurs in the layers immediately adjacent to the lamp and the fluorescence is localized. Under conditions in which the glow is especially pronounced, the admission of even 5 mm of ethylene sufficed to extinguish the fluorescence as observed visually. Such experiments sufficed to indicate (a) the emission of resonance radiation from the lamp source and (b) the transfer of the energy to ethylene by collision.

Photo-polymerization experiments

The following Table I records the conditions under which the polymerization of ethylene under the influence of resonance radiation was attempted. In no case, between the reaction temperature limits of 132 and 255°C, was any acceleration of the polymerization by photosensitization observed. The results were uniformly negative nor was any "permanent" gas, showing a pressure at liquid-air temperatures, produced during the several runs.

Even at a pressure of 133 mm recorded in run 5 the only pressure diminution recorded can be accounted for by the thermal reaction discussed in the succeeding section. An attempt to study the sensitized polymerization in presence of hydrogen or the sensitized hydrogenation of ethylene is prevented by the ready reaction of sodium and hydrogen, in which respect this agent differs from the previously studied cases of mercury and cadmium.

TABLE I. *Photosensitized polymerization of ethylene by sodium resonance radiation.*

Run No.	Temp. (°C)	Pressure (mm at 25°C)	Time of Illumination (Hours)	Pressure Change (mm)
1	132	3.3	1.66	<0.1
2	184	4.8	10	<0.1
3	218	5.2	5.5	<0.1
4	255	5.25	5	<0.05
5	255	133	20	~1

TABLE II. *Thermal polymerization of ethylene in Pyrex vessels with and without a coating of sodium.*

Run No.	Temp. (°C)	Pressure (mm)	ΔP (mm)	Δt (hours)	$\Delta P/\Delta t$	Remarks
1	302	182	20.6	44	0.46	Sodium Present
2	302	154.8	26.4	63	0.42	Sodium Present
3	302	167	2.4	38	0.06	Sodium Absent
4	354	166	1.0	23	0.04	Sodium Absent
5	354	180	22.0	17	1.3	Sodium Present
6	354	183	26.5	22	1.2	Sodium Present
7	302	184	23.8	70	0.34	Sodium Present
8	354	182	30.3	21	1.4	Sodium Present
9	255	181	23.0	232	0.1	Sodium Present

Catalytic polymerization of ethylene

It was thought that sodium vapor might be an efficient agent for the removal of traces of oxygen from ethylene gas and that, therefore, the thermal polymerization of ethylene might be reduced thereby, since, as is well known, traces of oxygen accelerate the polymerization process.[8] A series of experiments on the rate of thermal polymerization carried out in reaction vessels coated with a bright metallic sodium deposit are recorded in Table II.

Comparison of Experiments 3 and 4, in the absence of sodium, with the others in presence of sodium shows a marked accelerating influence on polymerization due to the presence of sodium. Experiment 9 indicates that the influence is measurable already at 255°C and accounts for the observed pressure change in the photosensitization experiment No. 5 of Table I under similar temperature and pressure conditions. That the influence of the sodium is catalytic is evident from the activation energy of the process. From Experiments 6, 7 and 8 we deduce $E=20$ kcal. The less accurate combination of Experiments 7 and 9 gives $E=17$ kcal. These values are much lower than the accepted value for thermal polymerization of 35–42 kcal.[3, 4] This catalytic reaction makes difficult the study of photosensitization in the higher temperature ranges, but illumination with resonance radiation in this temperature interval produced no noticeable acceleration.

[8] Lenher, J. Am. Chem. Soc. **53**, 3752 (1931).

Discussion

The absence of any polymerization of ethylene photosensitized by sodium diminishes markedly any expectation that examples of photosensitization using sodium will be found. Acetylene and hydrogen both react with sodium vapor and many other common reactants are similarly reactive towards sodium. It would seem, therefore, that there is little prospect of extending the list of atom-photosensitized reactions to this element.

The quenching of the sodium resonance radiation by ethylene indicates definitely that in the collisions with ethylene, at least 48 kcal. of energy per mole are transferred to the ethylene molecules. Although this is a larger energy than that required as activation energy in the thermal polymerization process no observable polymerization results. This is another example of the relative efficiency of thermal activation as compared with photoactivation. The negative result in this photosensitization confirms the view resulting from the studies with mercury and cadmium as activating agents that the efficiency of these latter is to be associated with their ability to produce, in the reaction system, free radicals which are efficient agents in the initiation of a polymerization chain. With respect to the optical and thermal methods of securing a particular reaction it should be observed that the method of calculation of activation energy in thermal processes takes account only of those collisions which, having the necessary activation energy, are successful, whereas, in the photosensitization studies, all the collisions are counted whether the energy is favorably located for reaction or not. Hence the lower apparent efficiency of light energy; hence, also, the observation that in thermal processes many collisions may occur with the necessary activation ernergy but unfavorable in the location of the activation. It is significant in this regard that Pease[3] computed from his data that the A factor in the velocity equation $Ae^{-E/RT}$ was of the order of 0.001 of that to be expected of a straight bimolecular process and that the existence of a chain of any marked length would cause a still greater discrepancy between the actual and theoretical magnitudes of A. These considerations do not, however, exclude the possibility that the activation energy deduced from thermal data may have a low value due to a reaction of ethylene with another substance of unknown nature, which reaction provides for the initiation of the chain. To this extent the thermal polymerization process is still obscure.

FEBRUARY, 1936 JOURNAL OF CHEMICAL PHYSICS VOLUME 4

The Homogeneous Unimolecular Decomposition of Gaseous Alkyl Nitrites

V. The Decomposition of Methyl Nitrite at Low Pressures

E. W. R. Steacie and D. S. Calder, *Physical Chemistry Laboratory, McGill University, Montreal*

(Received November 19, 1935)

The decomposition of methyl nitrite has been investigated from 0.005 to 5.0 cm in the temperature range 210–240°C. In this region the rate falls off steadily with diminishing pressure. The reaction is appreciably heterogeneous at the lower pressures. The results are in satisfactory agreement with the previous observations of Steacie and Shaw at higher pressures. The falling-off in rate with decreasing pressure is satisfactorily accounted for by the Rice-Ramsperger theory, assuming 13 degrees of freedom and a molecular diameter of 5.0×10^{-8} cm.

Introduction

In previous papers it has been shown that the decompositions of the gaseous alkyl nitrites constitute a series of simple first order reactions.[1] Recently Rice and Herzfeld[2] have suggested that the majority of first-order reactions may really be chain processes involving free radicals, and in a number of cases their suggestion has received striking experimental confirmation. A large

[1] Steacie and Shaw, (I) Proc. Roy. Soc. **A146**, 388 (1934); (II) J. Chem. Phys. **2**, 345 (1934); (III) ibid. **3**, 344 (1935); (IV) Proc. Roy. Soc. **A151**, 685 (1935).

[2] Rice and Herzfeld, J. Am. Chem. Soc. **56**, 284 (1934).

number of first-order reactions are therefore under suspicion. In the case of the nitrite decompositions, however, the work of Rice and Radowskas[3] on the free radical decomposition of ethyl nitrite makes it almost certain that no complicating chain process occurs. These reactions remain, therefore, among the few that are unequivocally unimolecular. It thus seems advisable to obtain more comprehensive data on these reactions, and the present communication deals with the decomposition of methyl nitrite at low pressures.

Experimental

The progress of the reaction was followed by observing the rate of change of pressure in a constant volume system. A mercury manometer and a set of McLeod gauges were used to cover the various parts of the pressure range investigated. Two Pyrex reaction bulbs were used. One of these had a volume of 336 cc and a surface-volume ratio of about 0.30 cm^{-1}, the other was packed with short lengths of 3-mm Pyrex tubing and had a surface-volume ratio of 4.5 cm^{-1}. The reaction bulb was immersed in a well-stirred oil bath, the temperature of which could be hand regulated to 0.1°C. The reaction bulb was connected by means of the shortest possible length of 1/4-inch tubing to the McLeod gauge or to the manometer. The connections to the pumping system and methyl nitrite supply were made through mercury seals, no stopcock grease being used in or near the reaction system.

Methyl nitrite was prepared and purified as previously described. It was stored as a liquid in a trap cooled with solid carbon dioxide. The desired amount for an experiment was obtained by filling a short length of capillary tubing with the gas to a predetermined pressure.

As previously mentioned, mercury seals were used in or near the reaction system. In other parts of the apparatus stopcocks were used, and these were lubricated with Apiezon *L* grease on account of its negligible vapor pressure. All connections were made of wide tubing to facilitate evacuation. Between runs the system was evacuated to at least 10^{-5} mm. If left standing after evacuation, the pressure at the end of 24 hours was always below 10^{-4} mm with the empty reaction vessel, and hence no trouble was experienced because of slow distillation from the walls of the vessel as reported by Rice and Sickman[4] in their investigation of the decomposition of ethyl ether at low pressures. In the packed vessel the effect was noticed to a very slight extent.

In carrying out an experiment, methyl nitrite was introduced by quickly lowering and raising the mercury seal separating the supply from the reaction system. After 15 seconds the mercury in the McLeod gauge was raised and the initial pressure read. Blank experiments made with the reaction vessel cold showed that this allowed ample time for the establishment of pressure equilibrium. After reading the initial pressure, the mercury in the gauge was lowered to a fixed point so located that the gas in the gauge was still cut off from the reaction vessel. After the lapse of a definite time the mercury was lowered so as to connect the gauge to the reaction vessel, and then raised again and the new pressure determined. By the use of this method only one point on the amount reacted-time curve was obtained from each experiment. It had the advantage, however, of permitting the use of gauges of large capacity, and at the same time keeping the dead space down to a few percent of the volume of the reaction system.

Calculation of Rates

From the initial and final pressure we may calculate the percent pressure increase which has occurred during the reaction time. This must be corrected for the fact that not all the gas in the system was in the reaction vessel. The correction for the volume of gas contained in the gauge is simple and certain, since this gas has been isolated during the entire experiment. The correction for the gas in the connecting tubing between the vessel and the gauge is less definite, however, since it is uncertain what assumption should be made regarding diffusion. Since the tubing was short and of 1/4-inch diameter, we have assumed that complete mixing occurred. In any case the error from this cause is of the same order of magnitude as the experimental error.

From the corrected pressure increase the "percent reaction" is calculated, assuming that 87 percent pressure increase corresponds to com-

[3] Rice and Radowskas, J. Am. Chem. Soc. **57**, 350 (1935).

[4] Rice and Sickman, J. Am. Chem. Soc. **56**, 1444 (1934).

plete reaction. The evidence for this will be given later. We thus have the percent reaction corresponding to a given time. From this the value of T_{40} (the time for 40 percent reaction) is calculated assuming that the reaction is first order. This is not quite justified, since we are dealing with a pressure region in which the reaction is tending to a higher order. No appreciable error is introduced, however, for the following reasons: (a) The times used were chosen so that the percent reaction was almost always in the range from 25 to 60. Theoretically the ratio T_{40}/T_{75} for a first-order reaction is 1.77 and for a second-order reaction 2.00. Hence even if the order were as high as 1.5, the error involved in the method of calculation would not be greater than 5 percent. (b) By trial it was found that in any single run the order did not deviate greatly from the first. (c) The results show no systematic variation with the value of the "percent reaction." The rate of reaction has therefore been reported throughout as $10^4/T_{40}$ sec.$^{-1}$.

Experimental Results

In all about 150 runs were made at four different temperatures. Table I gives a summary of the data for representative runs in the empty reaction vessel. The data for all runs are given in Fig. 1 in the form of a log $P-\log 10^4/T_{40}$ graph.

The results for the packed reaction vessel at 494.3°K are given in Table II. Similar results were obtained at other temperatures, but there seems to be no object in giving them in detail.

Some typical values of the total pressure increase at completion are given in Table III. The mean value for all runs was 87.0 percent, and this value has been used throughout in calculating the amount of reaction from the observed pressure increase. As in the investigation of Steacie and Shaw, it was found that after the pressure in any run had reached a maximum, there was a very slow decrease. The data in Table III represent the maximum pressure reached.

Discussion

The mean value of the pressure increase at completion is about 4.5 percent higher than that found by Steacie and Shaw. They found also that after rising to its maximum value the pressure decreased again slowly due to some sort of condensation. It seems probable that the higher value found here is due to diminished condensation at low pressures.

In Fig. 1 the reaction velocity data are plotted together with the high pressure rate calculated from Steacie and Shaw's equation

$$K=1.84\times10^{13}\, e^{-36400/RT}.$$

It will be seen that their rates are definitely higher than those found here. The discrepancy is equivalent to a difference of from 1 to 1.5° in the absolute temperature scale, and is therefore no greater than that which is usually found in comparing the results of different investigations.

A comparison of the results of Tables II and III shows that the reaction is appreciably heterogene-

Table I. *Data for representative experiments.*

Initial Pressure (cm)	Time (sec.)	Per-cent Reaction	T_{40} (sec.)	Initial Pressure (cm)	Time (sec.)	Per-cent Reaction	T_{40} (sec.)
			Temperature—484.3°K				
0.00533	7200	20.5	16000	0.131	7200	47.8	5640
0.0125	7200	20.0	16500	0.169	2700	26.6	6110
0.0257	7200	23.1	14000	0.468	2700	37.5	4010
0.0403	7200	28.2	11100	0.834	2700	43.6	3300
0.0537	7200	32.6	9310	1.43	2700	49.2	2790
0.0727	5400	29.3	7950	2.46	2700	53.3	2480
0.0943	7200	41.8	6790	5.79	manometer		1540
			Temperature—494.3°K				
0.00479	5400	15.3	16600	0.129	5400	62.1	2840
0.0107	5400	19.8	12500	0.268	1800	38.6	1880
0.0174	5400	25.0	9550	0.750	1800	54.1	1180
0.0381	5400	38.5	5670	1.67	1500	55.6	943
0.0604	5400	48.5	4150	1.87	manometer		1080
0.0748	5400	51.5	3800	6.00	manometer		590
			Temperature—504.4°K				
0.00687	3600	20.3	8100	0.288	1200	51.4	850
0.0120	3600	26.9	5860	0.515	1200	61.8	636
0.0246	3600	37.4	3920	0.766	1200	67.4	547
0.0437	3600	50.7	2600	1.59	1200	72.9	469
0.0615	3600	56.5	2210	1.16	manometer		540
0.0806	1200	32.9	1540	3.99	manometer		290
0.104	3600	69.9	1530	6.06	manometer		280
			Temperature—514.4°K				
0.00455	1500	11.3	6390	0.250	600	48.1	467
0.00999	1500	18.6	3720	0.493	600	61.1	324
0.0164	1500	23.9	2810	0.786	600	66.5	280
0.0310	1500	34.7	1820	1.14	600	71.0	247
0.0550	1500	39.3	1530	3.70	manometer		160
0.0840	1500	56.1	931	6.18	manometer		135
0.134	1500	64.0	751				

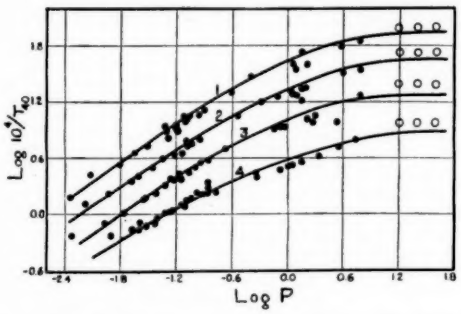

FIG. 1. Effect of pressure on rate. Curve (1) 514.4°K; (2) 504.4°K; (3) 494.3°K; (4) 484.3°K. Full circles—this investigation; open circles—Steacie and Shaw's high pressure rates.

ous at low pressures. Since the surface-volume ratio in the packed vessel was 15 times that in the empty vessel, we may calculate roughly that the reaction is about 5 percent heterogeneous at an initial pressure of 1.5 cm, about 15 percent at 0.05 cm, and about 40 to 50 percent heterogeneous at the lowest pressures employed. It follows that below about 0.05 cm the results have no great significance. Above this pressure an error will be introduced into the form of the log $P-\log 10^4/T_{40}$ curve, in the sense that the falling off in rate with diminishing pressure should be somewhat greater than that found. The general form of the curve, however, will not be altered sufficiently to affect seriously the subsequent calculations.

The average value of the energy of activation at pressures from 0.05 to 1.5 cm is found to be 36,100 calories per gram molecule in excellent agreement with Steacie and Shaw's value of 36,400. At lower pressures the heat of activation decreases rapidly with diminishing pressures. Such a decrease is to be expected on theoretical grounds, but it is doubtful in this case to what extent it is due merely to the increasing heterogeneity of the reaction.

It is to be noted that the curves in Fig. 1 show no sign of upward concavity as is the case with ethyl ether at low pressures.[4] There is therefore

TABLE II. *Experiments in packed reaction vessel at 494.3°K.*

Initial Pressure (cm)	Time (sec.)	Percent Reaction	T_{40} (sec.)
0.0224	1800	71.5	1100
0.0449	2700	64.6	1330
0.0745	3600	81.8	1080
0.0998	1800	61.1	973
0.600	1080	62.2	566
1.53	1080	65.3	521
1.96	manometer		360
5.26	manometer		370

TABLE III. *Pressure increase at completion.*

Temperature (°K)	Initial Pressure (cm)	Percent Pressure Increase at Completion	Temperature (°K)	Initial Pressure (cm)	Percent Pressure Increase at Completion
Empty Reaction Vessel					
484.3	0.0175	82.2	494.3	3.12	87.7
484.3	0.0603	87.5	504.4	0.0599	88.2
484.3	0.0782	89.2	504.4	4.49	85.6
484.3	1.66	83.2	514.4	0.00670	91.7
484.3	2.70	88.7	514.4	0.0213	87.6
494.3	1.86	83.4	514.4	6.41	86.6
Packed Reaction Vessel					
504.4	0.0532	85.0	504.4	0.0162	89.1
504.4	0.0758	79.8			

no indication of a second first-order region coming into existence at low pressures. This, however, would hardly be expected with as simple a molecule as methyl nitrite.

The falling off in rate as the pressure diminishes can be satisfactorily accounted for on the basis of Theory II of Rice and Ramsperger[5] if we assume a molecular diameter of 5.0×10^{-8} cm, and that 13 degrees of freedom are involved. In making the calculation the rates have been divided by 2, since on the basis of the Rice mechanism[3] two molecules are decomposed for each elementary act. As with the azo compounds the number of degrees of freedom involved is approximately half the total number avialable (30).

[5] Rice and Ramsperger, J. Am. Chem. Soc. **49**, 1617 (1927).

The Free Energies and Vapor Pressures of the Alkali Metals

A. R. GORDON, *Chemistry Department, University of Toronto*

(Received November 19, 1935)

The free energies of the diatomic alkali vapors K_2, Na_2 and Li_2 are calculated from spectroscopic data, and the equilibrium constants for the dissociation into the monatomic form are computed. With the aid of these constants, equations are deduced from the observed vapor pressures obtained by various investigators, which give the partial pressures of atoms and molecules in the saturated vapors for temperatures up to the normal boiling point. In the case of sodium and potassium, the entropy of the solid metal is computed from the vapor pressure equation, and is compared with that predicted by the third law of thermodynamics.

IN spite of the numerous investigations that have been carried out to determine the vapor pressures of the alkalis, there has still been some difficulty in reconciling the results that have been obtained by various methods, and a corresponding uncertainty as to the correct form of the vapor pressure equation. One reason for this is that molecule formation may be appreciable in the vapor phase, and although attempts have been made both experimentally and by means of the Gibson-Heitler equation to determine the degree of such association, there has still been a chance of appreciable error in allowing for this effect. Thanks primarily to the work of Loomis and his associates,[1] however, there are available data sufficient to permit a precise calculation of the equilibrium between atoms and molecules in the vapors, and the results of such calculations, together with their application to the vapor pressure data are recorded briefly here.

The spectroscopic constants used in the calculation of $(F^0-E_0^0)/T$ for K_2, Na_2 and Li_2 are listed in cm^{-1} in Table I; they are weighted averages computed for a nonisotopic gas from the table of Loomis[1] and the isotope abundance ratios of Brewer and Kueck,[2] by means of the familiar relations connecting the reduced mass of a molecule with the spectroscopic constants.[3] Even for the highest temperatures considered here, only the normal $^1\Sigma$ state of the molecule need be taken into account, since the excited $^1\Sigma$ and $^1\Pi$ states make only negligible contributions to the state sum. The table also gives the values[1, 4] of ΔE_0^0 in calories per mole for the reaction $M_2=2M$.

The resulting $(F^0-E_0^0)/T$ are listed in Table II,[5] and were computed by methods already described;[6] because of the small values of the fundamental frequencies such calculations would be exceedingly laborious if integral approxima-

TABLE I.

	K_2	Na_2	Li_2
ω_e	92.49	159.2	352.0
$\omega_e x_e$	0.352	0.73	2.5
B_0	0.05593	0.1543	0.6776
$-D_0\times10^6$	0.0827	0.586	10.22
	0.000218	0.00082	0.00728
ΔE_0^0	11800	17515	26275

TABLE II.

	$-(F^0-E_0^0)/T$			$\log K=\log (P_M)^2/(P_{M_2})$		
$T°K$	K_2	Na_2	Li_2	K_2	Na_2	Li_2
298.1	51.093	46.685	39.320	−5.247	−9.165	−15.540
300	51.148	46.738	39.369	−5.190	−9.081	−15.414
400	53.645	49.163	41.639	−2.962	−5.797	−10.500
500	55.606	51.077	43.447	−1.617	−3.816	− 7.539
600	57.224	52.659	44.953	−0.715	−2.490	− 5.558
700	58.603	54.009	46.246	−0.067	−1.538	− 4.138
800	59.807	55.188	47.379	+0.420	−0.823	− 3.070
900	60.877	56.235	48.388	0.800	−0.264	− 2.237
1000	61.841	57.178	49.298	1.105	+0.184	− 1.570
1200	63.53	58.83	50.89	1.562	0.857	− 0.564
1400	64.98	60.24	52.26	1.887	1.339	+ 0.155
1600	66.25	61.47	53.45	2.129	1.702	0.697
1800	67.39	62.58	54.52	2.315	1.981	1.118
2000	68.41	63.58	55.48	+2.464	+2.204	+ 1.456
$S^0_{298.1}$	59.706	55.024	47.081			

[1] Loomis, Phys. Rev. **38**, 2153 (1931). See this paper for a bibliography for the alkali molecular spectra.

[2] Brewer and Kueck, Phys. Rev. **46**, 894 (1934).

[3] For a discussion of the validity of averaging the spectroscopic constants for the various isotopic varieties of molecule present, and then treating the particular element as nonisotopic, see Giauque and Overstreet, J. Am. Chem. Soc. **54**, 1731 (1932); see also Gordon and Barnes, J. Chem. Phys. **1**, 692 (1933).

[4] Loomis and Nusbaum, Phys. Rev. **40**, 380 (1932).

[5] As is now customary, none of the entries includes the nuclear spin contribution. The constants used were $hc/k=1.4324$, $R=1.9869$, additive constant for the translational free energy $=-7.267$. $(F^0-E_0^0)/T$ can be interpolated using not more than second differences; in the case of the equilibrium constants, it is better to interpolate $T\cdot\log K$.

[6] Gordon and Barnes, J. Chem. Phys. **1**, 297 (1933).

tions[7] were not used to avoid summation over all values of the vibrational quantum number. It should be noted in passing that with these molecules, the use of the rigid rotator-harmonic oscillator approximation to the energy levels (such as is employed in the simple Gibson-Heitler equation) would lead to very considerable errors. For example, in the case of potassium, it would predict for 2000° and 1000° 67.69 and 61.56, respectively, as the values of $-(F^0-E_0^0)/T$ instead of 68.41 and 61.84 as given in Table II; similarly for sodium, the entries for 2000° and 1000° would be 63.07 and 56.98 with resulting errors of 0.51 and 0.20 cal./deg., respectively.

Values of $(F^0-E_0^0)/T$ for the atoms can be readily computed since for $T<2000°$ only the normal ^2S state (of quantum weight 2) need be considered. From these and the values of ΔE_0^0 given in Table I, $\log K=\log (P_M)^2/(P_{M_2})$ for the three metals can be obtained, and is entered in the last three columns of Table II. As an example of the errors introduced by the use of the simple Gibson-Heitler equation for these vapors, it should be noted that for 1000° and 2000° in the case of sodium, the equation would give $K=1.69$ and $K=207$, respectively, as compared with the exact values from Table II, *viz.* 1.53 and 160. Experimental determinations of the degree of association of the alkali vapors have been made by Lewis[8] using a magnetic deflection method, but his values of the equilibrium constants are all considerably larger than those recorded in Table II.

Of the three alkalis, sodium has by far the most complete and concordant vapor pressure data; the work of Edmondson and Egerton,[9] of Thiele[10] and of Rodebush and his associates[11, 12, 13] covers a range of temperature of nearly 700° and a range of pressure from 1/10,000 of a millimeter to nearly 500 millimeters. After allowing for the partial pressure of the molecules by means of Table II, the "best" equation[14] to fit the vapor pressures of the atoms (in mm of mercury) is given by

$$\log p_{Na}=11.3245-26{,}087/4.575T \\ -1.174\log T. \quad (1)$$

When used in conjunction with Table II, this leads to vapor pressures which in general agree with the results of experiment over the whole range to better than ±0.5 percent and with no drift in the deviations.

From Eq. (1), ΔE_0^0 for the reaction $Na(l)=Na(g)$ is 26,087 cal.; the latent heat of fusion of sodium[15] is 600 cal., and hence from the heat capacity data for crystalline sodium of Simon and Zeidler,[15] ΔE_0^0 for the reaction $Na(s)=Na(g)$ is 26,040 cal. Similarly, from Eq. (1), the entropy of $Na(g)$ and the data of Simon and Zeidler for the range 298°–371°, $S^0_{298.1}$ for crystalline sodium is 12.15 cal./deg.—in close but possibly fortuitous agreement with the "third law" value 12.2 cal./deg.

Fiock and Rodebush[16] have measured the vapor pressure of potassium for the range 679°–1033°K (pressures from 4.6 to 783 mm); molecule formation is less prominent than with sodium, but is still appreciable. After allowing for the partial pressure of K_2 by means of Table II, p_K (in mm) can be represented by the equation[17]

$$\log p_K=11.410-22{,}210/4.575T \\ -1.275\log T. \quad (2)$$

Eq. (2), in conjunction with Table II, predicts vapor pressures for this range which agree with Fiock and Rodebush's results within their estimated experimental error of ±1 percent. The agreement between these data for relatively high temperatures and those for the lower range (340°–470°K), however, is not nearly so satisfactory as in the case of sodium. For example,

[7] To ensure numerical accuracy in the integral approximations, the calculation was carried out for 2000° and 1000° for each gas with two different values of M, see reference 6, Eq. (12), p. 304. Note also the misprint in the expression for I_2 of Eq. (14), p. 304; the coefficient of the last term should be $(1/2r)$, not $(\frac{1}{2}r)$ as printed.

[8] Lewis, Zeits. f. Physik **69**, 804 (1931).

[9] Edmondson and Egerton, Proc. Roy. Soc. **A113**, 520 (1927).

[10] Thiele, Ann. d. Physik (5) **14**, 937 (1932).

[11] Rodebush and de Vries, J. Am. Chem. Soc. **47**, 2488 (1925).

[12] Rodebush and Walters, J. Am. Chem. Soc. **52**, 2654 (1930).

[13] Rodebush and Henry, J. Am. Chem. Soc. **52**, 3159 (1930).

[14] The coefficient of the last term assumes with Thiele (reference 10) Rengade's value for heat capacity of liquid sodium—7.30 cal./deg./gram-atom (Rengade, Comptes rendus **156**, 1897 (1913)).

[15] Simon and Zeidler, Zeits. f. physik. Chemie **123**, 383 (1926).

[16] Fiock and Rodebush, J. Am. Chem. Soc. **48**, 2522 (1926).

[17] The coefficient of the last term corresponds to a heat capacity for liquid potassium of 7.50 cal./deg./gram-atom; see reference 15.

for 373.2°K, Eq. (2) predicts $P_K(=P)=1.32\times10^{-5}$ mm, while the equations fitted to their experimental results by Edmondson and Egerton,[9] Mayer [18] and Neumann and Völker[19] give 1.82, 3.01 and 1.89×10^{-5}, respectively.

From Eq. (2), from the heat of fusion of potassium (575 cal.) and from the thermal data of Simon and Zeidler,[15] ΔE_0^0 for the reaction $K(s)=K(g)$ is 22,230 cal.; while from Eq. (2), the entropy of gaseous monatomic potassium and the heat capacity data of Simon and Zeidler, $S^0_{298.1}$ for crystalline potassium is 14.60 cal./deg.—definitely *less* than the third law value, 15.2 cal./deg. The reason for this discrepancy is not immediately apparent, but it should be noted that the Neumann-Völker vapor pressure equation leads to a value of $S°_{298.1}$ in agreement with the third law value, but is in definite disagreement with Fiock and Rodebush's results even when allowance has been made for the molecule formation.

In the case of lithium, Hartmann and Schneider[20] have measured the vapor pressure in the range 1204°–1353°K (pressures of from 17 to 94 mm); after correcting their observed pressures for p_{Li_2} by means of Table II, the pressure of the lithium atoms can be represented (as a rule to better than one percent by the equation)

$$\log p_{Li}=11.889-38{,}900/4.575T-1.174\log T. \quad (3)$$

The normal boiling points for the three alkalis and the partial pressures of atoms and molecules at the boiling point in the saturated vapors, predicted by Eqs. (1), (2) and (3) and Table II are:

	K	Na	Li
T_B	1030°	1162°	1599°
p_M	716 mm	658 mm	648 mm
p_{M_2}	44 mm	102 mm	112 mm

[18] Mayer, Zeits. f. Physik **67**, 240 (1931).
[19] Neumann and Völker, Zeits. f. physik. Chemie **A161**, 33 (1932).
[20] Hartmann and Schneider, Zeits. f. anorg. Chemie **180**, 275 (1929).

FEBRUARY, 1936 JOURNAL OF CHEMICAL PHYSICS VOLUME 4

Electron Distribution in $(NH_4)_2C_2O_4\cdot H_2O$ and the Structure of the Oxalate Group

S. B. HENDRICKS AND M. E. JEFFERSON, *Fertilizer Investigations, Bureau of Chemistry and Soils, Washington, D. C.*
(Received November 21, 1935)

The electron distribution of $(NH_4)_2C_2O_4\cdot H_2O$ projected on (001) was obtained by a Fourier analysis making use of quantitative intensity measurements of x-ray scattering from (*hk*0). This analysis combined with a determination of the atomic parameters perpendicular to (001) gave the complete structure. Separations of covalently linked atoms in the $C_2O_4^{--}$ group are C−C, 1.581±0.01A; C−O, 1.25±0.02A; and C−O, 1.23±0.02A with the angle O−C−O = 129°±2°. In this compound the O−C−O parts of an oxalate group are in planes at an angle of 28° while in $H_2C_2O_4\cdot 2H_2O$, α and β $H_2C_2O_4$ the parts are coplanar.

Introduction

THE crystal structures of a number of oxalates have been determined by the usual methods of analysis of x-ray diffraction data. In $H_2C_2O_4\cdot 2H_2O$,[1] α $H_2C_2O_4$ and β $H_2C_2O_4$[2] the oxalate group apparently has a center of symmetry and thus the four oxygen atoms of the group must be coplanar but cannot be crystallographically equivalent. Atomic separations as found for these compounds and for KHC_2O_4, $RbHC_2O_4$, $K_2C_2O_4\cdot H_2O$, and $Rb_2C_2O_4\cdot H_2O$ are C−C, 1.57 to 1.60A; C−O, 1.20 to 1.30A; and angle O−C−O, 125°–134°.[3] A more accurate determination of these values and a knowledge of the possible equivalence of the oxygen atoms can be obtained from a Fourier analysis of the electron distribution on a given plane.

[1] W. H. Zachariasen, Zeits. f. Krist. **89**, 442 (1934).
[2] S. B. Hendricks, Zeits. f. Krist. **91**, 48 (1935).
[3] Note *X-rays in Theory and Experiment*, by A. H. Compton and S. K. Allison (New York, 1935), p. 444 *et seq.*, for a logical development of the subject.

W. L. Bragg[4] has shown that the electron density per unit area at any point (x, y) in a projection with a center of symmetry is given by

$$\sigma(x, y) = \frac{1}{AZ} \sum_{-\infty}^{\infty} n \sum_{-\infty}^{\infty} m F_{nm} \cos 2\pi(nx+mz),$$

where n and m are the indices of planes in a zone whose axis is normal to the plane of projection, F_{nm} is the structure amplitude of the scattered wave, A is the area of the plane of projection, and Z is the total number of electrons in the projected volume. To evaluate this series it is necessary to have values of F_{nm} for all planes of a zone and these can be derived from the measured intensities which are proportional to F_{nm}^2.[5] The signs of F_{nm}, however, are only to be found from an approximate analysis of the structure by the usual methods.

It is perhaps apparent that the plane selected for the projection should be one that gives the minimum overlapping of atoms and groups in the projection. Further, in the case of an oxalate group with a center of symmetry, the most desirable plane would be one that is parallel to the plane of the oxygen atoms. These conditions are best fulfilled by a projection of the structure of $(NH_4)_2C_2O_4 \cdot H_2O$ on (001). This compound, as it will develop, is of particular interest in that the oxalate group has a twofold axis rather than a center of symmetry and there is the possibility of formation of hydrogen bonds with the ammonium ion and the water molecule.

Experimental Procedure and Approximate Analysis of the Structure Projected

Previous work[6] on ammonium oxalate monohydrate led to the space group $P2_12_1$ with $2[(NH_4)_2C_2O_4 \cdot H_2O]$ in a unit of structure having $a = 8.06$A, $b = 10.34$A, $c = 3.82$A. We have verified the space group assignment and have found $a = 8.04$A, $b = 10.27$A, and $c = 3.82$A; the first two values being determined from high order reflections of the pinacoids and the last from a layer line photograph about the c axis.

Intensities of reflections for $(hk0)$ were measured for Mo $K\alpha$ radiation from a constant source with an argon-filled ionization chamber; the ionization current being measured by an FP54 vacuum tube direct current amplifier. The sample of $(NH_4)_2C_2O_4 \cdot H_2O$ was a cylindrical one, 0.1 cm in radius (r), with its axis parallel to $(kh0)$ and it was illuminated through a narrow slit. The linear absorption coefficient (μ) measured with monochromatic Mo $K\alpha$ radiation is 1.42, and thus $\mu r = 0.14$. With this arrangement the maximum error that could be introduced into the intensity measurement due to varying absorption in the sample[7] would be less than one percent. These measurements were reduced to absolute values by comparison with the integrated reflection from (400) for Mo $K\alpha$ radiation on an extended face of NaCl, this being taken as 0.98×10^{-4} from the work of James and Firth.[8] The square of the structure amplitude, F_{nm}^2, was found according to the following expressions for a mosaic crystal:

$$\rho_{nm} = \text{integrated reflection} = 2Qre^{-2\mu r}$$

$$Q = \left(\frac{Ne^2}{mc^2} F_{nm}\right)^2 \lambda^3 \frac{1+\cos^2 2\theta}{2 \sin 2\theta} = 2.19 \times 10^{-8} \theta F_{nm}^2,$$

where

$$\theta = \frac{1+\cos^2 2\theta}{\sin 2\theta},$$

N is the number of scattering units per unit volume, and the other terms have their usual significance. μ was taken in the first analysis as the linear absorption coefficient since it was thought that a correction for extinction could best be based on a knowledge of the structure and the atomic scattering factors. In the end it appeared, however, that extinction must be quite small.

The general positions of the space group $P2_12_1$ are

$$xyz; \quad 1/2+x, \quad 1/2-y, \quad \bar{z},$$
$$\bar{x}\bar{y}z; \quad 1/2-x, \quad 1/2+y, \quad \bar{z},$$

which lead to special positions on the twofold axes, $00\,Z$, $1/2\;1/2\;\bar{Z}$; and $1/2\;0\;Z$; $0\;1/2\;\bar{Z}$. Because of interatomic distance requirements the oxalate groups must be at one of these sets and the H_2O molecules at the other, say $1/2\;0\;Z$; $0\;1/2\;\bar{Z}$. The NH_4, C, O_1 and O_2 atoms are in sets of general positions, thus giving thirteen parameters defining the structure.

[4] W. L. Bragg, Proc. Roy. Soc. **A123**, 537 (1929).
[5] W. L. Bragg, Zeits. f. Krist. **69**, 118 (1928).
[6] J. F. Wood, Proc. Univ. of Durham Phil. Soc. **7**, 111 (1928).
[7] F. C. Blake, Rev. Mod. Phys. **5**, 169 (1933).
[8] James and Firth, Proc. Roy. Soc. **A117**, 62 (1927).

TABLE I. *Observed and calculated values of the structure amplitudes (F) for (hk0) of* $(NH_4)_2C_2O_4 \cdot H_2O$ *· Mo Kα.*

h\k	0	1	2	3	4	5	6	7	8	9	10
0 obs			25.2		27.0		11.2		11.8		11.8
calc			18.5		30.6		8.0		6.7		10.0
1 obs		23.5	15.5	13.4	28.9	21.6	17.4	11.5	0.0	13.1	12.2
calc		18.4	10.0	10.1	33.2	13.8	11.9	7.9	0.4	11.7	7.5
2 obs	3.2	12.6	0.0	29.9	19.4	36.1	21.9	6.4	18.4	14.8	9.9
calc	6.0	10.1	3.1	25.5	12.0	44.6	13.3	6.7	13.2	7.2	7.2
3 obs		32.5	29.7	15.2	6.7	0.0	13.3	12.2	9.4	6.6	10.6
calc		38.6	33.8	9.9	3.6	1.4	10.3	9.1	6.9	7.0	6.0
4 obs	29.4	8.3	25.2	25.1	10.9	14.5	0.0	12.3	10.6	(3.3)	(9.4)
calc	21.6	2.6	25.8	23.9	8.1	9.5	0.5	9.3	6.5	2.0	5.7
5 obs		10.2	8.0	0.0	(3.8)	(5.7)	(3.0)	23.5	0.0		
calc		5.8	9.1	1.1	3.8	3.3	2.0	19.8	1.4		
6 obs	7.7	8.2	6.8	22.0	0.0	(2.8)	0.0	8.6	0.0	(7.3)	
calc	4.5	4.8	5.3	19.0	0.4	3.7	2.6	7.7	0.2	3.5	
7 obs		13.8	15.5	16.6	0.0	(6.6)	(7.8)	(7.2)	(3.8)		
calc		9.8	10.0	12.0	1.5	4.2	2.6	3.4	2.5		
8 obs	8.2	0.0	(7.5)						7.8		
calc	7.8	1.6	2.1						5.8		
10 obs	16.5	0.0	(7.1)								
calc	8.2	1.0	4.4								

Parenthetical values are visually estimated from an equatorial zone (*hk*0) Weissenberg photograph. Bars indicate negative values.

In deriving the approximate projection on (001) it was assumed that the oxalate group has a coplanar arrangement of atoms of the configuration previously found. It would then follow that this plane is parallel to (001) and this is supported by the cleavage parallel to that direction and *c* as the direction of vibration of the slow ray. The high polarizability of the NH_4^+ ion makes impossible further use of the optical data in the structure analysis.[9] To find the projection on (001) it is necessary to find the parameters of the ammonium group and the orientation of the oxalate group, which requires two parameters in both the *a* and *b* directions. The approximately normal intensities for reflections from (10.0.0) and (0.10.0) (note Table I) suggest that the majority of the atoms scatter in phase from these planes. This fact, the intensities from other orders of the pinacoids, and the absence of (220) require the following approximate parameters:

X_C, 0.095; X_{O_1}, 0.21; X_{O_2}, 0.11; X_{NH_4}, 0.40; Y_C, 0.03; Y_{O_1}, −0.05; Y_{O_2}, 0.145; Y_{NH_4}, 0.24.

The above parameter values were used in calculating the signs of $F_{(hk0)}$, use being made of assumed scattering curves for the various atoms and groups as follows: NH_4^+ as in NH_4Cl,[10] O and C as in urea[11] and water below $\sin\theta/\lambda = 0.20$ similar to NH_4^+ and above that value similar to O. A Fourier analysis was made using these signs and the resulting improved parameters were used in a final calculation of the signs and values of $F_{(hk0)}$ listed in Table I, as well as in the final Fourier analysis. It is to be emphasized that the final analysis does not depend upon arbitrary assumptions used in deriving the approximate structure.

The method suggested by Beevers and Lipson[12] was used for summing the double Fourier series and this greatly shortened the labor involved. Projected electron densities were calculated for values of *x* and *y* by steps of 0.02 save in the region near atomic centers where the interval was reduced to 0.01. Final values on the open scale are listed in Table II and the resulting contour map is shown as Fig. 1. The final parameters were taken as the average values for the centers of the contour areas and they are listed in Table III. The variation in these as determined from various contours did not exceed 0.001. An arbitrary splitting of the projection into areas per atom led to the results shown in Table III. The projected number of electrons exceeds that required by a neutral water molecule and is less than that required

[9] S. B. Hendricks, Zeits. f. Krist. (A) **91**, 290 (1935).
[10] Wyckoff and Armstrong, Zeits. f. Krist. **72**, 324 (1929–30).
[11] Wyckoff, Zeits. f. Krist. **81**, 108 (1932). The carbon data are combined with Bernal's results from graphite.
[12] Beevers and Lipson, Phil. Mag. **17**, 855 (1934).

TABLE II. *Calculated values of the projected electron density (σ) on (001) for $(NH_4)_2C_2O_4 \cdot H_2O$.*

$x\backslash y$	0.00	0.02	0.04	0.06	0.08	0.10	0.12	0.14	0.16	0.18	0.20	0.22	0.24
0.00	2.00	1.69	1.11	0.92	1.27	1.70	1.69	1.38	1.20	1.33	1.49	1.41	1.29
0.02	2.11	2.00	1.36	0.94	1.06	1.44	1.61	1.33	0.96	0.97	1.18	1.16	1.00
0.04	2.60	2.85	2.27	1.43	1.06	1.32	1.70	1.79	1.48	1.14	0.86	0.91	0.73
0.06	3.51	4.37	3.89	2.52	1.59	1.79	2.79	3.35	2.86	2.07	1.13	0.79	0.67
0.08	4.39	5.79	5.38	3.53	2.51	2.79	4.59	5.73	4.96	2.96	1.30	0.75	0.84
0.10	4.56	6.07	5.62	3.64	2.42	3.63	6.27	7.86	6.70	3.80	1.38	0.73	1.17
0.12	3.46	4.80	4.38	2.65	1.89	3.63	6.79	8.60	7.20	3.82	1.13	0.51	1.28
0.14	2.22	2.84	2.55	1.45	1.20	3.04	6.03	7.63	6.30	3.11	0.52	0.07	0.98
0.16	1.66	1.38	1.27	0.90	1.03	2.52	4.48	5.49	4.46	2.11	0.15	0.00	0.61
0.18	1.97	0.93	0.96	1.05	1.40	2.06	2.87	3.24	2.62	1.27	0.22	0.00	0.43
0.20	2.34	0.99	1.03	1.58	1.92	1.76	1.70	1.59	1.30	0.86	0.60	0.59	0.71
0.22	2.05	0.86	1.00	1.56	1.80	1.48	1.10	0.88	0.86	0.96	1.07	1.17	1.11
0.24	1.36	0.61	0.79	1.30	1.47	1.30	1.10	1.06	1.13	1.24	1.43	1.49	1.39
0.26	0.84	0.68	0.93	1.22	1.36	1.41	1.53	1.71	1.69	1.55	1.45	1.40	1.33
0.28	0.86	1.06	1.40	1.54	1.58	1.64	1.96	2.19	2.13	1.75	1.44	1.28	1.23
0.30	1.01	1.35	1.75	1.78	1.62	1.71	1.95	2.16	2.11	1.74	1.60	1.62	1.52
0.32	1.02	1.29	1.59	1.64	1.47	1.47	1.55	1.54	1.47	1.63	2.15	2.67	2.57
0.34	0.94	1.03	1.21	1.12	1.07	1.16	1.19	1.05	1.10	1.74	3.10	4.26	4.28
0.36	1.06	1.08	1.18	1.05	1.06	1.19	1.19	0.93	0.97	2.08	4.22	5.83	5.94
0.38	1.40	1.39	1.32	1.19	1.12	1.42	1.45	1.19	1.32	2.64	4.94	6.81	6.69
0.40	1.74	1.73	1.45	1.07	1.03	1.31	1.50	1.33	1.48	2.73	4.98	6.49	6.27
0.42	2.20	2.12	1.43	0.68	0.51	0.81	1.13	1.13	1.21	2.30	4.07	5.15	4.83
0.44	3.37	3.01	1.64	0.33	0.00	0.25	0.68	0.75	0.80	1.52	2.77	3.57	3.27
0.46	5.49	4.74	2.60	0.57	−0.24	0.09	0.54	0.77	0.43	0.88	1.77	2.31	2.03
0.48	7.76	6.64	3.89	1.29	0.24	0.36	0.68	0.58	0.33	0.67	1.19	1.56	1.57

$x\backslash y$	0.26	0.28	0.30	0.32	0.34	0.36	0.38	0.40	0.42	0.44	0.46	0.48	0.50
0.00	1.25	1.30	1.11	0.75	0.54	0.64	0.75	0.59	0.64	1.83	4.49	7.45	8.75
0.02	0.97	1.09	1.12	0.94	0.62	0.47	0.48	0.52	0.88	1.79	3.93	6.51	7.76
0.04	0.70	0.84	1.11	1.07	0.72	0.34	0.12	0.26	0.47	1.17	2.55	4.50	5.49
0.06	0.67	0.72	0.93	1.34	0.88	0.53	0.36	0.34	0.51	0.85	1.64	2.67	3.37
0.08	0.97	0.88	0.82	0.96	1.10	1.02	0.86	0.81	0.86	1.31	1.27	1.77	2.20
0.10	1.44	1.05	0.67	0.84	1.27	1.48	1.39	1.17	1.19	1.25	1.37	1.53	1.74
0.12	1.65	1.28	0.59	0.58	1.26	1.56	1.40	1.09	1.07	1.27	1.28	1.36	1.40
0.14	1.48	1.13	0.63	0.71	1.21	1.37	1.01	0.71	0.83	1.21	1.33	1.16	1.06
0.16	1.02	0.94	0.76	0.89	1.23	1.20	0.71	0.51	0.81	1.26	1.27	1.10	0.94
0.18	0.77	0.76	0.82	1.20	1.36	1.13	0.69	0.60	1.00	1.42	1.40	1.13	1.02
0.20	0.62	0.71	0.93	1.24	1.36	1.10	0.78	0.87	1.23	1.50	1.38	1.05	1.01
0.22	0.97	0.83	0.88	1.06	1.02	1.03	0.90	0.96	1.53	1.77	1.53	1.02	0.86
0.24	1.24	0.96	0.86	0.86	0.70	0.54	0.64	1.44	2.30	2.82	2.50	1.64	0.84
0.26	1.22	1.03	0.95	0.85	0.59	0.37	0.79	2.06	3.81	4.95	4.54	2.98	1.36
0.28	1.15	1.11	1.17	1.08	0.71	0.33	0.83	2.86	5.47	7.18	6.73	4.48	2.05
0.30	1.26	1.15	1.29	1.38	0.99	0.49	0.96	3.13	6.23	8.22	7.67	5.10	2.34
0.32	1.93	1.32	1.32	1.45	1.35	0.66	0.90	2.74	5.65	7.25	6.63	4.17	1.97
0.34	3.07	1.75	1.25	1.40	1.35	0.87	1.26	1.44	3.84	4.82	4.23	2.72	1.66
0.36	4.11	2.17	1.23	1.28	1.44	1.15	0.96	1.47	2.33	3.43	2.09	1.80	2.22
0.38	4.71	2.39	1.27	1.36	1.51	1.52	1.18	1.29	1.58	1.40	1.17	1.84	3.46
0.40	4.37	2.36	1.44	1.47	1.60	1.16	1.14	1.29	1.37	1.16	1.13	2.27	4.56
0.42	3.42	2.03	1.58	1.66	1.54	1.07	0.93	1.22	1.39	1.28	1.39	2.45	4.39
0.44	2.41	1.73	1.68	1.79	1.52	0.88	0.79	1.02	1.33	1.31	1.34	2.15	3.51
0.46	1.75	1.57	1.90	2.00	1.33	1.20	1.05	1.35	1.33	1.21	1.22	1.79	2.60
0.48	1.44	1.54	1.83	1.70	1.25	1.38	1.50	1.63	1.38	0.94	1.10	1.64	2.11

for carbon, while the other values correspond to O_1^-, O_2 and NH_4^+. These particular values depend upon choice of area but it is to be noted that the value of σ is greater for O_1 than for O_2 and that this would be more pronounced if the area of O_2 were increased or that of O_1 decreased. The oxygen atoms thus apparently have neither equivalent surroundings nor similar electron distributions.

Values of $F_{(hk0)}$ calculated using the above

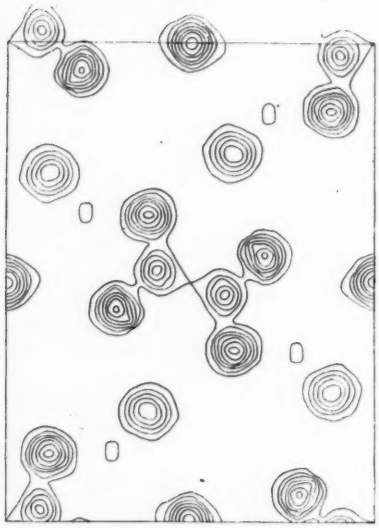

FIG. 1. The approximate electron distribution of $(NH_4)_2C_2O_4 \cdot H_2O$ projected on (001), with a contour interval of 1 electron/A^2, the lowest contour being 2.

parameters and the indicated atomic scattering curves are listed in Table I. The agreement is not perfect, a major part of the discrepancy undoubtedly being due to the use of the particular scattering curves. All absent reflections, however, are in close agreement and these are particularly sensitive for testing the possible correctness of a structure. Agreement between calculated and observed values of $F_{(hk0)}$ for strong reflections indicates the absence of extinction.

In this projection the separation of the atoms in a $C_2O_4^{--}$ group are C−C, 1.581A; O_1−C, 1.216A; and O_2−C, 1.200A with the angle O−C−O=124°. Since the oxalate group has a twofold axis the projected separation of the carbon atoms is their true separation while the O−C distances and the angle O−C−O are minimum values.

Complete Structure Analysis and Discussion

In order to complete the structure analysis it is necessary to determine the parameters along the *c* axis, the normal to the plane of the Fourier analysis. Trial and error methods can safely be used at least in determining the geometry of the oxalate group. *The observed intensities (004)a., (014)m.w., (034)m. cannot be explained if the atoms of the C_2O_4 group are coplanar.* Systematic consideration of the intensities of (00*l*) and (0*kl*) leads to the parameters listed in Table III. Agreement between intensities estimated visually from a Weissenberg photograph and calculated values of $F_{(0kl)}/f_O$ are listed in Table IV; the assumption being made that $f_{NH_4}=f_O=f_{H_2O}=2f_C$, where f_i is the scattering power. These parameter values are probably accurate to 0.01 for the atoms of the $C_2O_4^{--}$ group and 0.03 for NH_4^+ and H_2O. Distances within the oxalate group are thus found to be: C−C=1.581±0.01A; O_1−C=1.25±0.02A; and O_2−C=1.23±0.02A with the angle, O−C−O=129°±2°. Measurements on other oxalates mentioned in the introduction agree with these values within limits of experimental error; this being particularly true for $H_2C_2O_4 \cdot 2H_2O$ as analyzed by Zachariasen who found C−C=1.59±0.07A; O−C=1.25±0.05A and the angle O−C−O =126°±3°. The angle between the O−C−O plane and (001) is 14° and thus the angle between the two O−C−O planes of an oxalate group is 28°, this being diagrammatically shown in Fig. 2.

Arrangements of atoms surrounding NH_4^+ ions and water molecules are diagrammatically shown in Fig. 2. Water molecules are tetra-

TABLE III. *Parameter values and electron counts for $(NH_4)_2C_2O_4 \cdot H_2O$.*

Atom	Parameters			Electron Count		
	x	y	z	Area, A^2	Av. σ (001)	No. of Electrons
C	0.092	0.027	0.07	2.25	2.218	5.0
O_1	0.200	−0.056	0.14	5.00	1.870	9.3
O_2	0.118	0.142	0.00	4.58	1.763	8.1
NH_4	0.386	0.228	0.43	5.70	1.763	10.1
H_2O			−0.20	6.32	1.740	11.0

TABLE IV. *Estimated intensities of reflection for (0kl), Cu Kα radiation, of $(NH_4)_2C_2O_4 \cdot H_2O$ and calculated values of F/fo.*

k/l	1	2	3	4
0	1.4, s.	1.3, m. s.	$\overline{0.4}$, a.	0.0, a.
1	0.5, m.	1.0, m.-m.s.	1.3, m.-m.s.	0.7, w.
2	1.8, v.s.	1.0, m.	1.0, m.w.	0.5, v.w.
3	0.0, a.	0.9, m.	0.5, w.	1.7, m.
4	$\overline{1.0}$, m.s.	0.7, w.	1.5, m.-m.s.	1.0, m.w.-w.
5	0.2, a.	0.7, w.	1.1, m.	0.2, a.
6	$\underline{1.5}$, m.s.	$\underline{0.1}$, v.w.	0.6, a.	
7	$\overline{1.3}$, m.	$\overline{0.3}$, a.		
8	$\overline{0.2}$, a.	$\underline{0.7}$, v.w.		
9	$\underline{0.8}$, v.w.	$\underline{1.8}$, m.s.		
10	1.1, w.	1.4, m.w.		

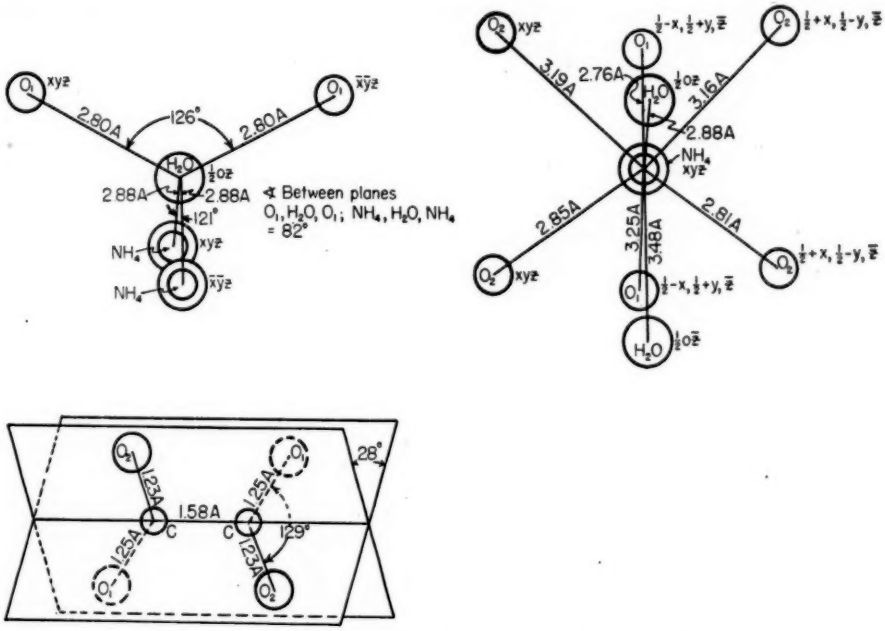

FIG. 2. The configuration of the oxalate group and the atomic surroundings of the water molecule and the ammonium ion in $(NH_4)_2C_2O_4 \cdot H_2O$.

hedrally surrounded by two NH_4^+ ions and two oxygen atoms, (O_1), having the higher value of σ. The minimum distances of approach NH_4-H_2O and H_2O-O_1 considerably exceed the value of 2.55A required for hydrogen bond formation, but the tetrahedral arrangement is in agreement with Bernal's and Fowler's[13] model of the water molecule. Ammonium ions too are tetrahedrally surrounded by two sets of oxygen atoms as shown in the figure. Interatomic distances for one set are near 2.80A and for the other near 3.20A.

The observation that the planes of the $O-C-O$ parts of the $C_2O_4^{--}$ group are at an angle of 28° to one another is particularly interesting since the group is a plane one in $H_2C_2O_4 \cdot 2H_2O$ and α and β $H_2C_2O_4$. Indeed it is the first instance yet encountered in crystal structure analysis where a group has different configurations in various salts. However, such a result is neither improbable nor unexpected due to the possibility of rotation about the $C-C$ single bond. The effect is similar to that which leads to the optical activity of diphenyl derivatives[14] as brought about by the steric effects of appropriate groups.

The separation of the carbon atoms in the $C_2O_4^{--}$ group, namely 1.58 ± 0.01A, considerably exceeds the value 1.54A found for the carbon to carbon distance in other aliphatic compounds that have been studied. This is possibly a result of repulsion between the negatively charged $(-CO_2^-)$ parts of the group.

Several comments should be made relative to previous work on oxalates. Structure analyses of $K_2C_2O_4 \cdot H_2O$, $Rb_2C_2O_4 \cdot H_2O$, KHC_2O_4 and $RbHC_2O_4$ were based on the assumption that the atoms of the $C_2O_4^{--}$ group were coplanar. Reconsideration of the data from the first two compounds shows that the CO_2 parts of a C_2O_4 group might be displaced by as much as 10° from a coplanar arrangement, the angle being $0° \pm 10°$. This does not seem to be probable for the other two salts but it is perhaps the factor that prevented a successful analysis of the structure of $NaHC_2O_4 \cdot H_2O$. Such a rotation of the CO_2 parts of the $C_2O_4^{--}$ group in ammonium oxalate monohydrate partially accounts for the departure of its optical properties from values predicted on the basis of a coplanar $C_2O_4^{--}$ group.

We are indebted to Lola S. Deming for aid in summing the various Fourier series.

[13] Bernal and Fowler, J. Chem. Phys. **1**, 515 (1933).
[14] See for instance R. Adams and H. C. Yuan, Chem. Rev. **12**, 261 (1933).

A Study of the Evaporation of Small Drops and of the Relationship Between Surface Tension and Curvature

J. L. SHERESHEFSKY AND SYLVIA STECKLER,[1] *Howard University, Washington, D. C.*

(Received November 12, 1935)

The rates of evaporation of *n*-dibutyl phthalate droplets ranging from 3μ to 0.5μ in radius were measured in a Hoag type of Millikan's oil-drop apparatus under different conditions of vapor pressures. The data obtained are interpreted in two ways. One interpretation is based on an equation derived from Fourier's equation of diffusion; the results thus obtained show that the surface tensions of the droplets decrease with increasing curvature. The other is based on an equation derived on the basis of an assumption of a vapor film surrounding the evaporating droplet; the results obtained here lead to the validation of Lord Kelvin's equation. An explanation is also given for the abnormally high values of surface tension obtained by Woodland and Mack.

THE capillary condensation hypothesis suggested by Zsigmondy[2] in explanation of adsorption in porous bodies prompted a number of scientific workers[3] to study the mechanism of the adsorption process by the application of the Kelvin[4] equation

$$\ln (P/P_0) = \pm 2\sigma V/RTr, \qquad (1)$$

where P/P_0 is the relative vapor pressure of a liquid surface of radius of curvature r with respect to a plane surface, V is the molar volume of the liquid, σ is the surface tension which is assumed to be independent of curvature,. and R and T have the usual significance. The sign of the right-hand term depends on whether the surface is concave or convex, the minus referring to liquids in capillaries and the plus to droplets.

The results of this application were rather perplexing, since in many instances[5] the calculated radii of the pores were less than the known diameters of the molecules of the adsorptive. On the other hand, Patrick[6] and co-workers extended the Zsigmondy hypothesis by assuming that the surface tension in small closed capillaries is increased because of a negative hydrostatic pressure in the surface, and were able to show the independence of the volume of adsorption from temperature and from the chemical nature of the adsorptive, thus showing the applicability of a modified Kelvin relationship.

In this connection, Shereshefsky,[7] studying the vapor pressure of water in small capillaries several μ in diameter, found the lowerings considerably greater than the corresponding values obtained from the Kelvin equation. These results were interpreted to indicate an increase in the surface tension,, and therefore the need for extending this relationship. However, Goodris and Kulikova,[8] in studying the evaporation of water droplets of radii approximately equal to those of the capillaries, found the Kelvin equation to hold.

Recently Woodland and Mack,[9] applying the same method in a study of the rate of evaporation of droplets of dibutyl phthalate and dibutyl tartrate, report exceedingly high values for the surface tensions of these substances when calculated with the aid of the Kelvin equation. These high values they seek to explain by assuming that the evaporating droplets are surrounded by a layer of vapor from 0.5μ to 0.6μ in thickness.

In view of these discordant results together with the high values of surface tension and the unlikely thickness of the vapor layer reported by the latter workers, we undertook this study of the Kelvin relationship.

[1] Part of thesis submitted in partial fulfillment for the degree of Master of Science in Chemistry at Howard University.

[2] Zsigmondy, Zeits. f. anorg. Chemie **71**, 356 (1911).

[3] Anderson, Zeits. f. physik. Chemie **88**, 191 (1914); Coolidge, J. Am. Chem. Soc. **46**, 596 (1924).

[4] Thomson, Phil. Mag. [4] **42**, 448 (1871).

[5] J. W. McBain, *The Sorption of Gases and Vapors by Solids* (George Routledge & Sons, London, 1932), p. 437.

[6] McGavack, Jr. and Patrick, J. Am. Chem. Soc. **42**, 946 (1920); Patrick and Greider, J. Phys. Chem. **29**, 1031 (1925); Patrick, Preston and Owens, J. Phys. Chem. **29**, 421 (1925); Patrick and Eberman, J. Phys. Chem. **29**, 220 (1925).

[7] Shereshefsky, J. Am. Chem. Soc. **50**, 2966 (1928).

[8] Goodris and Kulikova, J. Russ. Phys.-Chem. Soc., Phys. Part **56**, 167 (1924).

[9] Woodland and Mack, Jr., J. Am. Chem. Soc. **55**, 3149 (1933).

Apparatus and Method

Similar to Goodris and Kulikova[8] and Woodland and Mack[9] we studied the rate of evaporation of tiny liquid droplets by utilizing the method developed by Millikan[10] in the oil-drop experiment. It was also considered desirable first to obtain data that would lend themselves to direct comparison with the work of Woodland and Mack. For this reason the Hoag[11] modification of the oil-drop apparatus and droplets of *n*-butyl phthalate[12] were used in this preliminary investigation.

The set-up included an a.c. power supply unit[13] to furnish the required plate potentials, which could be varied in a continuous manner over a range of 0–850 volts. The output of the unit was stabilized with a voltage regulator[14] connected in series with the input. This arrangement reduced the fluctuations in the line to ± one percent.

Four series of experiments were carried out in which droplets ranging from 3.0 to 0.5μ in radius were studied. In one series droplets were allowed to evaporate in a condenser chamber saturated with dibutyl phthalate vapor. This condition was obtained by placing micro-boats containing the liquid in convenient positions in the condenser. In the second series the evaporation of a number of droplets was allowed to proceed under conditions in which the condenser chamber contained activated charcoal. In a third series of experiments the charcoal was replaced by small sheets of blotting paper which were placed against the upper and lower plates. In this connection it may be pointed out that the blotting paper had no dielectric properties and merely affected the distance between the plates. But as the ratio e/d, as evident from Eqs. (2) and (3) given in the following section, is determined by the measured values of V and m, an error in the value of d is of no consequence to the purposes of this investigation. In the latter two series the condenser was taken apart, cleaned, and fresh charcoal or blotting paper introduced for each droplet studied. In the fourth series similar measurements were carried out under reduced pressures. This necessitated a more complicated apparatus which will be described in a forthcoming paper.

[10] Millikan, Phys. Rev. **32**, 389 (1911); Millikan, *The Electron* (University of Chicago Press, 1917), p. 168.
[11] W. M. Welch Co., Chicago.
[12] Eastman Kodak Co., Rochester.
[13] G–M Laboratories, Chicago.
[14] Delta Manufacturing Co., Cambridge, Mass.

Results

As it is hardly possible to include in this paper all the data and calculations obtained for the large number of droplets investigated, we are presenting complete data for only two phthalate droplets; these were studied in a chamber containing blotting paper. They were chosen because of the relatively large change in their radii during the period of observation, as well as because they are approximately of the same radius as the phthalate particle reported by Woodland and Mack. A further reason for selecting them was the fact that they show considerable differences in the rate of evaporation at comparable radii.

The data for these droplets are contained in Tables I and II. The observed values are given

Table I. *Data of evaporation of droplet No. 20.* Temperature 21°C; No. of charges, 28; density, 1.051.

1	2	3	4	5	6
Time (min.)	Plate Potential (volts)	Tangent (volt/sec.)	Radius μ	Rate of Evapor. (g/sec. cm)	Rate of Evapor. (g/sec. cm²)
2	221.5	0.127	1.673	7.060×10^{-11}	3.358×10^{-8}
4	206.0	.125	1.634	7.125	3.470
8	176.4	.119	1.550	7.161	3.677
12	148.0	.114	1.463	7.240	3.939
16	122.0	.107	1.372	7.262	4.218
20	97.0	.101	1.270	7.368	4.616
24	73.5	.093	1.156	7.474	5.149
28	52.6	.084	1.036	7.565	5.809
32	34.0	.074	0.895	7.684	6.828
36	18.3	.062	.728	7.880	8.610

Table II. *Data of evaporation of droplet No. 22.* Temperature 21°C; No. of charges, 5; density, 1.051.

1	2	3	4	5	6
Time (min.)	Potential (volts)	Plate Tangent (volt/sec.)	Radius μ	Rate of Evapor. (g/sec. cm)	Rate of Evapor. (g/sec. cm²)
1	323	0.660	1.068	10.25×10^{-11}	7.63×10^{-8}
2	283	.660	1.022	10.72	8.35
3	245	.637	0.974	10.83	8.83
5	172	.568	.866	10.89	10.01
7	107	.508	.739	11.43	12.32
8	77	.462	.662	11.55	13.88
9	51	.405	.577	11.65	16.07
10	28	.334	.473	11.72	19.70

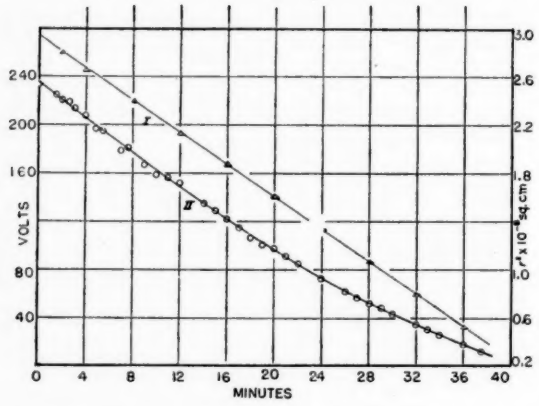

FIG. 1. The evaporation of droplet No. 20. Curve I—The time variation of the surface. Curve II—The variation of the plate potential with time.

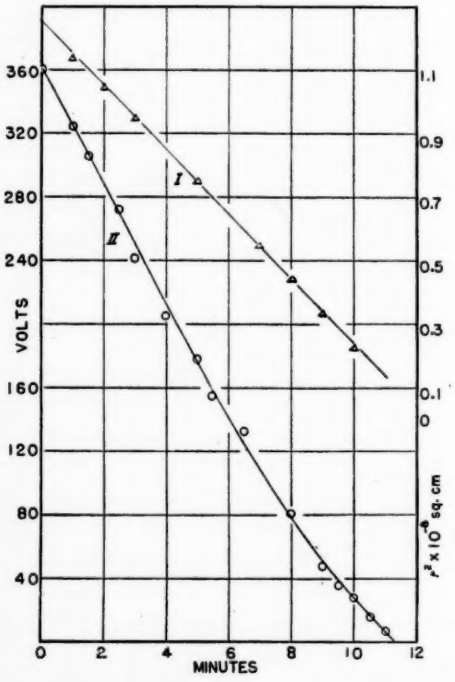

FIG. 2. The evaporation of droplet No. 22. Curve I—The time variation of the surface. Curve II—The variation of the plate potential with time.

in the first two columns; the values of the third column were obtained with a tangent meter from the voltage-time curves given in Figs. 1 and 2 drawn on a larger scale. The remaining columns were calculated from the first three by the application of the equations given below:

1. Stokes' law

$$v = 2gr^2\rho/9\eta, \tag{2}$$

where v is the rate of free fall, r is the radius of the droplet, ρ is the density of the liquid, and η is the viscosity of air.

2. The relationship between the electrical field, the charge and the mass of the droplet

$$Ve/d = mg = (4/3)\pi r^3 \rho g, \tag{3}$$

where V is the plate potential, d is the distance between the plates, e is the charge of the droplet, g is the acceleration constant, and m is the mass of the particle. In the fifth column are given the rates of evaporation expressed in grams per second per cm radius of droplet. In the sixth column are given the rates of evaporation in grams per second per sq. cm of surface of the droplet.

It is of importance to point out that differences in the rates of evaporation as appreciable as those shown in the above tables were obtained with the largest number of droplets studied in these experiments. Furthermore, these differences were observed both when the evaporation was taking place in a condenser saturated with phthalate vapor and when the condenser contained an adsorbing material. Thus droplets 1 and 2 in Table III evaporated presumably under equal environmental conditions, since the chamber in each instance was saturated with phthalate vapor; but the first droplet showed a rate of evaporation almost twice as large as the second, in spite of the fact that the former was a larger droplet. The same is also true of droplets 7 and 11 which were evaporating in a chamber containing charcoal, and of droplets 18 and 21 which were evaporating in a chamber containing sheets of blotting paper.

It was also observed that the rate of evaporation was affected by the relative number of droplets entering the condenser. This number, not easily controllable, varied widely from experiment to experiment, as it depended on the hand pressure applied to the rubber bulb of the atomizer and the relative direction of the nozzle with respect to the perforations in the upper plate of the condenser. When the number of the droplets thus introduced into the chamber was relatively large, the rate of evaporation of the

TABLE III. *Evaporation of droplets of n-butyl phthalate under various conditions.*

1 No. of Droplet	2 Length of Obs. (min.)	3 Initial Radius μ	4 Final Radius μ	5 Rate of Evapor. (g/radius) Initial	6 Final	7 Condition of Condenser	8 σ(calc.) (ergs/sq. cm)
1	26	1.33	1.28	0.643×10^{-11}	0.670×10^{-11}	Saturated	6.2×10^{3}
2	46	1.27	1.22	0.371	.388	Saturated	5.8
3	32	1.10	1.00	.860	.946	Saturated	5.1
4	30	0.92	0.85	.549	.595	Saturated	4.2
7	58	2.20	2.01	1.347	1.457	Charcoal	10.2
11	32	1.25	1.18	0.719	0.761	Charcoal	5.7
12	21	0.63	0.45	.951	1.331	Charcoal	2.7
18	30	2.66	1.80	17.120	18.230	Blotting paper	6.9–1.2
21	10.5	1.25	0.89	8.09	10.43	Blotting paper	6.0–3.5
Woodland & Mack	29.5	1.25	0.75	4.08	5.27	Charcoal	1.4–2.3

droplet under observation was generally slower, and *vice versa*.

It is therefore very likely that the apparent inconsistencies pointed out above are due to a variation in the degree of saturation of the chamber and of the adsorbing material. All the droplets, except the ones held for observation, whether charged or uncharged, fell to one or the other plate. While many of them in reaching the surface of the plates may have spread, a large fraction undoubtedly adhered in some modified droplet form, and caused a supersaturated atmosphere. It also explains why in the case of the blotting paper where all the droplets reaching the plates were absorbed the rate of evaporation was so much higher.

However, all droplets, each under its own environmental conditions, behaved consistently alike as evidenced by the linear time variation of the surface shown in curve 1, Figs. 1 and 2, where the square of the radius is plotted against the time.

Treatment of Results

Maxwell[15] pointed out that the rate of diffusion and the rate of heat conduction are equivalent processes and that mathematically analogous equations can be applied to both phenomena. Therefore, in a hollow sphere which is large in comparison with the droplet and which is lined with an absorbing medium, a droplet held in the center will evaporate as fast as the vapors are carried away by diffusion to the absorbing walls. As the conditions of the present experiments approximate this ideal arrangement, the radial flow of vapor from the droplet to the walls of the condenser may be described by the Fourier equation

$$d\rho/Ddt = d^2(r\rho)/rdr^2, \tag{4}$$

where D is the diffusion coefficient, ρ is the density of the vapor, and r is the radial distance from the center of the droplet.

Assuming that for short time intervals the densities of the vapor in the different parts of the system are constant, the above equation becomes

$$d^2(r\rho)/rdr^2 = 0, \tag{5}$$

which on integration gives equation

$$\rho = A + B/r, \tag{6}$$

where A and B are constants.

From this general equation relating the density of the vapor with the radial position, after introducing appropriate boundary conditions, there is obtained[16]

$$-dm/dt = -4\pi r^2 D d\rho/dr = 4\pi r_1 R_0 D(\rho_1 - \rho_0)/(R_0 - r_1), \tag{7}$$

where dm/dt is the rate of evaporation of the droplet, ρ_1 is the density of the vapor at the distance r_1 equal to the radius of the droplet, and ρ_0 is the density of the vapor at a distance R_0 equal to the radius of the hollow sphere.

When r_1 is small in comparison with R_0, Eq. (7) can be simplified to

[15] Maxwell, *Scientific Papers* (1890), Vol. II, p. 639.

[16] Ingersoll and Zobel, *Mathematical Theory of Heat Conduction* (Ginn and Company, 1913), p. 27.

$$-dm/dt=4\pi Dr_1(\rho_1-\rho_0), \quad (8)$$

which on assuming the vapor to obey the gas laws can be put into the form

$$-dm/dt=4\pi r_1 MD(p_1-p_0)/RT. \quad (9)$$

This equation, in which p_1 is the vapor pressure of the droplet, becomes identical with that derived by Langmuir,[17] when p_0 the vapor pressure of the absorbing medium is negligible with respect to p_1. Langmuir applied this equation to explain the results of Morse[18] who found the rates of evaporation of small iodine spheres to be proportional to the radius.

Assuming the droplet to be a perfect sphere, its mass m is given by

$$m=(4/3)\pi r^3\rho. \quad (10)$$

Neglecting the variation of the density with the radius and differentiating, we obtain

$$dm/dt=4\pi r^2\rho dr/dt=\tfrac{1}{2}r\rho dS/dt, \quad (11)$$

where S is the area of the droplet. Combining with Eq. (9), we obtain

$$-dS/dt=8\pi MD(p_1-p_0)/\rho RT. \quad (12)$$

This equation, first derived by Whytlaw-Gray and Whitaker[19] to explain results obtained by them in a study of the vapor pressure of small water droplets, is in agreement with the constant rate of change of surface also found in our experiments, as shown in Figs. 1 and 2.

In view of the appreciable effect of the vapor pressure of the absorbing medium upon the rate of evaporation of a droplet discussed in the preceding section, it is evident that p_0 in Eq. (9) cannot be assumed to be negligible, and that the rate of evaporation per unit radius, $(1/r_1)dm/dt$, is proportional to the difference (p_1-p_0) of the vapor pressures. This fact most likely explains why Woodland and Mack[9] in assuming the rate of evaporation per unit radius to be directly proportional to the vapor pressure of the droplet have obtained from the Kelvin equation abnormally high values of surface tension; also the equally high values shown in column 8 of Table III and in column 6 of Tables IV and V. There is, however, a difference in that our values unmistakably decrease with decrease in droplet size, while the values of Woodland and Mack show a tendency to vary in the opposite direction.

One method of testing the validity of the Kelvin equation is to calculate the absolute surface tension values corresponding to different droplet radii. As the application of this method to the available data is prevented by the lack of knowledge of p_0 in Eq. (9), it is possible to obtain evidence as to the constancy of σ from calculated relative values.

Putting Eq. (9) into the form

$$\Delta m_1=K_1(p_1-p_0), \quad (13)$$

where $\Delta m_1=(1/r_1)dm/dt$ and $K_1=4\pi MD/RT$, we obtain for the relative rate of evaporation per unit radius for two droplets of radii r_1 and r_2 the expression

$$\Delta m_2/\Delta m_1=(p_2-p_0)/(p_1-p_0). \quad (14)$$

Rearranging we get

$$p_2/p_1=\Delta m_2/\Delta m_1+p_0/p_1(1-\Delta m_2/\Delta m_1) \quad (15)$$

or in generalized form

$$p_n/p_1=\Delta m_n/\Delta m_1+p_0/p_1(1-\Delta m_n/\Delta m_1), \quad (16)$$

where the relative vapor pressure p_n/p_1 of the droplets of radii r_n and r_1 are expressed in terms of the measured quantities Δm and the constant but unknown quantity p_0/p_1.

Combining the Kelvin equation in the exponential form with Eq. (16) we obtain

$$e^{2\sigma V(1/r_n-1/r_1)/RT}=\Delta m_n/\Delta m_1+p_0/p_1(1-\Delta m_n/\Delta m_1). \quad (17)$$

It is evident that by taking an arbitrary value of σ, preferably the measured value, in Eq. (17) we should, if the surface tension is independent of curvature, obtain a constant value of p_0/p_1 for all values of r_n.

The application of this equation to the available data is shown in Tables IV and V. In column 3 of these tables are given the values of the left-hand member of the equation; in column 4 the values of $\Delta m_n/\Delta m_1$, and in column 7 the values of the ratio of the vapor pressure of the

[17] Langmuir, Phys. Rev. **12**, 368 (1918).
[18] Morse, Proc. Am. Acad. **45**, 362 (1910).
[19] Whytlaw-Gray and Whitaker, Proc. Leeds Phil. Soc., Sci. Part I (1926).

TABLE IV. *Surface tension and curvature. Droplet No. 20.*

1 Time (min.)	2 Radius (Obs.) μ	3 P_n/P_1 Relative v.p. (Kelvin)	4 Relative Rate of Evapor. (unit radius)	5 Relative Rate of Evapor. (unit surface)	6 σ calc. (ergs/sq. cm)	7 p_0/p_1	8 σ calc. (ergs/sq. cm)	9 p_0/p_1
2	1.673	1.00000	1.0000	1.0000	—	—	—	—
4	1.634	1.00010	1.0092	1.0334	3.05×10^3	0.9890	32.6	0.9970
8	1.550	1.00034	1.0143	1.0950	1.38	.9766	15.6	.9964
12	1.463	1.00061	1.0255	1.1730	1.34	.9758	15.0	.9965
16	1.372	1.00093	1.0286	1.2561	1.00	.9675	10.9	.9964
20	1.270	1.00134	1.0436	1.3746	1.04	.9693	11.7	.9964
24	1.156	1.00189	1.0584	1.5334	0.96	.9676	11.0	.9965
28	1.036	1.00260	1.0715	1.7299	.85	.9636	9.9	.9964
32	0.895	1.00368	1.0084	2.0334	.75	.9584	8.6	.9965
36	0.728	1.00550	1.1162	2.5640	.64	.9527	7.6	.9965

TABLE V. *Surface tension and curvature. Droplet No. 22.*

1 Time (min.)	2 Radius (obs.) μ	3 P_n/P_1 Relative v.p. (Kelvin)	4 Relative Rate of Evapor. (radius)	5 Relative Rate of Evapor. (surface)	6 σ calc. (ergs/sq. cm)	7 p_0/p_1	8 σ calc. (ergs/sq. cm)	9 p_0/p_1
1	1.068	1.00000	1.000	1.000	—	—	—	—
2	1.022	1.00064	1.047	1.095	5.04×10^3	0.995	32.6	0.9969
3	0.974	1.00154	1.057	1.147	2.80	.988	15.2	.9957
5	.866	1.00295	1.063	1.312	1.29	.977	6.3	.9951
7	.739	1.00406	1.113	1.614	1.18	.974	6.6	.9951
8	.662	1.00565	1.127	1.819	0.96	.969	4.8	.9951
9	.577	1.00766	1.137	2.107	.74	.960	4.1	.9949
10	.473	1.01621	1.143	2.583	.57	.947	3.0	.9952

absorbing medium and that of the droplet at its largest radius.

Since the vapor pressure of the absorbing medium is determined by the initial conditions of each experiment and is undoubtedly constant during the whole period of observation, the decreasing ratio p_0/p_1 is a definite indication of a decreasing value of σ with decreasing droplet size. The actual values of surface tension based on the assumption that the surface tension of the droplet at its largest radius was 32.6 ergs/sq. cm are given in column 8. They were obtained from Eq. (15) by using the first value of p_0/p_1 and calculating for σ. A similar tendency is also to be observed in the values of σ in column 6 obtained from the Kelvin equation on the basis of the erroneous assumption that $p_0=0$, that is, that $\Delta m_n/\Delta m_1=p_n/p_1$.

To explain the abnormally high values of σ they have obtained, Woodland and Mack postulated the presence of a layer of vapor surrounding the evaporating droplet. The thickness of this layer they calculate by applying Eq. (9) in which they neglect the term p_0. Following this method of calculation we obtain values for the thicknesses of the vapor layer considerably larger than theirs. Thus, as shown in Table VI

TABLE VI. *The thickness of vapor layer.*

Droplet No. 20			Droplet No. 22		
Radius (obs.) μ	Radius (calc.) μ	Thickness of Vapor Layer μ	Radius (obs.) μ	Radius (calc.) μ	Thickness of Vapor Layer μ
1.673	3.316	1.643	1.068	4.814	3.746
1.634	3.347	1.713	1.022	5.035	4.013
1.550	3.363	1.813	.974	5.087	4.113
1.463	3.401	1.938	.866	5.115	4.249
1.372	3.411	2.039	.739	5.367	4.628
1.270	3.461	2.191	.662	5.425	4.763
1.156	3.510	2.354	.577	5.472	4.895
1.036	3.553	2.517	.473	5.505	5.032
0.895	3.609	2.714			
0.728	3.701	2.973			

the values for droplet 20 increase from one to four times the radius of the droplet, and for droplet 22 the thicknesses are even greater. It seems hardly plausible, in view of the mean free path under the present experimental conditions being about 0.01μ, that the postulated saturated

layer should exceed so considerably this value. This is also borne out by the agreement between our observations and Eq. (12). This equation as shown above was derived from Eq. (9) in which r_1, on the assumption of a vapor layer, stands for the radius of the evaporating vapor sphere, and from Eq. (11) in which r stands for the observed radius of the liquid droplet. From this it is seen that the agreement of the observed rate of change of surface with theory is possible either on the assumption that the ratio r_1/r is constant but larger than one, or that $r_1=r$. The first assumption must be ruled out, since as pointed out above the ratio r_1/r constantly increases with decreasing r; it therefore follows that within the experimental error the radii of the liquid droplet and of the vapor sphere coincide, and that the possible difference between r_1 and r does not exceed 0.02μ. However, it is possible that the value of 3.1×10^{-6} mm for p_1 used in these calculations is too small, as indicated by the extrapolated value of 7.8×10^{-5} mm obtained from the vapor pressure measurements of Hickman.[20] On the other hand, it is obvious that for droplet 7 in Table III we would obtain negative values for the thickness of the vapor layer.

Though the values for the thickness of the layer are too large to be accepted as evidence, there are other indications pointing to the possible correctness of the vapor-layer idea. One such indication is the constant rate of change of surface exhibited by the droplets in these experiments. As evident from Eq. (12) this behavior requires that (p_1-p_0) be constant; and, therefore, that p_1, the vapor pressure of the evaporating droplet, be constant during the whole period of observation. This condition would seem possible in the light of the Kelvin relationship if the droplet at a certain distance from it is surrounded by a vapor film of constant pressure.

Let us assume that this film is within one mean free path from the surface of the droplet. In the region between the film and the surface of the droplet the number of molecules of vapor per cc is given by $N=\bar{N}p_1/RT$, where $\bar{N}$ is Avogadro's number and p_1 is the vapor pressure of the droplet. Of these molecules moving with the velocity u, 1/6 will be directed towards the film. The number of molecules that will pass in time dt an element of area $dxdy$ in the plane of the film is

$$N'=(1/6)dxdyudt\bar{N}p_1/RT. \qquad (18a)$$

Similarly, the number of vapor molecules passing $dxdy$ from a region of thickness udt adjacent to the other side of the film is

$$N''=(1/6)dxdyudt\bar{N}p_0/RT, \qquad (18b)$$

where p_0 is the partial pressure of the vapor in this region. The net transfer of molecules through the element $dxdy$ in the film is

$$N_1=(1/6)dxdyudt\bar{N}(p_1-p_0)/RT,$$

and the mass transferred is

$$w_1=(1/6)dxdyudtM(p_1-p_0)/RT, \qquad (19)$$

where M is the molecular weight of the vapor. This net transfer represents the mass which escapes the region between the droplet and the film and which diffuses to the walls of the vessel. The rate of evaporation per sq. cm is therefore

$$\Delta m_1=(2M/9\pi RT)^{\frac{1}{2}}(p_1-p_0), \qquad (20)$$

since $u=(8RT/\pi M)^{\frac{1}{2}}$. For simplicity and similar to Eq. (13) it can be written in the form

$$\Delta m_1=K_2(p_1-p_0). \qquad (21)$$

There is one important distinction between this equation and Eq. (13). In the latter Δm_1 is the rate of evaporation per unit radius, while here it represents the rate per unit area.

Relating the rate of evaporation of a droplet of radius r_n and of vapor pressure p_n to that of a droplet of radius r_1 and of vapor pressure p_1, we obtained an expression equal in form to Eq. (16). Then combining it with the Kelvin equation we obtain an expression which is analogous to Eq. (17), and which equally allows the evaluation of the variation of surface tension with curvature.

The results obtained in following the same method of calculations as in the case of the diffusion equation are presented in Tables I, II, IV and V. In the sixth column of Tables I and II observed rates of evaporation expressed in

[20] Hickman, J. Phys. Chem. **34**, 627 (1930).

grams per second per sq. cm are given. In the fifth column of Tables IV and V are given the relative rates of evaporation per sq. cm, and in the ninth column of the same tables the values of p_0/p_1. It is to be observed that the values of p_0/p_1 are constant to a remarkable degree, the maximum deviation being in Table IV about 0.06 percent and in Table V about 0.2 percent, and the deviation from the average being 0.04 and 0.15 percent, respectively. If we were to exclude in each table the first value of this ratio corresponding to time intervals in which the steady state was probably not yet established, the deviations from the average would be reduced to about 0.01 percent in the case of both droplets. This fact seems therefore to indicate the validity of the Kelvin relationship for droplets ranging in size from 1.67μ to 0.47μ; and since there is no reason to suspect any different behavior for droplets larger than 1.67μ, the Kelvin equation seems to hold for all droplet sizes down to 0.5μ, and most likely also for radii reasonably smaller.

The contradictory results obtained from these two interpretations of the process of evaporation of liquid spheres are not at all surprising. If there is no discontinuity at the surface of the evaporating droplet, in the sense that the density gradient varies continuously from the surface of the liquid down to the absorbent, then the assumption of a vapor film or vapor layer around the droplet together with the conclusion based upon this assumption are erroneous. On the other hand, if the idea of a film of vapor or an equivalent form of discontinuity is correct, then Eq. (17) and the conclusions based upon it are not valid, since the Kelvin equation in the present form is not applicable to vapor spheres. In this connection it is worth pointing out that for a similar reason there is a serious objection to the use of the Kelvin equation for the calculation of surface tensions of solids from evaporation measurements.

On theoretical grounds there is little reason to suspect that in microscopic droplets surface forces would extend beyond a distance of a few molecular layers. However, there are numerous investigations recorded in the literature in which evidence of surface forces acting through relatively great distances is presented. For instance, Trillat[21] and Perrin[22] from x-ray measurements and Taylor[23] from measurements of the index of refraction on liquid films find evidence pointing to a possible orientation extending through a relatively large number of molecular diameters. Derjaguin[24] reaches similar conclusions from measurements of the resistance to the movement of an oscillating lens presented by water surfaces.

The distances through which the surface forces are reported to act are of the same order of magnitude as the diameters of the droplets in the present experiments. Unfortunately, it was not possible from our data to determine whether the range of action of the surface forces of the droplets was equally great, since we were only able to obtain relative values of the surface tensions. However, the decreasing surface tension with increasing curvature obtained on the basis of one of the mechanisms of evaporation discussed above can only be explained[25] on the assumption that the surface forces of the droplets extend through distances equally great as those reported by other investigators. But to establish this it would be necessary to determine first which of the mechanisms represents the process of evaporation of tiny droplets.

---

[21] Trillat, Comptes rendus **180**, 1839 (1935).
[22] Perrin, Kolloid Zeits. **51**, 2 (1930).
[23] Taylor, J. Opt. Soc. Am. **23**, 309 (1933).
[24] Derjaguin, Zeits. f. Physik **84**, 657 (1933).
[25] The effect of electrification on surface tension was shown by J. J. Thomson in *Application of Dynamics to Physics and Chemistry* (Macmillan and Company, 1888), p. 165, to be negligible. Nor is it likely that contamination of the surface is responsible for the effect observed, since the surface tensions of substances considered to be contaminants and of the liquid are nearly alike, and high concentrations would have to be assumed to approach quantitatively anywhere near the lowerings observed.

The Thermal Decomposition of Divinyl Ether

H. AUSTIN TAYLOR, *New York University, University Heights*

(Received October 31, 1935)

The thermal decomposition of divinyl ether has been studied at temperatures between 460° and 500°C, and at pressures from 30 to 1000 mm. That the reaction has a chain mechanism, chains being broken on the walls at low pressure and in the gas phase at high pressure, is concluded from the effects of (a) increased surface, (b) added nitrogen (c) varying temperature coefficient with pressure and (d) induced decomposition with azomethane. The over-all order at high pressure is three-halves judged both from the individual velocity constants during a run and from the variation of velocity constant with pressure.

THE thermal decomposition of numerous relatively complex organic compounds has been shown to proceed with an over-all first order rate. This has been satisfactorily accounted for by the free radical chain theory in many instances for which experimental data are available; a treatment confirmed by a specific rate enhancement upon introduction of free radicals either thermally or photochemically. The theoretical treatment of certain reactions however from this point of view is not without difficulty and rival theories must not be overlooked. The ethers constitute a series, the decompositions of which seem undoubtedly to follow a chain mechanism, and analysis of the chain steps has furnished indirect evaluations of the activation energies of various radical-molecule reactions. Divinyl ether being unsaturated might be expected to furnish additional evidence for or against the free radical mechanism as a general scheme for ether decompositions. This choice would seem particularly interesting since from the point of view of a direct decomposition into product molecules the reaction would appear to be very simple. The prevalent view of ether decomposition prior to the chain mechanism suggestion, considered the possibility of a hydrogen transfer across the oxygen in the ether molecule followed by rupture to yield a hydrocarbon and an unstable residue which subsequently decomposed. Thus for methyl ether the hydrogen transfer would yield methane and formaldehyde. The parallel for divinyl ether would suggest the formation of ethylene and ketene, the latter in turn yielding ethylene and carbon monoxide. If the reaction were to proceed at temperatures below which ethylene polymerizes and decomposes, the products expected would be very simple and the reaction kinetics therefore easier of interpretation even than those of the saturated ether. Such a procedure, however, is not found. On the contrary the complexity appears to be even greater. Evidence is presented that the reaction has a chain mechanism and from a theoretical point of view at least will be equally as complex as diethyl ether in the contingency of multiple interacting chains with possibly doubtful establishment of a steady state.

EXPERIMENTAL

The divinyl ether employed was a Merck product obtained through the courtesy of Dr. Major to whom thanks are due. It was furnished containing one-hundredth of a percent of an oxidation inhibitor and for the first series of experiments was distilled from this. The boiling point was 28.3°C in agreement with that found by Miles and Menzies.[1] Subsequent experiments were performed with the sample direct without further purification with no change in the decomposition rates. This is to be expected in view of the nonvolatility of the inhibitor present. It may be well to remark at this stage that polymerization of the liquid ether was observed on a few occasions but in all such cases oxygen may have been present. The liquid under its own vapor pressure alone showed no tendency to polymerize and the vapor maintained for long periods of time at temperatures where decomposition was just too slow to measure showed no volume decrease.

[1] Miles and Menzies, J. Phys. Chem. **37**, 425 (1933).

The experimental procedure was similar to that previously reported for static studies from this laboratory. The reaction vessel of Pyrex glass was about 250 cc capacity. During an attempt to find a limiting rate at high pressure condensation of some product of the reaction in the capillaries outside the furnace necessitated an auxiliary heating of these to about 80°C. In the lower pressure range this was not found necessary.

To investigate the products of decomposition several dynamic experiments were made. The ether vapor was forced through a small capillary under constant pressure, thence through a furnace, by varying the temperature of which the products corresponding to more or less reaction as desired could be found.

Results and Discussion

The results of a typical static experiment in the early stages are given in Table I.

Table I. *Initial Pressure 339 mm; temperature 500°C.*

Time (min.)	Pressure Change	k_{uni} (sec.$^{-1}$)	k_{bi} (sec.$^{-1}$)
1	48	2.54×10^{-3}	8.11×10^{-6}
2	87	2.47	8.49
3	119	2.40	8.86
4	147	2.37	9.41
5	169	2.30	9.78
6	187	2.23	10.1
7	201	2.14	10.2
8	216	2.11	10.8
10	237	2.00	11.4
12	252	1.89	11.9

The endpoint of the reaction appeared to be somewhat erratic varying between 1.05 and 1.24 for the ratio of pressure change to initial pressure. No systematic variation with temperature was found though the higher the initial pressure the greater in general was the endpoint ratio. In Table I, are included the values of the unimolecular and bimolecular velocity constants calculated in the usual way but assuming an endpoint ratio of unity; the time unit is the second, the concentration unit in k_{bi} being the pressure directly observed in mm mercury. Since only the relative variation is required this is satisfactory. It will be observed that k_{uni} decreases whilst k_{bi} increases, the latter somewhat more rapidly than the former. The over-all order during a run is thus between one and two. For comparison of results at different pressures and temperatures use has therefore been made of the extrapolated first order constant obtained graphically from the pressure-time ratios in the early stages. This at least may be expected to give a more nearly true initial decomposition rate of the pure substance even when the products of reaction do affect the rate, than any other simple method.

Table II contains these data for the various pressures and temperatures studied. Numerous other experiments were made at lower pressures down to about one mm. In all these cases, however, a marked induction period was ob-

Table II.

Initial Pressure (mm)	$k\times10^4$ (sec.$^{-1}$)	Initial Pressure (mm)	$k\times10^4$ (sec.$^{-1}$)
460°C		480°C	
18	1.48	33	4.04
26.5	1.57	60	4.86
45	1.85	98	6.30
65	2.10	126	7.94
77	2.16	167	7.98
83	2.41	199	8.79
103	2.90	353	10.9
170	3.49	377	11.5
210	3.77	475	13.0
302	4.14	561	13.7
417	4.40	691	14.7
520	4.81	817	15.3
702	5.22	977	17.1
891	5.61		
1008	5.95	490°C	
1050	6.03	19	5.25
470°C		35	6.21
19	2.19	60	8.05
27	2.47	101	9.57
54.5	3.06	112	11.2
94	3.52	183	13.7
143	4.65	260	16.0
198	5.89	358	18.2
327	6.63	401	18.7
421	7.52	738	22.6
551	7.86	871	23.9
637	8.63	942	26.5
760	9.21		
1056	10.1		
500°C		470°C added surface	
22	7.58		
30	8.33		
57	11.7	39	1.92
102	15.4	89	2.53
110	16.1	133	3.01
204	20.4	288	5.06
339	26.1	474	6.74
439	28.3		
491	28.5		
587	31.5		
762	36.1		
928	39.9		

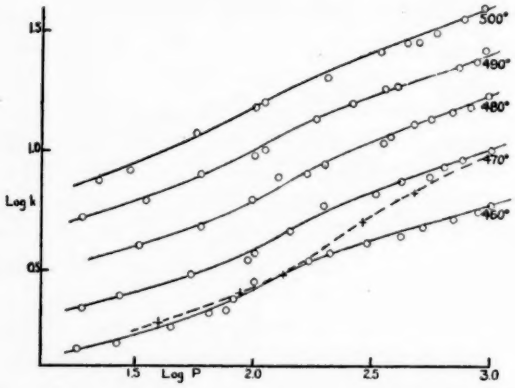

FIG. 1. Curves showing the variation of initial reaction rate with pressure at 460°, 470°, 480°, 490° and 500°C.

servable, greater at lower temperatures. The data are not included even though the slope of the pressure-time curve after the induction period would seem to fall well on the log k − log p plot. Experience with several reactions with induction periods has shown that such agreement is frequently fortuitous and always misleading.

The above data are plotted in the figure, the resulting curves being reminiscent of the type found in diethyl ether and propylamine[2] but not at all like those to be expected for a simple unimolecular reaction which would be concave downwards. There does seem to be evidence that the curves are becoming concave downwards at the highest pressures measured though the rate of approach to a limit is too slow to justify any extrapolation. At the lowest pressures studied too, there does not appear to be any indication of a limiting value. The average slope of the curves is about 1/3 corresponding to a 4/3 order and at the highest pressures the slope is 1/2, that is the reaction is 3/2 order.

The effect of added surface is shown in Fig. 1 by the dotted curve. The reaction vessel was filled with short lengths of 5-mm tubing, the ends being fire-polished, whereby the calculated surface to volume ratio was increased 3.5 times. At the highest pressures the effect is very small but in the lowest pressure range the rate is decreased to an extent approximately equivalent to a decrease of ten degrees in temperature. This fact alone is suggestive of a chain mechanism for the reaction.

[2] O. K. Rice and D. V. Sickman, J. Am. Chem. Soc. **56**, 1444 (1934); **57**, 22 (1935).

Table III contains the data obtained in a study of the effect of various gases added to the system. The gas labeled products was simply the residue after some divinyl ether had completely decomposed. An examination of these data shows that the effect of added gases is in general to reduce the rate of reaction. With the exception of hydrogen there is no reason to suspect from the results that specific chemical action was occurring in any case. With hydrogen, although the initial rate was the same as that for the ether alone the pressure-time curve reached its endpoint sooner yielding a value 0.9 as compared with 1.1 to 1.2 as previously mentioned. It seems likely that this reduction of the endpoint ratio, is due to hydrogenation of unsaturated bodies shown later to be present. This does not absolutely preclude of course the possibility that chemical action might have occurred for example with the products even though the endpoint is apparently unchanged. Thus the ratio for 100 mm ether alone at 500°C was 1.12 and for 112 mm ether in presence of 112 mm of product was also 1.12. The point is mentioned because the effect of products in reducing the initial rate of decomposition seems considerably greater in the lower ether pressure range than is found for example with the more probably inert gas nitrogen. Since ethylene and carbon monoxide are among the products their effects were tested separately but showed no such marked reduction of the rate as did the products. When a sufficiently large excess of ethylene was used a

TABLE III.

ETHER PRESSURE (mm)	ADDED GAS PRESSURE (mm)	T°C	$k \times 10^4$ (sec.$^{-1}$)
110	None	500	16.1
112	Products, 112	500	12.7
116	Products, 240	500	10.1
103	Products, 350	500	8.15
100	Nitrogen, 100	500	16.3
200	None	470	5.50
200	Nitrogen, 204	470	5.42
344	None	470	6.92
344	Nitrogen, 153	470	6.05
464	None	470	7.76
464	Nitrogen, 100	470	6.83
111	Hydrogen, 99	500	16.1*
102	Ethylene, 96	500	16.3
109	Ethylene, 202	500	15.0
103	Carbon Monoxide, 104	500	16.2

* Endpoint reduced to 0.9.

relatively small rate reduction was observed. The results for nitrogen are particularly illuminating. For pressures of the ether around 100 to 200 mm even twice that amount of nitrogen has a relatively small effect. At higher ether pressures a considerably smaller amount of nitrogen causes a marked reduction in the initial decomposition rate. Now it is precisely in this higher range of ether pressures that the effect of surface is least, hence that the reaction is a chain reaction, chains being broken on the walls at lower pressures and in the gas phase at higher pressures would seem a possible explanation. It would thus appear possible that the curves shown in the figure are complex, the one showing the variation with pressure of the over-all rate of reaction heterogeneously terminated, the other homogeneously. The apparent inflection should then correspond to a pressure at which the homogeneous and heterogeneous effects become approximately equal. It would be interesting to study the reaction in presence of very extensive surfaces at considerably higher pressure and also in large volume with a correspondingly small surface at lower pressure, to give an idea of the variation of the heterogeneous and homogeneous effects over a larger pressure range. The indication herein is that the log k − log p plot is concave upwards for the heterogeneous effect and the reverse for the homogeneous. The former is explicable on the basis of increasing saturation of the surface for deactivation or chain breaking; the latter since the over-all order is less than two whereas deactivating or chain-breaking collisions are presumably bimolecular.

An examination of the figure shows that the log k − log p plots for the different temperatures are not parallel but approach each other in the low pressure range and diverge from each other at higher pressures. This is tantamount to saying that the energy of activation increases with increasing pressure. Thus it is found that around 30 mm pressure the mean energy of activation, calculated from the curves for the different temperatures at constant pressure, is 47,000 calories; at 100 mm it is 50,000 whilst at 300 mm, 51,000 calories. Such a variation is outside the limits of experimental error, which should not be more than 1000 calories, and would be inexplicable for a simple reaction. In a chain of reactions with the possibility of more than one chain carrier such a variation is at least explicable if not in fact to be expected.

In an effort to determine the products of the reaction a small amount of the liquid divinyl ether was sealed in a small bomb and completely decomposed at 450°C. The resulting gases were then analyzed. The bomb after the decomposition was dark brown in color but showed no signs of free carbon. A few drops of a colorless liquid were present which possessed an odor suggesting a paraffin hydrocarbon which volatilized around 70°C. A C−H balance from the gas analyses gave an end product with the formula $CH_{1.5}$. The data for the analyses are given in Table IV. Included in the table are the analyses

TABLE IV.

	Complete Decomposition (Percent)	Partial Decomposition 450	475	500°C
CO	60.3	89.6	89.0	86.4
C_2H_2	1.6	1.5	1.4	1.6
C_2H_4	7.1	2.9	3.3	3.0
CH_4	17.1	3.8	4.0	5.0
C_2H_6	13.9	2.2	2.2	3.9

made in the dynamic experiments by the method outlined above. The effluent gases from the furnace were bubbled through water to remove soluble products including unchanged ether, the gases in the above analyses being collected over water. The presence of ketene in the effluent gas was demonstrated by treatment with alkali and subsequent identification of acetic acid. The multiplicity of products renders a complete systematization of mechanism extremely difficult. However even a cursory review of the possibilities of chain reactions in this decomposition will indicate the complexities to be expected.

There is very little evidence to indicate definitely what types of disruptions may be expected in a molecule as unsaturated as divinyl ether. The only apparent rule relative to unsaturated compounds[3] is that with a doubly bound carbon atom, the alpha-bonds are stronger than normal whereas the beta-bonds are weaker. Actually in divinyl ether there are no beta-bonds

[3] F. O. Rice and K. K. Rice, *Aliphatic Free Radicals* (Johns Hopkins Press, 1935).

unless the C−O bonds may be considered as beta to the farther double bond. It would seem probable though that the ether linkages would be slightly weaker in this case than for the saturated ethers and hence the primary break would certainly occur there. Beyond that there is little precedent to indicate the relative strengths of the remaining bonds. The following equations summarize the majority of the more obvious possibilities.

$$CH_2 : CH-O-CH : CH_2 \rightarrow CH_2 : CHO + CH_2 : CH$$
$$CH_2 : CH + CH_2 : CH-O-CH : CH_2 \rightarrow CH_2 : CH_2 + CH_2 : COCH : CH_2$$
$$CH_2 : CH + CH_2 : CH-O-CH : CH_2 \rightarrow CH_2 : CH_2 + CH : CH-O-CH : CH_2$$
$$CH_2 : COCH : CH_2 \rightarrow CH_2 : CO + CH_2 : CH$$
$$CH : CH-O-CH : CH_2 \rightarrow CH \vdots CH + CH_2 : CHO$$
$$CH_2CHO \rightarrow CH_3 + CO$$
$$CH_3 + CH_2 : CH-O-CH : CH_2 \rightarrow CH_4 + CH_2 : COCH : CH_2$$
$$CH_3 + CH_2 : CH-O-CH : CH_2 \rightarrow CH_4 + CH : CH-O-CH : CH_2$$
$$2CH_2 : CH \rightarrow C_4H_6$$
$$2CH_3 \rightarrow C_2H_6$$
$$CH_3 + CH_2 : CH \rightarrow CH_4 + CH \vdots CH$$

There is therefore a high probability of at least two distinct chain carriers with the possibility of two alternative modes of reaction of each, one of which regenerates itself whilst the other regenerates the second carrier. The two schemes are therefore considerably interlocked and judicious assumptions could easily account at least qualitatively for a variation of reaction order and a variation of energy of activation with pressure. Furthermore, as numerous efforts, which find no place here, have shown, judicious choice from among the above can give a three-halves order reaction rate which in most cases corresponds to an over-all activation energy around 50,000 calories as observed. It seems useless to be more specific at the present time until further evidence is forthcoming.

It should be remarked in passing that the presence in quantity of acetylene and butadiene in the final products should not be expected since decomposition of the former sets in markedly around 500°C, of the latter below 400°C, whilst polymerization of acetylene could account for the presence of condensable products observed in the high pressure runs. Moreover it should not be overlooked that addition reactions as well as polymerizations are possible in a system as unsaturated as that of vinyl ether and its products, though it is doubtful if they are likely to any appreciable extent under the temperature conditions used herein.

The most hopeful indication of further evidence seems to be forthcoming from work now in progress in this laboratory by F. P. Jahn on the decomposition of divinyl ether induced thermally by azomethane. The reaction proceeds quite rapidly at 330°C with less than ten percent of azomethane. The over-all order is about three-halves though a resolution of this into the separate orders relative to the ether and azomethane alone has not yet been made. It is not certain that the induced reaction is identical with the decomposition here studied; a lower endpoint signifies a difference. Such a difference may however actually afford a means of distinguishing between the many possible chains suggested.

I. Calculation of Energy of H_3 Molecule

J. HIRSCHFELDER, H. EYRING AND N. ROSEN, *Frick Chemical Laboratory of Princeton University and the Institute for Advanced Study*

(Received November 22, 1935)

The potential energies for linear symmetrical configurations of the triatomic hydrogen molecule have been calculated by the variational method with hydrogen-like 1*s* atomic orbitals by varying the "effective charge" and the amount of all polar and homopolar states in the eigenfunction. The lowest energies (in kcal./mole = 1/23.06 ev) and corresponding separations between neighboring atoms (in Bohr radii) are given in the table. The activation energies are for the reaction $H+H_2 \rightarrow H_2+H$, and are calculated with the same type of approximation for H_2 and H_3. All of the difficult three-center integrals for the repulsions between pairs of electrons were calculated explicitly in ellipsoidal coordinates without the use of infinite series.

	Heitler-London	H.L. plus Polar	Wang	Wang plus Polar	Experiment
$E_{H_3}-3EH$	−53.11	−60.39	−56.16	−67.09	−103.
r_{H_3}	2.00	2.00	1.89	1.84	
Act. Energy	19.07	13.63	30.68	25.15	7.

INTRODUCTION

THE simplest triatomic systems are those formed from three hydrogen nuclei. The neutral triatomic molecule is of particular interest since it is the intermediate in reactions of the type

$$D+H_2 \rightarrow DHH \rightarrow DH+H \qquad (1)$$

and also in the ortho-para hydrogen conversion.

Various approximations for the energy have been considered for H_3. London[1] proposed to use hydrogen atomic orbitals and to neglect all but the diatomic Coulombic and exchange integrals. This led to values for H_3 very much too high as is known by comparison with experiment and certain of the terms neglected are of the same order of magnitude as those which are retained. Coolidge and James[2] have calculated the energy for a single configuration of the linear symmetric H_3 molecule using hydrogen atomic orbitals to form the lowest homopolar state. Their particular configuration gives an energy more than a half volt higher than they would have obtained for a somewhat larger interatomic distance. A discussion of the criticism of James and Coolidge of the semi-empirical method of calculating activation energies will be given in a forthcoming paper in the light of this work and the results of the method itself.

In the present paper the variational method for the energy is carried through for all the linear symmetric configurations using hydrogen-like atomic orbitals (of the 1*s* type) to form the four following eigenfunctions:

(a) the best homopolar function.

(b) the best linear combination of polar and homopolar functions.

(c) the eigenfunction of (a) with the "effective charge" varied to give the lowest energy.

(d) the eigenfunction of the type in (b) obtained by simultaneous variation of the screening constant and the polar-homopolar composition.

II. THE ENERGY OF THE TRIATOMIC HYDROGEN MOLECULE

All of the integrals used in the calculation of the energy of the triatomic hydrogen molecule are defined and discussed in the appendix. The Hamiltonian operator for the electronic energy is:

$$H=H_A+H_B+H_C+H_D, \qquad (2)$$

where

$$H_A=-(h^2/8\pi^2m)[\nabla_1^2+\nabla_2^2+\nabla_3^2]$$

$$=\text{kinetic energy of the electrons,}$$

$$H_B=e^2[r_{ab}^{-1}+r_{ac}^{-1}+r_{bc}^{-1}]$$

$$=\text{energy of mutual repulsions of nuclei,}$$

$$H_C=-e^2\sum_{i=1}^{3}[r_{ai}^{-1}+r_{bi}^{-1}+r_{ci}^{-1}]$$

$$=\text{energy of attraction of electrons to the nuclei,}$$

$$H_D=e^2[r_{12}^{-1}+r_{13}^{-1}+r_{23}^{-1}]$$

$$=\text{energy of mutual repulsions of electrons.}$$

[1] F. London, Zeits. f. Physik **46**, 455 (1928); **50**, 24 (1928).

[2] A. S. Coolidge and H. M. James, J. Chem. Phys. **2**, 811 (1934).

Here a, b and c are atoms arranged in the symmetrical linear configuration with b the central atom. The distance between neighboring atoms is Ra_0 ($a_0=0.528$ Angstrom, i.e., the radius of the first Bohr orbit for atomic hydrogen). The electrons are denoted by 1, 2, and 3. r_{ij} is the distance between the ith and jth particle. The calculated energy for the molecule is given as:

$$E=\int\int\int \Psi^* H\Psi d\tau_1 d\tau_2 d\tau_3 / \int\int\int \Psi^*\Psi d\tau_1 d\tau_2 d\tau_3. \quad (3)$$

By the variational principle E is the actual energy of the molecule when Ψ is really an eigenfunction of H, and E is greater than the lowest energy of the molecule when Ψ is only an approximate eigenfunction. In this treatment we obtain the energy using various types of approximate eigenfunctions built from the $1s$ hydrogenic atomic orbitals:

$$a(1)=(z^3/\pi)^{\frac{1}{2}}e^{-zr_{a1}}, \quad b(1)=(z^3/\pi)^{\frac{1}{2}}e^{-zr_{b1}}, \quad c(1)=(z^3/\pi)^{\frac{1}{2}}e^{-zr_{c1}}, \quad (4)$$

where z is the "effective nuclear charge." These eigenfunctions must be antisymmetric with respect to an interchange of any two electrons because of the Pauli exclusion principle. Without loss of generality they are taken as eigenfunctions for S^2 and S_z, the square and the z component of the total spin, respectively; the lowest energy usually corresponds to the lowest allowed value of S^2. The fact that H is symmetric with respect to an interchange of atoms a and c, allows the eigenfunctions to be separated into symmetric and antisymmetric functions with respect to this interchange, and the two types of functions are noncombining. In the London approximation, i.e., where the multiple exchange and overlap integrals are neglected, it is easy to show that the antisymmetric eigenfunctions correspond to the states of lowest energy. This is also found to be the case in the present calculation.

1. The Heitler-London approximation

The simplest form of eigenfunction which we can take for the triatomic hydrogen molecule corresponds to a pure homopolar state with $z=1$. This eigenfunction is the three-atom analog of that used by Heitler and London[3] (H.L.) for the normal diatomic hydrogen molecule, and we should expect the energy obtained in this manner for the triatomic molecule to be of the same order of accuracy. There are two eigenfunctions of this type which can be formed: ψ_5 is symmetric with respect to an interchange of atoms a and c and corresponds to the bond $a-c$; ψ_1 is antisymmetric in this respect and corresponds to a bond between a and b alternating with a bond between b and c. With the abbreviated notation:

$$\begin{pmatrix} a & b & c \\ \alpha & \beta & \alpha \end{pmatrix} = (3!)^{-\frac{1}{2}} \begin{vmatrix} a(1)\alpha(1) & b(1)\beta(1) & c(1)\alpha(1) \\ a(2)\alpha(2) & b(2)\beta(2) & c(2)\alpha(2) \\ a(3)\alpha(3) & b(3)\beta(3) & c(3)\alpha(3) \end{vmatrix}, \quad (5)$$

where $\alpha(1)$ and $\beta(1)$ are spin functions of electron 1 which are eigenfunctions, respectively, for $S_{z1}=\frac{1}{2}h/2\pi$, $-\frac{1}{2}h/2\pi$.

$$\psi_1 = 2\begin{pmatrix} a & b & c \\ \alpha & \beta & \alpha \end{pmatrix} - \begin{pmatrix} a & b & c \\ \beta & \alpha & \alpha \end{pmatrix} - \begin{pmatrix} a & b & c \\ \alpha & \alpha & \beta \end{pmatrix}, \quad (6)$$

$$\psi_5 = \begin{pmatrix} a & b & c \\ \alpha & \alpha & \beta \end{pmatrix} - \begin{pmatrix} a & b & c \\ \beta & \alpha & \alpha \end{pmatrix}. \quad (7)$$

These correspond to the electronic energies:

$$E_{11}=\frac{\int\int\int \psi_1 H\psi_1 d\tau_1 d\tau_2 d\tau_3}{\int\int\int \psi_1\psi_1 d\tau_1 d\tau_2 d\tau_3} = \frac{a^2b^2c^2+a^2bcbc-b^2acac-abbcac}{1+I_{00}^2(R)-I_{00}^2(2R)-I_{00}(2R)I_{00}^2(R)}, \quad (8)$$

$$E_{55}=\frac{\int\int\int \psi_5 H\psi_5 d\tau_1 d\tau_2 d\tau_3}{\int\int\int \psi_5\psi_5 d\tau_1 d\tau_2 d\tau_3} = \frac{a^2b^2c^2+b^2acac-a^2bcbc-abbcac}{1+I_{00}^2(2R)-I_{00}^2(R)-I_{00}(2R)I_{00}^2(R)}, \quad (9)$$

where we have used the notation: $I_{00}(R)=(1/\pi)\int e^{-r_a-r_b}d\tau$,

$$a^2bcbc=(a(1)b(2)c(3)\,|\,H\,|\,a(1)c(2)b(3)), \quad \text{etc.} \quad (10)$$

These energy components are plotted in Figs. 1 and 2.

The energy of the symmetrical state, ψ_5, is shown in Fig. 3, curve V. It corresponds to a

[3] Heitler and London, Zeits. f. Physik **44**, 455 (1927).

strong repulsion between the three hydrogen atoms.

The energy of the state ψ_1 (antisymmetric with respect to a and c) is shown in Fig. 3 as curve I. The energy is less than for the three separated atoms and greater than for a diatomic hydrogen molecule and a hydrogen atom. The lowest energy is -53.11 kcal./mole for the separation of 2.0 a_0 between neighboring atoms. This is to be compared with the energy of the diatomic hydrogen molecule calculated by Heitler and London and Sugiura,[4] -72.18 kcal./mole. If a linear symmetrical molecule really corresponds to the activated state, then the activation energy for the reaction $H+H_2 \rightarrow H_2+H$, will be 19.07 kcal./mole by this calculation. However this approximation for the diatomic molecule is 36 kcal. or 1.6 ev higher than the experimental value of -108.6 kcal. Comparing the experimental activation energy (5.5 to 7.3 kcal.),[5] one sees that the energy obtained here for the triatomic molecule must be about 0.6 ev less accurate than that for the diatomic molecule.

James and Coolidge calculated the energy of the triatomic hydrogen molecule for the single

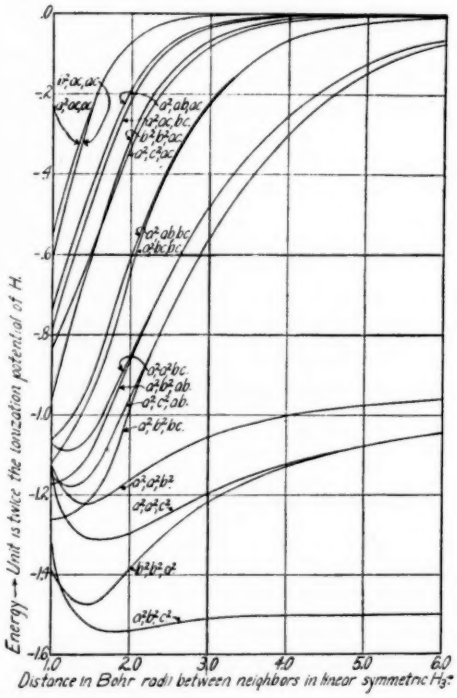

FIG. 1. The energy matrix components for H_3.

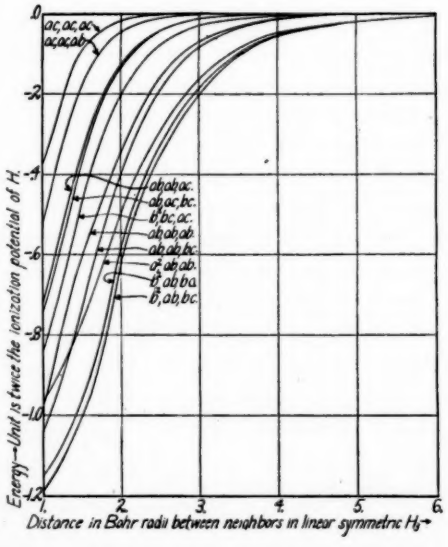

FIG. 2. The energy matrix components for H_3.

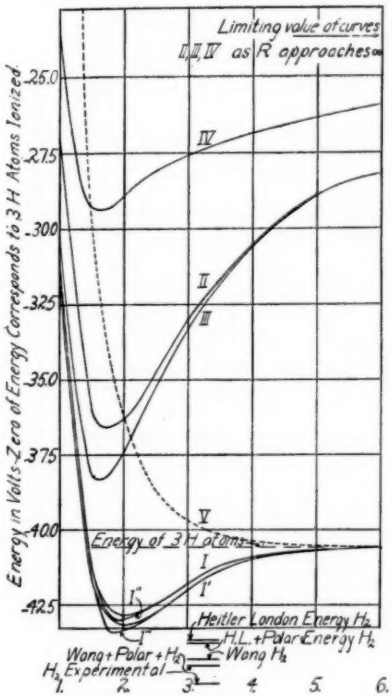
Limiting value of curves I, II, IV as R approaches ∞
Energy in Volts—Zero of Energy Corresponds to 3 H Atoms Ionized
Energy of 3 H atoms
Heitler London Energy H3
H.L. + Polar Energy H3
Wang + Polar + H2
Wang H3
H2 Experimental

FIG. 3. H to H distance of neighbors in Bohr radii. Potential curves for various states of linear symmetrical H_3.

[4] Y. Sugiura, Zeits. f. Physik **45**, 484 (1927).

[5] It appears that the zero-point energy in the activated complex is within one or two kcal./mole the same as that for the normal H_2 molecule (6.2 kcal./mole). See A. and L. Farkas, Proc. Roy. Soc. **A152**, 124 (1935); K. Geib and P. Harteck, Zeits. f. physik. Chemie Bodenstein Festband, 849 (1931).

internuclear separation $R=1.7\ a_0$. For this point they obtained the energy of -39.7 kcal./mole which is in good agreement with our value for this separation.

2. Heitler-London plus polar states

A slightly better approximation to the energy of the triatomic hydrogen molecule may be obtained by including the polar states in the eigenfunction. There are three polar states which are antisymmetric with respect to an interchange of a and c and which must be considered. ψ_2 corresponds to two electrons on atom a and one on c alternating with two on c and one on a. ψ_3 corresponds to two electrons on b and one electron alternating between a and c. ψ_4 corresponds to one electron on b and two electrons alternating between a and c:

$$\psi_2=\begin{pmatrix}a\ a\ c\\ \alpha\ \beta\ \alpha\end{pmatrix}-\begin{pmatrix}c\ c\ a\\ \alpha\ \beta\ \alpha\end{pmatrix}, \tag{11}$$

$$\psi_3=\begin{pmatrix}a\ b\ b\\ \alpha\ \beta\ \alpha\end{pmatrix}+\begin{pmatrix}b\ b\ c\\ \alpha\ \beta\ \alpha\end{pmatrix}, \tag{12}$$

$$\psi_4=\begin{pmatrix}b\ c\ c\\ \alpha\ \beta\ \alpha\end{pmatrix}+\begin{pmatrix}a\ a\ b\\ \alpha\ \beta\ \alpha\end{pmatrix}. \tag{13}$$

The energy components are shown in Figs. 1 and 2. By letting S_{ij} be the matrix components of unity:

$$S_{ij}=\int\int\int\psi_i\psi_j d\tau_1 d\tau_2 d\tau_3$$

and H_{ij} the matrix components of H:

$$H_{ij}=\int\int\int\psi_i H\psi_j d\tau_1 d\tau_2 d\tau_3.$$

The energies are given as the roots of the secular equation:

$$|H_{ij}-ES_{ij}|=0. \tag{14}$$

We are interested only in the lowest root of this equation, the other roots corresponding to higher states of the molecule. The composition of the eigenfunction which leads to the lowest energy value may be written as

$$\Psi=c_1(S_{11})^{-\frac{1}{2}}\psi_1+c_2(S_{22})^{-\frac{1}{2}}\psi_2+c_3(S_{33})^{-\frac{1}{2}}\psi_3+c_4(S_{44})^{-\frac{1}{2}}\psi_4. \tag{15}$$

The c_i are the solutions to the set of linear equations:

$$(S_{11})^{\frac{1}{2}}c_iE=c_1H_{i1}(S_{11})^{-\frac{1}{2}}+c_2H_{i2}(S_{22})^{-\frac{1}{2}}+c_3H_{i3}(S_{33})^{-\frac{1}{2}}+c_4H_{i4}(S_{44})^{-\frac{1}{2}},\quad i=1,\ 2,\ 3,\ 4. \tag{16}$$

The absolute values of the c_i are chosen so that Ψ is normalized to unity. Fig. 4 shows the c_i plotted as functions of the internuclear separation R.

The energy of the pure polar states 2, 3 and 4 are shown by curves II, III and IV, respectively, of Fig. 3. They correspond to much higher energies than the homopolar state. However, these states interact and the best linear combination of the four gives an energy level which is considerably lower than the homopolar. It is customary to designate such improvement by the term "resonance energy"; its physical significance is the improvement of the faulty charge distribution due to the approximate nature of the original eigenfunctions. The best linear combination is shown as curve I′ in Fig. 3. The minimum energy which this type of eigenfunction yields is -60.39 kcal./mole for $R=2.0\ a_0$.

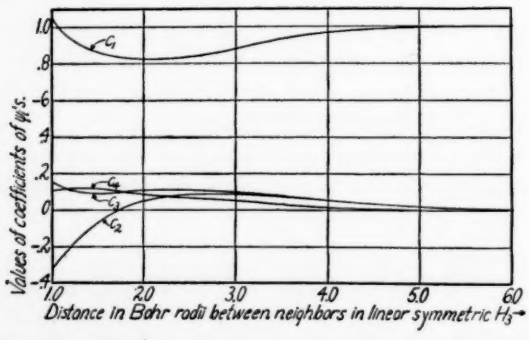

FIG. 4. Coefficients of $\Psi=c_1\psi_1+c_2\psi_2+c_3\psi_3+c_4\psi_4$. Ψ and ψ_i's are normalized to unity. ψ_i's are not orthogonal.

Weinbaum[6] calculated the energy of the diatomic hydrogen molecule using the same type of eigenfunction, i.e., homopolar plus polar states, and he obtained -74.02 kcal./mole. Comparing the energy of the triatomic molecule with this, one finds that the calculated activation energy for the reaction $H+H_2\rightarrow H_2+H$ is (except for zero-point energy) 13.63 kcal./mole. This activation energy is in fair agreement with the experimental value of 5.5 to 7.3 kcal./mole. Unfortunately the eigenfunctions are still too

[6] S. Weinbaum, J. Chem. Phys. **1**, 593 (1933).

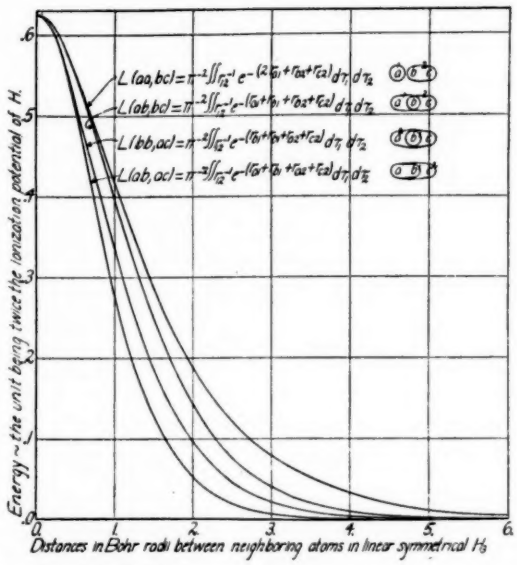
Energy ~ the unit being twice the ionization potential of H.
Distances in Bohr radii between neighboring atoms in linear symmetrical H3

FIG. 5. Potential between pairs of electrons having eigenfunctions involving three centers.

approximate for this agreement to have real significance, since the absolute value of the energy of the diatomic molecule with which we are comparing the energy of the triatomic molecule is 34 kcal./mole too large.

3. The Wang type of eigenfunction

In the diatomic hydrogen molecule, Wang[7] obtained a considerable improvement over the Heitler-London energy value by varying the "effective nuclear charge," z, in the atomic orbitals. This same type of variation may be carried out for the triatomic molecule without introducing any new integrals. Our method is similar to that used by Wang and by Coulson.[8]

The overlap integral $I_{00}(R)$ goes into $I_{00}(\rho)$ where $\rho=zR$. The nuclear attraction and electronic repulsion integrals become the same integrals as functions of ρ instead of R except that they are multiplied by z.

The kinetic energy gives rise to three separate integrals:

$$\int a(1)(-(h^2/8\pi^2m)\nabla_1^2)a(1)d\tau_1 \rightarrow z^2e^2/2a_0,$$

$$\int b(1)(-(h^2/8\pi^2m)\nabla_1^2)a(1)d\tau_1 \rightarrow [-\tfrac{1}{2}z^2I_{00}(\rho)+z^2J_{00}(\rho)]e^2/a_0,$$

$$\int c(1)(-(h^2/8\pi^2m)\nabla_1^2)a(1)d\tau_1 \rightarrow [-\tfrac{1}{2}z^2I_{00}(2\rho)+z^2J_{00}(2\rho)]e^2/a_0.$$

By combining the energy components it is easy to show that the energy in units of e^2/a_0 for the pure homopolar state 1 has the form

$$(E)_z=z[(E)_{z=1}+(z-1)A_{11}/S_{11}],$$

where A_{11} is a function of ρ.

Now keeping $zR=\rho$ constant, we can vary z to give the lowest energy:

$$(\partial E/\partial z)_\rho=0=(E)_{z=1}+(2z-1)A_{11}/S_{11},$$

$$z_{\min}=-\tfrac{1}{2}(E)_{z=1}S_{11}/A_{11}+\tfrac{1}{2},$$

$$E_{\min}=-S_{11}[(E)_{z=1}-A_{11}/S_{11}]^2/(4A_{11}).$$

$E_{\min}$ is the lowest energy that may be obtained for a particular value of zR but not necessarily for a particular value of R. However, if ρ is now varied to give the lowest value of $E_{\min}$, the latter will agree with the lowest possible value of E which can be obtained by varying both R and z.

This process corresponds to the Wang approximation for the diatomic hydrogen molecule. In the diatomic molecule the variation of z led to an energy of -86.94 kcal./mole which is an improvement of 14.8 kcal./mole over that for $z=1$. In the triatomic molecule this variation leads to an energy of -56.16 kcal./mole (at the point $R=1.889$ a_0 and with $z=1.059$), an improvement of only 3.05 kcal. This is 4.23 kcal./mole worse than for the H.L. plus polar states value. See Fig. 3, curve I'' for the values of $E_{\min}$. The corresponding activation energy for the $H+H_2 \rightarrow H_2+H$ reaction which we calculate as the difference between diatomic and triatomic energy is then 30.78 kcal./mole.

4. Wang plus polar states approximation

The variation of the "effective nuclear charge," z, was carried out for the eigenfunction in which the polar states are included. The variation of z and of the composition of the eigenfunction was carried out by successive approxima-

[7] S. C. Wang, Phys. Rev. **31**, 579 (1928).
[8] C. A. Coulson, Proc. Camb. Phil. Soc. (2) **31**, 244 (1935).

tions. First, the composition of the eigenfunction was taken to be the same as that previously obtained for the H.L. plus polar states approximation; a value of the best z for that composition was then obtained. The composition was then varied for that value of z. This last step improved the energy by only 0.35 kcal./mole at the point $\rho=2.0$; it was therefore deemed unprofitable to go back and readjust z. The energy values are shown as curve I''' in Fig. 3. The value for the Wang plus polar states approximation for the diatomic hydrogen molecule is -92.24 kcal./mole as obtained by Weinbaum. Since the minimum value which we find for the energy of the triatomic hydrogen molecule to this approximation is -67.09 kcal./mole for $R=1.841\ a_0$ and $z=1.087$, the calculated activation energy then becomes 25.15 kcal./mole. This activation energy is 17 kcal./mole larger than the experimental value. This approximation is the best that we can obtain without using more elaborate eigenfunctions and calculating new three-center integrals. It is not surprising that the variation of the screening constant on the three atoms simultaneously gives little improvement in the energy since one would expect that the central and outer atoms really ought to have different screening constants. However, such a treatment would involve the evaluation of additional integrals and has not been attempted here.

Appendix

Integrals

The three hydrogen nuclei, a, b, c lie symmetrically on a straight line with a separation of R times the first Bohr radius for atomic hydrogen, a_0; and 1 and 2 are electrons.

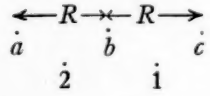

If the molecular eigenfunctions are compounded from 1s hydrogen-like atomic orbitals each having the same screening constant, all of the troublesome three-center integrals may be carried through directly in terms of ellipsoidal coordinates without resorting to ponderous or slowly converging infinite series. The convenient units $e^2/a_0=27.058$ ev $=623.96$ kcal./mole for the energy and $a_0=0.528\times10^{-8}$ cm for the length, are used here. The ellipsoidal coordinates are:

$$\lambda_n=(r_{in}+r_{jn})/R',$$

$$\mu_n=(r_{in}-r_{jn})/R',$$

$$\phi_n=\text{azimuthal angle of } n,$$

where i and j are the foci, R' is the distance between them, r_{in} and r_{jn} are the distances of the arbitrary point n to i and j, respectively.

The basic integral in this work is:

$$K(n, ij)=\pi^{-1}\int_{\text{all space}}\int\int r_{n1}^{-1}\exp(-r_{1i}-r_{1j})d\tau_1. \tag{17}$$

The integration of $K(n, ij)$ is simple in ellipsoidal coordinates where i and j are foci. It may be obtained as a by-product of Sugiura's calculation of

$$\pi^{-2}\int\int r_{12}^{-1}\exp(-r_{a1}-r_{b1}-r_{a2}-r_{b2})d\tau_1 d\tau_2.$$

Schuchowsky[9] and Gordadse[10] have also obtained it.

$$K(n, ij)=[K_0(R', \lambda_n)+\mu_n^2 K_2(R', \lambda_n)], \tag{18}$$

where:

$$K_0(R', \lambda_n)=(4R')^{-1}[3(\lambda_n^2+1)D-6\lambda_n I_{00}(R')+(6\lambda_n-2R')\exp(-R'\lambda_n)],$$

$$K_2(R', \lambda_n)=3(4R')^{-1}[-(3\lambda_n^2-1)D+6\lambda_n I_{00}(R')-(6\lambda_n+2R')\exp(-R'\lambda_n)],$$

$$D=I_{00}(R')[(\log(\lambda_n+1)/(\lambda_n-1))+Ei(-R'(\lambda_n-1))]-F(R')Ei(-R'(\lambda_n+1)),$$

$$I_{00}(R')=(\tfrac{1}{3}R'^2+R'+1)\exp(-R'),$$

$$F(R')=(\tfrac{1}{3}R'^2-R'+1)\exp(+R').$$

[9] A. Schuchowsky, Acta Physicochimica U.S.S.R. **1**, 901 (1934).
[10] G. Gordadse, Zeits. f. Physik **96**, 542 (1935).

Here $Ei(-x)$ is the integral logarithm, defined by

$$Ei(-x) = -\int_x^\infty x^{-1} \exp(-x)dx.$$

Values of $Ei(-x)$ for x greater than 15 were calculated from the asymptotic expansion of $Ei(-x)$. Two special examples of $K(n, ij)$ are the two three-center integrals which arise from the attraction of the electrons to the nuclei. $K(a, bc)$ is $K(n, ij)$ in which $R'=R$, $\mu_n=1$, $\lambda_n=3$. $K(b, ac)$ is $K(n, ij)$ in which $R'=2R$, $\mu_n=0$, $\lambda_n=1$.

There are four three-center multiple exchange integrals which arise from the mutual electronic repulsions. We shall consider them in order.

1. $$L(aa, bc) = \pi^{-2}\int\int r_{12}^{-1} \exp(-2r_{a1}-r_{b2}-r_{c2})d\tau_1 d\tau_2.$$

If we integrate over the coordinates of electron 1, $L(aa, bc) = K(a, bc) - T(a, bc)$,

where $$T(a, bc) = \pi^{-1}\int (1+r_{a2}^{-1}) \exp(-2r_{a2}-r_{b2}-r_{c2})d\tau.$$

By putting this in ellipsoidal coordinates with a and c as foci and integrating over the azimuthal angle ϕ_2,

$$T(a, bc) = 2R^3\int_1^\infty\int_{-1}^1 [(\lambda^2-\mu^2)+R^{-1}(\lambda-\mu)] \exp(-3R\lambda-R\mu-R(\lambda^2+\mu^2-1)^{\frac{1}{2}})d\mu d\lambda.$$

By making the substitution:

$$t = \mu+(\lambda^2+\mu^2-1)^{\frac{1}{2}},$$

μ is expressible rationally in terms of t:

$$\mu = \tfrac{1}{2}t-\tfrac{1}{2}t^{-1}(\lambda^2-1).$$

$T(a, bc)$ is now free from radicals:

$$T(a, bc) = \int_1^\infty\int_{\lambda-1}^{\lambda+1} [k(\lambda)t^2+\cdots+k'(\lambda)t^{-4}] \exp(-3R\lambda-Rt)dtd\lambda,$$

where $k(\lambda), \cdots k'(\lambda)$ are polynomials. This is readily integrated to give:

$$\begin{aligned} 81T(a, bc) = {} & (e^{-3R}/16)[131/3R+1670+2256R+624R^2]-(e^{-5R}/16)[131/3R+34+160R] \\ & -[116/9R+116/3+44R+16R^2][Ei(-2R)+2\log 2]e^{-3R} \\ & +e^{3R}Ei(-8R)[116/9R-116/3+44R-16R^2]. \end{aligned} \quad (19)$$

2. $$L(bb, ac) = \pi^{-2}\int\int r_{12}^{-1} \exp(-2r_{b1}-r_{a2}-r_{c2})d\tau_1 d\tau_2.$$

The integration over the first electron coordinates gives: $L(bb, ac) = K(b, ac) - T(b, ac)$,

where $$T(b, ac) = \pi^{-1}\int (1+r_{b2}^{-1}) \exp(-2r_{b2}-r_{a2}-r_{c2})d\tau_2.$$

Again by using the ellipsoidal coordinates with a and c as foci and integrating over ϕ_2:

$$T(b, ac)=2R^3\int_1^\infty\int_1^1(\lambda^2-\mu^2)[1+R^{-1}(\lambda^2+\mu^2-1)^{-\frac{1}{2}}]\exp(-2R\lambda-2R(\lambda^2+\mu^2-1)^{\frac{1}{2}})\cdot d\mu d\lambda.$$

The substitution $s=\lambda+(\lambda^2+\mu^2-1)^{\frac{1}{2}}$ enables λ to be expressed rationally in terms of s,

$$\lambda=\tfrac{1}{2}s-\tfrac{1}{2}s^{-1}(\mu^2-1),$$

and thereby eliminates radicals from the integral, which may be evaluated directly.

$$105T(b, ac)=16R^4(7+2R^2)[Ei(-2R)-2Ei(-4R)]+e^{-2R}[16R^5-8R^4+64R^3-40R^2+52R$$
$$+108-51/R]+e^{-4R}[-16R^5+4R^4-58R^3+15.5R^2-8.5R+33.375+51/R]. \quad (20)$$

3. $L(ab, ac)=\pi^{-2}\int\int r_{12}^{-1}\exp(-r_{a1}-r_{c1}-r_{a2}-r_{b2})d\tau_1 d\tau_2.$

The integration over the first electron coordinates gives:

$$L(ab, ac)=\pi^{-1}\int K(2, ac)\exp(-r_{a2}-r_{b2})d\tau_2.$$

By expressing this in ellipsoidal coordinates with foci at a and c and integrating over ϕ_2,

$$L(ab, ac)=2R^3\int_1^\infty[C_0K_0(2R, \lambda)+C_2K_2(2R, \lambda)]d\lambda, \quad (21)$$

where

$$C_0=\int_{-1}^1(\lambda^2-\mu^2)\exp(-R\mu-R(\lambda^2+\mu^2-1)^{\frac{1}{2}})d\mu,$$

$$C_2=\int_{-1}^1(\lambda^2-\mu^2)\mu^2\exp(-R\mu-R(\lambda^2+\mu^2-1)^{\frac{1}{2}})d\mu.$$

The same substitution used in $L(aa, bc)$ makes the integration of C_0 and C_2 possible. The last integration over λ would also be carried through analytically, but the integrand involves so many separate terms that it is much easier to carry through the last integration numerically. C_0 and C_2 as well as $K_0(2R, \lambda)$ and $K_2(2R, \lambda)$ were evaluated for a large number of values of λ for each value of R considered. The final integrand was obtained by accurate curve fitting with functions of the form:

$$f(\lambda)\exp(-2R\lambda)+g(\lambda)\exp(-4R\lambda),$$

where $f(\lambda)$ and $g(\lambda)$ are polynomials. Care was taken that these functions had the proper behavior for large values of λ and that they had no extraneous oscillations. The final integration was carried out with these functions. The values obtained for the integral are probably correct to five figures after the decimal point, in atomic units, i.e., 0.005 kcal.

4. $$L(ab, bc)=\pi^{-2}\int\int r_{12}^{-1}\exp(-r_{a1}-r_{b1}-r_{b2}-r_{c2})d\tau_1 d\tau_2.$$

After integrating over the coordinates of electron 1,

$$L(ab, bc)=\pi^{-1}\int K(2, ab)\exp(-r_{b2}-r_{c2})d\tau_2.$$

By integrating over the azimuthal angle and putting this in the ellipsoidal coordinates with a and b as foci.

$$L(ab, bc)=\frac{R^3}{4}\int_1^\infty [M_0K_0(R, \lambda)+M_2K_2(R, \lambda)]\exp(-\tfrac{1}{2}R\lambda)d\lambda, \tag{22}$$

where

$$M_0=\int_{-1}^{1}(\lambda^2-\mu^2)\exp(\tfrac{1}{2}R\mu-\tfrac{1}{2}R(\lambda^2+\mu^2-6\mu\lambda+8)^{\frac{1}{2}})d\mu,$$

$$M_2=\int_{-1}^{1}\mu^2(\lambda^2-\mu^2)\exp(\tfrac{1}{2}R\mu-\tfrac{1}{2}R(\lambda^2+\mu^2-6\mu\lambda+8)^{\frac{1}{2}})d\mu.$$

Here the substitution

$$z=3\lambda-\mu+(\lambda^2+\mu^2-6\mu\lambda+8)^{\frac{1}{2}}$$

makes μ_2 expressible in terms of z in a rational manner:

$$\mu_2=-\tfrac{1}{2}z+3\lambda+4z^{-1}(1-\lambda^2),$$

and the integrations over z may be carried out analytically. The final integration over λ, just as in the case of $L(ab, ac)$, might be carried through analytically but the large number of terms in the integrand at this point makes such a task extremely laborious. The M_0 and M_2 as well as the $K_0(R, \lambda)$ and $K_2(R, \lambda)$ were computed for a large number of values of λ for each value of R considered and the integrand was accurately "curve-fitted." The curve fitting in this case was much more difficult than in the previous case and it was necessary to fit a number of sections and integrate these separately. The final numerical values for these integrals are probably also correct to five places after the decimal point in atomic units (0.005 kcal./mole). In Fig. 5 the four integrals just discussed are plotted against internuclear separation.

Fig. 8 shows the four three-center integrals as functions of the internuclear separation R. They each approach 5/8 as R approaches zero. The value of these integrals for ordinary interatomic distances in molecules are of the same order of magnitude as those for two centers although they become comparatively negligible for large separations.

Previous to this work, the three-center multiple exchange integrals have always been treated by expanding $1/r_{12}$ and at least two of the exponential factors in the integrand in terms of a doubly infinite series of spherical harmonics about one of

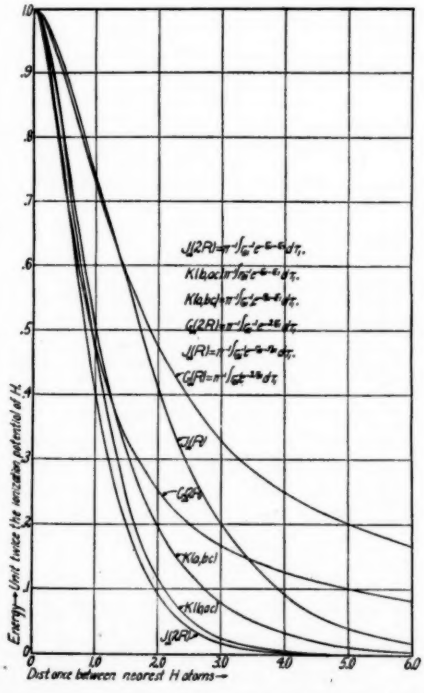

FIG. 6. Some two- and three-center energy integrals.

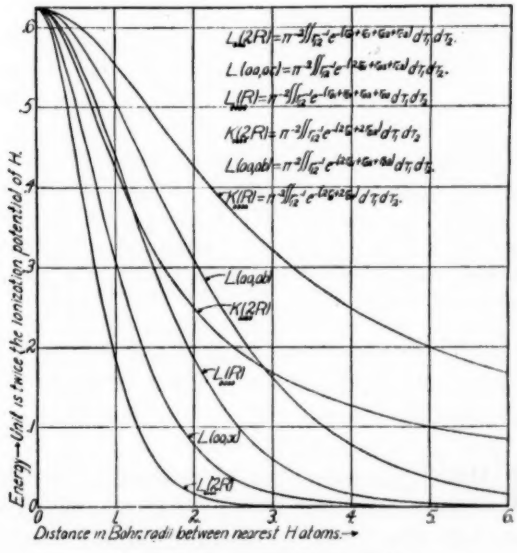

FIG. 7. Some energy integrals.

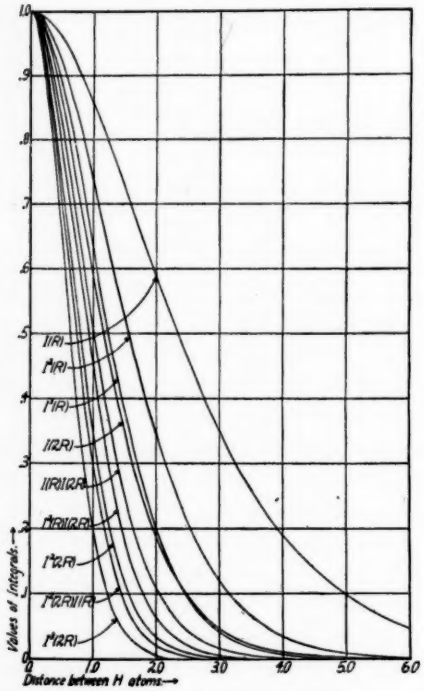

FIG. 8. Normalizing integrals.

the centers.[11] The resulting integrations may then be carried through by making use of the orthogonality properties of the spherical harmonics. However, the series which must be evaluated, converges slowly except for small internuclear distances and the terms are ponderous. Coolidge and James have used this method for the internuclear separation of 1.7 a_0 and obtained agreement with our values to within half a kcal./mole for $L(aa, bc)$, $L(bb, ac)$ and $L(ab, bc)$ but their value of $L(ab, ac)$ is some two kcal./mole smaller than ours.

The one- and two-center integrals which occur in this treatment have been previously used for the diatomic hydrogen molecule.[12] The integrals for nuclear attraction are shown in Fig. 6, those for electronic repulsion in Fig. 7. The overlap integrals and all the combinations of them required for H_3 are given in Fig. 8.

We wish to express our appreciation to the American Philosophical Society for financial assistance during the course of this work.

[11] A. S. Coolidge, Phys. Rev. **42**, 189 (1932), used this method for H_2O. Some work along this line has been done by Hershtenkorn (Diss., M.I.T., June 1932) and by A. A. Frost at Princeton.

[12] See, e.g., N. Rosen, Phys. Rev. **38**, 2099 (1931).

FEBRUARY, 1936 JOURNAL OF CHEMICAL PHYSICS VOLUME 4

II. Calculation of Energy of H_3^+ Ion

J. HIRSCHFELDER, H. EYRING AND N. ROSEN, *Frick Chemistry Laboratory of Princeton University, and the Institute for Advanced Study*

(Received November 22, 1935)

The potential energies for linear symmetrical configurations of H_3^+ have been calculated by the same methods used in the previous paper (I). The energies at the minimum in kcal./mole and the corresponding distances between neighboring atoms in Bohr radii for the various approximations are:

Heitler-London	− 91.92 at 2.00;
H.L. plus polar	−108.64 at 2.00;
Wang Approx.	−130.89 at 1.55;
Wang plus polar	−155.35 at 1.52.

It follows from the use of the variational method that the energy of binding of a proton to H_2 is greater than 46.8 kcal./mole. If we use the same Wang plus polar approximation for H_2 and H_3^+ we obtain for this binding energy 63.11 kcal./mole. The reaction $H_2^+ + H_2 \rightarrow H_3^+ + H$ may be exothermal and cannot be more than slightly endothermal.

THERE is experimental evidence that H_3^+ ions are formed whenever H_2 is ionized at any but the lowest pressures.[1] This probably occurs by the following secondary processes:

[1] H. D. Smyth, Rev. Mod. Phys. **3**, 347 (1931); Phys. Rev. **4**, 452 (1925); W. Bleakney, Phys. Rev. **40**, 496 (1932); **35**, 1180 (1930); Hogness and Lunn, Phys. Rev. **26**, 44 (1925); Brasefield, Phys. Rev. **31**, 52 (1928); Dorsch and Kallmann, Zeits. f. Physik **53**, 80 (1929).

$$H_2^+ + H_2 \rightarrow H_3^+ + H, \quad (1)$$

$$H^+ + H_2 \rightarrow H_3^+, \quad (2)$$

$$H + H_2^+ \rightarrow H_3^+, \quad (3)$$

of which the first is ordinarily the most important. In this paper only the linear symmetric configurations are considered. The calculation of the energy of the triatomic hydrogen ion is then very similar to that of the triatomic hydrogen molecule treated in the paper immediately preceding (I). The same integrals are used and the same types of approximations considered. The lowest energy states for the triatomic hydrogen ion are found to be symmetric with respect to an interchange of atoms a and c in the electronic eigenfunctions as contrasted with the H_3 case.

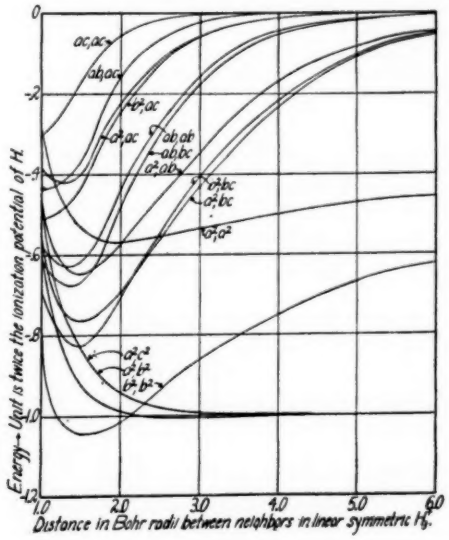

FIG. 1. The energy matrix components for H_3^+.

1. Energy of Lowest Bond State

The simplest type of eigenfunction which we can form from the atomic orbitals considered in paper I corresponds to a bond between the atoms a and b alternating with a bond between b and c.

$$\psi_1 = (2)^{-1}[a(1)b(2)+a(2)b(1)+b(1)c(2)+b(2)c(1)][\alpha(1)\beta(2)-\alpha(2)\beta(1)].$$

This state corresponds to the energy:

$$E_{11} = \frac{a^2b^2+b^2ac+abab+abbc}{1+I_{00}(2R)+2I_{00}^2(R)}.$$

Values for the energy components are given in Fig. 1. The energy is shown in Fig. 2 as curve I. The lowest value which we obtained for the energy was -91.92 kcal./mole.

2. Heitler-London Plus Polar States Type of Eigenfunction[2]

The energy for the triatomic hydrogen ion can be considerably improved if we include in the eigenfunction linear combinations of two polar states and two homopolar states so as to get the minimum energy for the combination. The eigenfunctions which can be formed from the atomic orbitals considered, and which are symmetrical with respect to an interchange of atoms a and c are: (1) bond eigenfunction between a and b plus a bond eigenfunction between b and c; (2) bond between a and c; (3) both electrons on the central atom b; (4) both electrons alternately on a and then on c.

$$\psi_2 = \tfrac{1}{2}[a(1)c(2)+c(1)a(2)][\alpha(1)\beta(2)-\alpha(2)\beta(1)],$$

$$\psi_3 = 2^{-\frac{1}{2}}b(1)b(2)[\alpha(1)\beta(2)-\alpha(2)\beta(1)],$$

$$\psi_4 = \tfrac{1}{2}[a(1)a(2)+c(1)c(2)][\alpha(1)\beta(2)-\alpha(2)\beta(1)].$$

The calculation of the energy involves the same formal processes as in the equivalent approximation for the triatomic molecule. The energy components are shown in Fig. 1. The energy for the pure states 1, 2, 3 and 4 are shown as curves I, II, III, IV, respectively, in Fig. 2. The energy of the ion is then obtained by the solution of a fourth-order secular equation. The values are shown graphically in Fig. 2 as curve I′. At large internuclear separations there is a strong interaction between the two homopolar states (1) and (2). It is interesting that for distances so large that states ψ_1 and ψ_2 have practically attained their asymptotic energies, their interaction energy H_{12} is still appreciable. At small separations there is a strong interaction between (1) and the polar state (3). Fig. 3 shows the coefficients c_i of the normalized Ψ giving the total normalized eigenfunction of

[2] Heitler and London, Zeits. f. Physik **44**, 455 (1927); S. Weinbaum, J. Chem. Phys. **1**, 593 (1933).

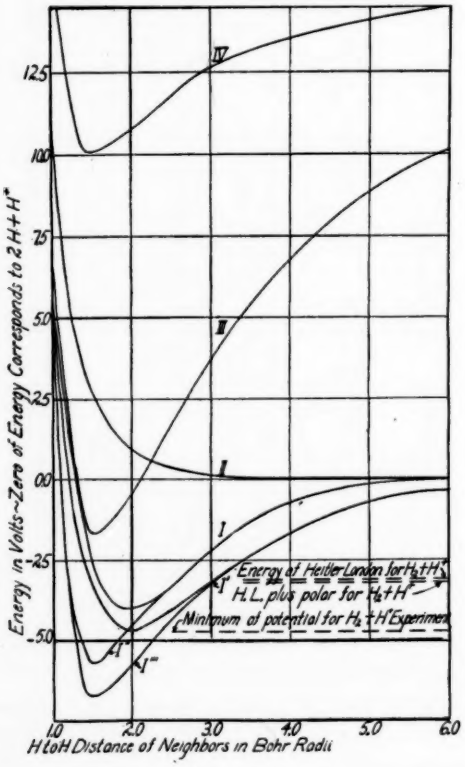

FIG. 2. Potential curves for various states of linear symmetrical H_3^+.

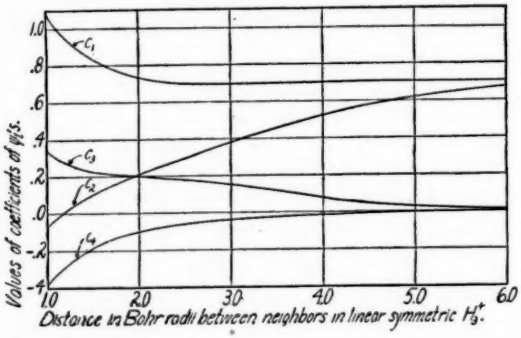

FIG. 3. Coefficients of $\Psi=c_1\psi+c_2\psi_2+c_3\psi_3+c_4\psi_4$. Ψ and the ψ_i's are normalized to unity. The ψ_i's are not orthogonal.

lowest energy. These c_i are similar to those defined for the triatomic molecule in paper I. The minimum energy that is obtained in this approximation is -108.64 kcal./mole at a separation of $2.0a_0$ between neighboring atoms. The improvement, it will be noticed, is 16.72 kcal./mole over the corresponding value for the lowest homopolar state.

3. WANG TYPE OF EIGENFUNCTION[3]

It is not difficult to vary the effective nuclear charge in exactly the same manner as for the triatomic hydrogen molecule in paper I. It should be emphasized again that because of the type of variation the value for E is the lowest for a particular value of $\rho=zR$ but not necessarily for any particular value of R except at that point at which it is a minimum for *both* z and R. Thus it will be noticed in the curve I'' of Fig. 2 which shows this energy as a function of R, that this method of varying z led to considerable improvement of the energy for separations near $R=2.0$ which is the most favorable separation when $z=1$. However, curve I'' merges into I' for larger or smaller separations and for these separations this particular way of varying z does not improve the energy. The lowest energy which is obtained in this approximation is -130.89 kcal./mole for the separation $R=1.546a_0$ and $z=1.294$. This is an improvement of 39 kcal./mole over the lowest bond state approximation. It is remarkable that the variation of the effective charge produces such a striking change in this energy when it made so little difference in the energy of the triatomic molecule.

4. WANG PLUS IONIC STATES EIGENFUNCTION

By varying the effective nuclear charge in the H.L. plus polar eigenfunction the energy of the triatomic hydrogen ion is improved considerably. Knowing the composition of this eigenfunction for $z=1$, we may find the energy of the molecule for this same composition as a function of z. The c_i are given in Fig. 3. z is then varied until E has a minimum value for the particular value of $\rho=zR$ considered. This value of E can be improved still further by varying the composition keeping z constant. This variation of the composition improved the result at the energy minimum by 2.87 kcal./mole. The value of the energy as a function of R is shown as curve I''' in Fig. 2. The minimum value of the energy has dropped to -155.35 kcal./mole for the separation of $R=1.525a_0$ which corresponds to $z=1.312$ and

[3] S. C. Wang, Phys. Rev. **31**, 579 (1928).

$zR=2.0a_0$. This is to be compared with the energy of the normal diatomic molecule calculated in this same manner by Weinbaum,[2] -92.24 kcal./mole. This calculation gives an energy of binding of a proton to the H_2 of 63.11 kcal./mole. This is very nearly equal to the energy of binding of a proton to a hydrogen atom, i.e., 64.04 kcal./mole. (The zero-point energy is not taken into account in either of these values.) Since the true energy of the diatomic hydrogen molecule is -108.6 kcal./mole instead of the calculated -92.2, the very smallest amount of binding energy which the triatomic ion could possibly have relative to a hydrogen molecule plus a proton is 46.8 kcal./mole. However, the actual binding energy of the proton to the hydrogen molecule will probably be larger instead of smaller than 63.11 kcal./mole. The reason for this supposition is that our experience with H_3 was that the accuracy for the three-center problem was poorer than that obtained for the two-center case by the corresponding method. In any event, the reaction $H_2^+ + H_2 \rightarrow H_3^+ + H$ should take place with at most a small amount of kinetic energy, and it is probable (not certain) that it can take place without any relative kinetic energy.

5. Remarks

From our calculations we find for the linear ion a moment of inertia of 2.15×10^{-40} g cm^2. If the same distances between neighboring atoms were preserved in the equilateral triangle model, the latter would have two moments of inertia having values of $\frac{1}{2}$ and $\frac{1}{4}$ of the above. It would require an increase of about 40 percent in the distances to double the latter moments of inertia. Allen and Sandeman[4] found three band systems in the secondary spectrum of a hydrogen filled Wood's discharge-tube, which they interpret as due to a triatomic hydrogen molecule or ion with a moment of inertia of 1.8×10^{-40} g cm^2. These bands are enhanced in the arc spectrum and under conditions favorable to the formation of H_3^+.

The equilateral triangle model for the triatomic hydrogen ion was considered by C. A. Coulson.[5] However, Coulson did not calculate the three-center multiple exchange integrals, and without them he was not able to place the energy of the molecule within any significant limits. He believed that the triatomic ion would be more stable in the equilateral triangle configuration than in the linear. His argument was based on the fact that the binding energy which two electrons exert on three centers is increased if the configuration is triangular. While this is undoubtedly true, the nuclear repulsions become much larger at the same time. For a separation between neighbors of $1.5a_0$ (which must be nearly the best separation for both cases) the energy of nuclear repulsion is 1040 kcal./mole for the three atoms in a linear symmetrical configuration and 1248 kcal./mole for the equilateral triangle. Thus only if the electronic binding for the triangle exceeds that for the line by over 200 kcal./mole can the former configuration be the more stable. This point requires further investigation.

We wish to express our appreciation to the American Philosophical Society for financial assistance during the course of this work.

---

[4] Allen and Sandeman, Proc. Roy. Soc. **A114**, 293 (1927).

[5] C. A. Coulson, Proc. Camb. Phil. Soc. (2) **31**, 244 (1935).

Normal Vibration Frequencies of the Molecule XYZ_3

JENNY E. ROSENTHAL,* *Chemistry Department, Columbia University*
AND
H. H. VOGE,** *Physics Department, Harvard University****

(Received December 16, 1935)

A very general expression is set up for the potential energy of the tetrahedral molecule XYZ_3. The normal vibration frequencies are given as functions of the constants in this expression. The equation for the parallel frequencies is shown to be essentially independent of the shape of the tetrahedron, while for the perpendicular case the two angles determining the molecular configuration must be taken into account. Connections are given between the general potential energy constants and the constants for the special forces used by Dennison and Sutherland.

SUBSTITUTED tetrahedral molecules of the type XYZ_3 form a large and important class, with many representatives among derivatives of methane, silane and other regular tetrahedral molecules. This class is of considerable interest in the study of molecular vibrations. A great deal of infrared and Raman spectrum data is available, from which it should be possible to derive definite conclusions concerning intramolecular forces. This requires, however, the existence of perfectly general expressions for the vibration frequencies. Such formulas will be derived in this paper.

The pentatomic molecule XYZ_3, in which three equivalent atoms are attached to the central atom Y, has geometric symmetry corresponding to the point group C_{3v}. According to the well-known results of group theory,[1,2] the molecule has three single vibrations of the parallel type, belonging to the symmetric representation A_1; and three doubly degenerate vibrations of the perpendicular type, belonging to the representation E. All six frequencies are permitted by the selection rules in both infrared absorption and Raman effect.

If the Hamiltonian is written in terms of variables of the proper symmetry, the secular equation for the normal frequencies of vibration factors into parts corresponding to the two representations. One cubic equation derives from A_1, and two identical cubics ensue from the variables transforming according to E. Symmetry coordinates which lead to the desired factorization have been described by Howard and Wilson.[3] For the purpose of formulating a general potential function, geometrical symmetry coordinates[2] are more convenient, and they are employed here. The geometrical symmetry coordinates satisfy all the conditions set down by Howard and Wilson, except that of conservation of angular and linear momenta.

The notation used is closely related to that introduced in a study of the vibrations of the molecule YX_4.[4] Thus δr_i indicates the mutual displacement between the central atom Y and one of the other atoms, while δq_{ij} represents a similar quantity for two peripheral atoms. The numbering is shown in Fig. 1. The shape of the tetrahedron is taken into account by means of two angles. θ represents the angle formed by a Y−Z bond with the axis of the YZ_3 pyramid, while φ is the angle between a line connecting X with Z and the same axis. M is the mass of the Y atom, while m and n are, respectively, the masses of the Z and X atoms. Since the parallel and perpendicular frequencies represent separate mathematical problems, they are treated in turn below.

PARALLEL FREQUENCIES

Take as the three independent geometrical symmetry coordinates

* Sarah Berliner Research Fellow of the American Association of University Women.
** National Research Fellow in Chemistry.
*** A large part of the work described in this and the following paper was done at the University of Michigan.
[1] E. B. Wilson, Jr., J. Chem. Phys. **2**, 432 (1934).
[2] J. E. Rosenthal and G. M. Murphy, to be published in Reviews of Modern Physics.
[3] J. B. Howard and E. B. Wilson, Jr., J. Chem. Phys. **2**, 630 (1934).
[4] J. E. Rosenthal, Phys. Rev. **46**, 730 (1934).

$$s_1=\delta r_1+\delta r_2+\delta r_3,$$
$$s_2=\delta r_4, \qquad (1)$$
$$s_3=\delta q_{12}+\delta q_{13}+\delta q_{23}.$$

Then the most general quadratic potential function may be written

$$2V=G_{11}s_1^2+G_{22}s_2^2+G_{33}s_3^2 +2(G_{12}s_1s_2+G_{13}s_1s_3+G_{23}s_2s_3). \qquad (2)$$

The kinetic energy written in terms of these variables and the masses is

$$2T=m(M+3m+n)^{-1}\{\tfrac{1}{3}(M+n)\sec^2\theta\dot{s}_1^2 +(n/m)(M+3m)\dot{s}_2^2+[(M+n)\sec^2\theta/9+\tfrac{1}{3}m]\dot{s}_3^2 +2[n\sec\theta\dot{s}_1\dot{s}_2-\tfrac{1}{3}(M+n)\tan\theta(\sec\theta/\sqrt{3})\dot{s}_1\dot{s}_3 -n(\tan\theta/\sqrt{3})\dot{s}_2\dot{s}_3]\}. \qquad (3)$$

Eqs. (2) and (3) lead by the usual methods to the cubic equation for the parallel frequencies.[5]

$$m^3\lambda^3-R_1m^2\lambda^2+R_2m\lambda-R_3=0,$$

where

$$R_1=(3/M)(3m\cos^2\theta+M)G_{11}+(m/Mn)(M+n)G_{22}-(6m/M)\cos\theta G_{12}+6(\sqrt{3})\sin\theta G_{13}+9G_{33},$$
$$R_2=(3m/Mn)(3m\cos^2\theta+M+n)(G_{11}G_{22}-G_{12}^2)+(9m/Mn)(M+n)(G_{22}G_{33}-G_{23}^2)$$
$$+(27\cos^2\theta/M)(3m+M)(G_{11}G_{33}-G_{13}^2)+6(\sqrt{3})\sin\theta(m/Mn)(M+n)(G_{22}G_{13}-G_{12}G_{23})$$
$$+18(\sqrt{3})\sin\theta\cos\theta(m/M)(G_{11}G_{23}-G_{12}G_{13})+54\cos\theta(m/M)(G_{13}G_{23}-G_{12}G_{33}), \qquad (4)$$

and

$$R_3=27\cos^2\theta(m/Mn)(3m+M+n)(G_{11}G_{22}G_{33}+2G_{12}G_{13}G_{23}-G_{11}G_{23}^2-G_{22}G_{13}^2-G_{33}G_{12}^2).$$

In making calculations it is convenient to substitute $\lambda=\omega^2$, ω being given in cm^{-1}, and to use the masses in atomic weight units. The constants G thus determined are of the dimensions mass $(cm^{-1})^2$. However, if the constants are desired in dynes/cm, it is necessary to set $\lambda=4\pi^2c^2\omega^2$ and to express the masses in grams per atom. To transform the force constants from the mass $(cm^{-1})^2$ units to dynes/cm, it is only necessary to multiply by 0.05863.

Formulas (4) seem to imply that the parallel frequencies depend explicitly on the angle θ, i.e., on the shape of the tetrahedron. This, however, is not the case. For if we introduce new constants F such that

$$G_{11}=3\sec^2\theta F_{11},$$
$$G_{22}=F_{22},$$
$$G_{33}=\tan^2\theta F_{11}+F_{33}-2\tan\theta F_{13},$$
$$G_{12}=(\sqrt{3})\sec\theta F_{12}, \qquad (5)$$
$$G_{13}=-(\sqrt{3})\tan\theta\sec\theta F_{11}+(\sqrt{3})\sec\theta F_{13},$$
$$G_{23}=-\tan\theta F_{12}+F_{23},$$

it is found upon substitution that the angle θ vanishes from Eqs. (4). This linear transformation of the constants corresponds to the use of the following geometrical symmetry coordinates:

$$s_1'=(\sqrt{3})\sec\theta s_1-\tan\theta s_3,\quad s_2'=s_2,\quad s_3'=s_3. \qquad (6)$$

The F_{ij} are then the constants in the general potential function written in these new variables. We have preferred to use the variables indicated

FIG. 1.

[5] As a check the problem has also been set up in symmetry coordinates of the type described in reference 3, and the formulas for both the parallel and perpendicular frequencies have been verified. The two methods represent different ways of treating the kinetic and potential energies, but are of course mathematically equivalent.

in (1), for then the coefficients in the potential energy are susceptible to a simple physical interpretation which will be discussed in the following paper.

Perpendicular Frequencies

While the treatment of this problem is exactly analogous to the one used for the parallel case, the resultant formulas for the frequencies are much more cumbersome. Their dependence on the angles θ and φ is inherent in the problem and cannot be eliminated by any substitutions. We use as the geometrical symmetry coordinates

$$s_4=\delta r_2-\delta r_3,\quad s_5=\delta q_{24}-\delta q_{34},\quad s_6=\delta q_{12}-\delta q_{13}. \tag{7}$$

The most general quadratic potential energy function consistent with C_{3v} may then be written

$$2V=G_{44}s_4^2+G_{55}s_5^2+G_{66}s_6^2 +2(G_{45}s_4s_5+G_{46}s_4s_6+G_{56}s_5s_6); \tag{8}$$

while the kinetic energy takes the form

$$2T=(m/t_0)[t_{44}\dot{s}_4^2+t_{55}\dot{s}_5^2+t_{66}\dot{s}_6^2 -2(t_{45}\dot{s}_4\dot{s}_5+t_{46}\dot{s}_4\dot{s}_6+t_{56}\dot{s}_5\dot{s}_6)], \tag{9}$$

where

$$\begin{aligned}
t_0&=\tfrac{1}{3}(\cot\varphi-\cot\theta)^2+(m/n)\operatorname{cosec}^2\theta\\
&\quad+(m/M)\operatorname{cosec}^2\varphi+\tfrac{1}{2}m(3m-n-M)/Mn,\\
t_{44}&=\tfrac{1}{3}(\cot^2\varphi+\tfrac{1}{2}+3m/2n)\operatorname{cosec}^2\theta,\\
t_{55}&=\tfrac{1}{3}(\cot^2\theta+\tfrac{1}{2}+3m/2M)\operatorname{cosec}^2\varphi,\\
t_{66}&=2(\cot\varphi-\cot\theta)^2/9+\tfrac{1}{3}(m/n)\operatorname{cosec}^2\theta\\
&\quad+\tfrac{1}{3}(m/M)\operatorname{cosec}^2\varphi+\tfrac{1}{2}(m^2/nM),\\
t_{45}&=\tfrac{1}{3}(\cot\varphi\cot\theta+\tfrac{1}{2})\operatorname{cosec}\varphi\operatorname{cosec}\theta),\\
t_{46}&=[\tfrac{1}{3}\cot\varphi(\cot\varphi-\cot\theta)+\tfrac{1}{2}(m/n)]\\
&\quad\times\operatorname{cosec}\theta/\sqrt{3},\\
t_{56}&=[\tfrac{1}{3}\cot\theta(\cot\theta-\cot\varphi)+\tfrac{1}{2}(m/M)]\\
&\quad\times\operatorname{cosec}\varphi/\sqrt{3}.
\end{aligned} \tag{10}$$

The frequencies are given by

$$m^3\lambda^3-P_1m^2\lambda^2+P_2m\lambda-P_3=0,\quad\text{with}$$

$$\begin{aligned}
P_1&=(3m\sin^2\theta/M+2)G_{44}+4\cos(\theta-\varphi)G_{45}+(3m\sin^2\varphi/n+2)G_{55}+3G_{66}+2(\sqrt{3})\sin\theta G_{46}\\
&\quad+2(\sqrt{3})\sin\varphi G_{56},\\
P_2&=3(3m\sin^2\theta/M+2-\sin^2\theta)(G_{44}G_{66}-G_{46}^2)+2(\sqrt{3})(3m\sin\varphi\sin^2\theta/M+2\sin\varphi\\
&\quad-2\cos(\theta-\varphi)\sin\theta)(G_{44}G_{56}-G_{45}G_{46})+6(2\cos\varphi\cos\theta+\sin\varphi\sin\theta)(G_{45}G_{66}-G_{46}G_{56})\\
&\quad+3(3m\sin^2\varphi/n+2-\sin^2\varphi)(G_{55}G_{66}-G_{56}^2)+[6m\sin^2\theta/M+4\sin^2(\theta-\varphi)\\
&\quad+9m^2\sin^2\varphi\sin^2\theta/Mn+6m\sin^2\varphi/n](G_{44}G_{55}-G_{45}^2)\\
&\quad+2(\sqrt{3})[2\cos\varphi\sin(\theta-\varphi)+3m\sin^2\varphi\sin\theta/n](G_{55}G_{46}-G_{45}G_{56}),\\
P_3&=3[2\sin^2(\theta-\varphi)+3\sin^2\varphi(2m/n+3m^2\sin^2\theta/Mn-m\sin^2\theta/M-m\sin^2\theta/n)+6m\sin^2\theta/M]\\
&\quad\times(G_{44}G_{55}G_{66}+2G_{45}G_{46}G_{56}-G_{44}G_{56}^2-G_{55}G_{46}^2-G_{66}G_{45}^2).
\end{aligned} \tag{11}$$

It should be pointed out that the general formulas given here can be applied to special types of potential energy functions such as valence forces, Urey and Bradley[6] forces, or other types based on simplified physical models. To obtain the corresponding equations for the frequencies, it is only necessary to find the connection between our general G_{ij}'s and the special constants and substitute it into Eqs. (4) and (11). For example, the relations

$$\begin{aligned}
G_{11}&=(1/9)a\sec^2\theta,\\
G_{22}&=c,\\
G_{33}&=(1/27)(b-2d\tan\theta+a\tan^2\theta),\\
G_{12}&=0,\\
G_{13}&=(1/9\sqrt{3})\sec\theta(d-a\tan\theta),\\
G_{23}&=0,
\end{aligned} \tag{12}$$

which are derived from the four constant potential function assumed by Sutherland and Dennison,[7] lead to the special formula they have given for the parallel frequencies of this molecule.

[6] H. C. Urey and C. A. Bradley, Jr., Phys. Rev. **38**, 1969 (1931).

[7] G. B. B. M. Sutherland and D. M. Dennison, Proc. Roy. Soc. **A864**, 250 (1935).

Potential Functions of Molecular Groups and the Vibrations of the Halogen Derivatives of Methane

H. H. VOGE,* *Physics Department, Harvard University*
AND
JENNY E. ROSENTHAL,** *Chemistry Department, Columbia University*

On the assumption of the invariance of the molecular groups YZ_3 and YX formulas are given connecting the potential energy constants of the molecules YZ_4, XYZ_3, ZYX_3, and ZX_4. The validity of the assumption is tested for the series CH_4, $ClCH_3$, $HCCl_3$, and CCl_4; the consistency of the results definitely shows it to be a very good approximation. The application leads to a determination of the general potential functions of all four molecules. Frequencies of $HCCl_3$ and $DCCl_3$ are calculated from those of CH_4, $ClCH_3$, and CCl_4, and are found to be in excellent agreement with the observed data. Predictions are made for the frequencies of $ClCD_3$. A certain ambiguity exists for the constants for the perpendicular frequencies of both $HCCl_3$ and $ClCH_3$, since two different chemically acceptable sets will account for the observed frequencies. A discussion of the methane constants shows that, while individual constants are quite sensitive to various methods of determination, certain linear combinations of them, to which a definite physical meaning can be attached, are practically invariant. The methane constants are used to redetermine the constants computed by Sutherland and Dennison for ethane; they yield an entirely different set, which, however, is equally suited to an explanation of the frequencies.

A CORRELATION of the vibrations of polyatomic molecules with intramolecular forces has been attempted many times on the basis of various simplified models, and some of these—notably the valence force assumption and its various modifications such as the Urey-Bradley field—have met with a certain amount of success. With reference to these simplified models, it has been possible to speak of force constants characteristic of certain bonds. However, a molecule can only be completely described in terms of a general potential function, and it is only the corresponding generalization of the bond constants that can have any definite meaning.

Spectroscopic observations on deuterium derivatives have enabled determination of the most general quadratic potential functions for certain simple hydrides; but in molecules where the hydrogens are of minor importance or completely absent, isotope shifts are too small to be of much help. An enticing alternative method of determining general potential functions is the assumption proposed by Sutherland and Dennison,[1] and others, that the forces remain constant within certain molecular groups in passing from one molecule to another. The validity of this assumption is a question of considerable physical interest, and, if substantiated, should enable calculation of the frequencies of molecules for which experimental data are not available.

In the present paper it is proposed to apply this method to the series YZ_4, XYZ_3, ZYX_3, YX_4, and to make a specific numerical test of the assumption for the special case CH_4, $ClCH_3$, $HCCl_3$, CCl_4. Stated more explicitly, our assumption means that the potential energy for the YZ_3 group is the same whether it is attached to an X or to another Z atom; and furthermore, that the force between Y and X is not changed by the nature of the other atoms in the molecule.[2] While there is no reason for supposing that the methyl group in methyl chloride is identical with that in methane, or that the CCl_3 radical remains entirely unchanged in passing from carbon tetrachloride to chloroform, it is believed that such an assumption is not far from the truth. Modern valence theory supports this idea, and experimental data appear to verify it. Thus the recent electron diffraction experiments of Sutton and Brockway,[3] in contradistinction to earlier observations, indicate that

* National Research Fellow in Chemistry.
** Sarah Berliner Research Fellow of the American Association of University Women.

[1] G. B. B. M. Sutherland and D. M. Dennison, Proc. Roy. Soc. **A864**, 250 (1935).

[2] This does not imply that the force between Y and X is the same as in the diatomic molecule YX. However such an extension of the assumption is not too unreasonable, and it might be worth while to check it by comparison with experimental data.

[3] L. E. Sutton and L. O. Brockway, J. Am. Chem. Soc. **57**, 473 (1935).

the Cl−C−Cl angle in $HCCl_3$ is very near the tetrahedral value, and Johnston and Dennison[4] conclude, from the moments of inertia, that the CH_3 group has the same dimensions in methane and in the methyl halides. Because there is no obvious connection between potential functions and dipole moments, the difference between the dipole moments of chloroform and methyl chloride does not seriously indict the assumption.

Connections between XYZ_3 and YZ_4 Constants

An analytic formulation of the assumption leads to a functional relationship between the constants[5] A, B, C, D and E of YZ_4, the constants[6] G_{11}, G_{12}, $\cdots$ G_{66} of XYZ_3, the constants $\bar{G}_{11}$, $\cdots$ $\bar{G}_{66}$ of ZYX_3, and the constants $\bar{A}$, $\bar{B}$, $\bar{C}$, $\bar{D}$ and $\bar{E}$ of YX_4.

We start by separating the quadratic potential function of YZ_4 into three parts V_1, V_2, V_3 corresponding to forces within the YZ_3 group, the YZ group, and the interactions between the two. Thus

$$V = V_1(\delta r_1, \delta r_2, \delta r_3, \delta q_{12}, \delta q_{13}, \delta q_{23}) + V_2(\delta r_4^2) + V_3, \quad (1)$$

where V_3 is a function of displacements of the type δq_{14}, and also contains terms linear in δr_4. For the notation, see I. In terms of the variables $s_1 \cdots s_6$, the potential energy of YZ_4 becomes[7]

$$\begin{aligned}
2V &= (9A/16+4B+4E-3D)s_1^2+(2/3)(A/4+4B-2D)s_3^2+2(2/3)^{\frac{1}{2}}(5D/2-3A/8-4B)s_1s_3 \\
&\quad +(3A/8)s_4^2+(A/16+B+C-D/2)s_6^2+2(3/8)^{\frac{1}{2}}(D-A/4)s_4s_6, \\
2V_2 &= (A/16+4B+4E+D)s_2^2, \qquad (2) \\
2V_3 &= (A/16+B+C-D/2)s_5^2+2[(4B+4E-3A/16-D)s_1s_2+(2/3)^{\frac{1}{2}}(A/8-4B+D/2)s_2s_3 \\
&\quad +(3/8)^{\frac{1}{2}}(D-A/4)s_4s_5+(A/16+B-C-D/2)s_5s_6].
\end{aligned}$$

By comparing Eqs. (2) with Eq. (2) of I, it is seen that the assumption stated above, which also postulates invariance of the tetrahedral angle in the group YZ_3, leads to the following relations:

$$\begin{aligned}
G_{11} &= 9A/16+4B+4E-3D, \\
G_{13} &= (-3A/8-4B+5D/2)(2/3)^{\frac{1}{2}}, \\
G_{33} &= (2/3)(A/4+4B-2D), \\
G_{44} &= 3A/8, \qquad (3) \\
G_{46} &= (D-A/4)(3/8)^{\frac{1}{2}}, \\
G_{66} &= A/16+B+C-D/2, \\
G_{22} &= \bar{A}/16+4\bar{B}+4\bar{E}+\bar{D}.
\end{aligned}$$

Similar relations for the quantities $\bar{G}_{ij}$ may be obtained by interchanging A and $\bar{A}$ etc. No connection is expected between the constants G_{12}, G_{23}, G_{45}, G_{55}, and G_{56} and the coefficients in the expression for V_3 for YZ_4, since, obviously, the forces between an X atom and a YZ_3 group are different from the forces between the same group and a Z atom. The expression for V_3 has, however, been given explicitly to permit a comparison of the magnitude of the interaction terms in YZ_4 and XYZ_3. It may be stated in this connection that the applicability of the formulas (3) (with the exception of the expression for G_{22}) is not limited to the XYZ_3 molecule but extends to other molecules containing the YZ_3 group.

Substitution of relations (3) into the expressions for the parallel and perpendicular frequencies (Eqs. (4) and (11) of I), where θ has been set equal to its value for a regular tetrahedron leads to Eqs. (4) and (5) given below. For the parallel frequencies

$$m^3\lambda^3 - m^2\lambda^2 R_1 + m\lambda R_2 - R_3 = 0,$$

with

[4] M. Johnston and D. M. Dennison, Phys. Rev. **48**, 868 (1935).

[5] Cf. J. E. Rosenthal, Phys. Rev. **45**, 538 (1934).

[6] Cf. the preceding paper on the vibrations of the XYZ_3 molecule. This will henceforth be referred to as I.

[7] It should be pointed out that the variables s are not geometrical symmetry coordinates for the molecule YZ_4, since they only satisfy the symmetry requirements of the group C_{3v}, and not those of the group T_d.

$$R_1=m(1/M+1/n)(\bar{A}/16+4\bar{B}+4\bar{E}+\bar{D})+(1+3m/M)(3A/16-D)+4(1+m/M)B$$
$$+4(3+m/M)E-2(m/M)G_{12},$$
$$R_2=-4m(1/M+1/n)[9G_{23}^2/4+2G_{12}G_{23}(3/2)^{\frac{1}{2}}]+(1+3m/M)(AB/2-D^2/2+2AE$$
$$+32EB-16ED)-4(m/M)[4G_{12}B-G_{12}D-G_{23}(8E-4B+3D/2)(3/2)^{\frac{1}{2}}]$$
$$-m(3/M+3/n+m/Mn)G_{12}^2+(m/Mn)(\bar{A}/16+4\bar{B}+4\bar{E}+\bar{D})[(M+n+3m)(3A/16-D) \quad (4)$$
$$+4(M+m+n)B+4(3M+3n+m)E],$$
$$R_3=m(1/M+1/n+3m/Mn)[(\bar{A}/16+4\bar{B}+4\bar{E}+\bar{D})(AB/2-D^2/2+2AE+32EB-16ED)$$
$$-3G_{23}^2(9A/16+4B+4E-3D)-(G_{12}^2/2)(A+16B-8D)-(3A/2+16B-10D)G_{12}G_{23}(3/2)^{\frac{1}{2}}].$$

The corresponding expression for the perpendicular frequencies is

$$m^3\lambda^3-m^2\lambda^2P_1+m\lambda P_2-P_3=0,$$

where

$$P_1=(3m\sin^2\varphi/n+2)G_{55}+(4/3)(2\sqrt{2}\sin\varphi+\cos\varphi)G_{45}+2(3)^{\frac{1}{2}}\sin\varphi G_{56}$$
$$+(7/16+m/M)A+3B+3C+D/2,$$
$$P_2=(5/4+3m/M)[A(B+C)-D^2]+3(3m\sin^2\varphi/n+1+\cos^2\varphi)[(B+C)G_{55}-G_{56}^2]$$
$$+\sin\varphi[(\sqrt{2}/3+\sqrt{2}m/M-\cot\varphi/12)A+4(\cot\varphi+\sqrt{2})(B+C)-(7\sqrt{2}/3+4\sqrt{2}m/M$$
$$+2\cot\varphi/3)D]G_{45}+(3)^{\frac{1}{2}}\sin\varphi[(2m/M+2/3-\sqrt{2}\cot\varphi/12)A-(\sqrt{2}\cot\varphi+2)D]G_{56}$$
$$-8\sin^2\varphi[(2\cot\varphi-\sqrt{2}/2)^2/9+m^2/Mn+3m/4n+2m(1+\cot^2\varphi)/3M]G_{45}^2 \quad (5)$$
$$+4(3)^{\frac{1}{2}}\sin^2\varphi[(1/3)\cot\varphi-(2/3)\sqrt{2}\cot^2\varphi-\sqrt{2}m/n]G_{45}G_{56}$$
$$+3\sin^2\varphi[(17\cot^2\varphi/72-5\sqrt{2}\cot\varphi/36+17/144+2m/3M+2m\cot^2\varphi/3M+7m/16n$$
$$+m^2/Mn)A+\tfrac{1}{3}\cot^2\varphi-\tfrac{1}{3}\sqrt{2}\cot\varphi+m/2n-1/2)D]G_{55},$$
$$P_3=\sin^2\varphi[(2\sqrt{2}\cot\varphi-1)^2/3+9m/n+8m/M+4m(3m-M-n)/Mn+8m\cot^2\varphi/M]$$
$$\times[\tfrac{3}{4}(AB+AC-D^2)G_{55}+(D-A/4)G_{45}G_{56}(6)^{\frac{1}{2}}-(A/8+2B+2C-D)G_{45}^2-3AG_{56}^2/4].$$

Discussion of the Methane Constants

All the theoretical expressions given above refer to the ω's, the frequencies with infinitesimal amplitudes. Since a sufficient number of combination bands is not known for any of the molecules treated to enable us to derive the ω's from the experimentally observed frequencies ν_i, the only way to proceed is to set $\nu_i=\omega_i$, thus introducing into the calculations an error of the order of magnitude of the anharmonicity corrections. However, since the anharmonicity is usually of the same sign, we may expect at least a partial cancelation of the errors, with a final result correct to about five percent. The constants discussed below are so adjusted as to give the best possible fit for the ν's. With these reservations we pass to the discussion of the methane constants.

The general formulas for the fundamental vibrations of methane [5] involve five force constants; and, with only four frequencies, an additional relationship is necessary for evaluation of the constants. This was obtained from the interaction between vibration and rotation by Dennison and Johnston,[8] who determined the constants and used them in the formulas of Rosenthal[5] to calculate the frequencies of the deuterium derivatives of methane. They obtained two alternate sets of constants and gave two sets of fre-

[8] D. M. Dennison and M. Johnston, Phys. Rev. **47**, 93 (1935).

quencies. The infrared absorption frequencies of CH_3D observed by Ginsburg and Barker[9] were found to agree well with one of the alternate sets calculated.[10] The observed frequencies may be used to recompute the five methane constants.[11] However, in the following the constants derived by Dennison and Johnston have been used, since they reproduce the CH_3D frequencies as well as the set calculated from the best individual observed frequency (2205). These constants are

$A=7.67\times10^5$ dynes/cm, $B=0.4760$, $C=0.3409$, $D=1.2779$, $E=0.1336$.

They are based on the methane frequencies

$$\nu_1=2915, \qquad \nu_2=1520,$$
$$\nu_3=3014 \qquad \nu_4=1304,$$

for which the assignments are quite certain.

As a matter of fact the two sets of constants are not, for our purposes, as widely divergent as they at first appear to be. While the individual constants calculated by the two methods may differ by as much as 13 percent, certain linear combinations of them which appear prominently in our potential functions are found to be practically invariant. Thus $A/16+4B+4E+D$ is equal respectively to 4.88×10^5 dynes/cm and 4.92, a difference of less than one percent. This particular quantity on our assumption corresponds to the constant of the C−H bond.

With the values of the methane constants known, it is possible to calculate the three constants a, b, d used by Sutherland and Dennison[1] to characterize the parallel vibrations of the CH_3 group. The analytic relationships may be found directly, or by way of Eqs. (12) I and Eqs. (3) of this paper. They are

$$a=9A/16+4B+4E-3D, \qquad b=8B+32E,$$
$$d=(\sqrt{2})(8E+3D/2-4B).$$

On substitution of the methane constants the values $a=3.67\times10^5$ dynes/cm, $b=13.95$, $d=3.59$ are obtained. These are to be compared to the values $a=8.24$, $b=8.01$, $d=\pm5.07$ which were chosen to fit ethane by Sutherland and Dennison; or $a=8.47$, $b=0.83$, $d=\pm5.39$ chosen to fit methyl chloride. In spite of the marked differences, the two sets of constants, when used in the formulas of reference 1, fit the observed parallel frequencies of ethane and methyl chloride equally well, and lead to the same values of the $X-CH_3$ bond constant c. This is another example of the situation mentioned above—only certain combinations of the constants (here $ab-d^2$ for instance) are important in the formulas for the frequencies. The sensitivity of the individual constants is due largely to the manner in which the potential function is defined. However it should be pointed out that the CH_3 constants a, b, d derived from the methane constants are more reasonable physically, since they indicate larger stretching and smaller bending forces than do the constants derived by Sutherland and Dennison.

Experimental Data

The frequencies employed are listed in Table I. Those for $ClCH_3$ are from infrared absorption of the gas.[12, 13, 14] 731.5 cm^{-1} is the weighed mean of the two isotopic lines for this vibration. 2924 is the average of the two observed lines 2880 and 2967, taken under the plausible assumption of Adel and Barker[12] that the pair is produced by resonance between ν_1 and $2\nu_4=2920$. There are few data for chloroform or carbon tetrachloride in the gaseous state, but since the frequencies of methane and methyl chloride are those for the free molecules, it has been thought advisable to correct the observed Raman spectra for the liquids $HCCl_3$ and CCl_4 in order to secure fre-

[9] N. Ginsburg and E. F. Barker, J. Chem. Phys. **3**, 668 (1935).

[10] Recently MacWood and Urey (J. Chem. Phys. **3**, 650 (1935)) have given the Raman spectrum of CH_3D. Their results agree moderately well with the infrared absorption spectrum except for an intense line at 2315 cm^{-1}, which they interpret as an overtone. The appearance of a strong overtone in the Raman effect is most unusual, but the force constants derived on the assumption that it is a fundamental are incompatible with the other CH_3D frequencies and the parallel frequencies of ethane. Resonance with the 2200 fundamental may help in explaining the intensity of this overtone.

[11] There is an error in the constants calculated by Ginsburg and Barker. For instance the values derived from CH_3D 2205 should be $A=8.69\times10^5$ dynes/cm, $B=0.437$, $D=1.33$ instead of $A=7.30$, $B=0.430$, $D=1.33$. Whenever their constants are referred to, it is the corrected values that are implied.

[12] A. Adel and E. F. Barker, J. Chem. Phys. **2**, 627 (1934).

[13] A. H. Nielsen and E. F. Barker, Phys. Rev. **46**, 970 (1934).

[14] E. F. Barker and E. K. Plyler, J. Chem. Phys. **3**, 367 (1935).

TABLE I. *Vibration frequencies in cm^{-1}, assignments, and corrections which have been added to secure gaseous frequencies.*

	$ClCH_3$	$HCCl_3$	$DCCl_3$	CCl_4	
	ν_1 2924	3033 15	2267 (11)	ν_1 467 (8)	A_1
||	ν_3 1355	683 (16)	666 (16)	ν_2 222 (5)	E
	ν_5 731.5	376 (10)	376 (10)		
	ν_2 3047	1225 (10)	916 (8)		
				ν_3 318 (5)	
⊥	ν_4 1460	776 (16)	753 (16)		T_2
				ν_4 782 7	
	ν_6 1020	271 (10)	271 (9)		

quencies for the gases throughout. The alteration in passing from liquid to gas is usually a shift toward greater frequency,[15] and that has been the uniform assumption in applying corrections. On the basis of the known displacements for certain CH_4 and $ClCH_3$ lines, as well as for 782 of CCl_4 and 3033 of $HCCl_3$,[16] small corrections to the Raman spectra of the liquids[17] have been made. In doing this, the approximate modes of vibration for these molecules described by Kohlrausch[18] have been employed to characterize lines, and the dipole moments of molecular groups have been accepted as the chief cause of the displacements. The corrections, which have been added to the observed spectra for the liquids to give the values listed, are also shown in Table I. Those not in parentheses are based upon direct experimental knowledge. Actually these corrections do not affect the calculations or conclusions to any extent, and their inclusion is a matter of minor importance. The frequency 782 for CCl_4 is the mean of the two resonating components[19] 768 and 797, observed in infrared absorption by Schaefer and Kern.[20] The assignments of frequencies are rendered quite certain by the observed character of the bands in the case of infrared absorption,[13, 14] and by polarization measurements[21] for the Raman lines. For CCl_4 the assignments are indicated in the table by the representation of T_d to which the vibration corresponds.

The perpendicular frequencies depend upon the molecular geometry, and it is necessary to know the relative bond distances before computations can be carried out. The values C−Cl =1.77,[22] C−H=1.08[23] have been used.

THE PARALLEL FREQUENCIES

We are now ready to apply the formulas derived above. In doing this, it is sometimes found that several alternate solutions for the constants are possible. The criterion for choosing between these, in addition to that of general self-consistency, is that the constants shall be physically reasonable. Thus large negative values, and those with large imaginary parts are considered suspect. Small imaginary parts are not sufficient cause for the rejection of constants, for they may be due to the uncertainties arising from anharmonicity, etc. Only small values of G_{12} and G_{23} are to be expected, for physical reasons.

The first application is to methyl chloride. When the methane constants are substituted in formulas (4), it is possible to solve for the three remaining constants G_{22}, G_{12} and G_{23}, by using the values of the three parallel frequencies of methyl chloride as given in Table I. Throughout unbarred constants refer to methane and methyl chloride, while barred constants refer to carbon tetrachloride and chloroform. The masses used are C=12.00, H=1.008, Cl=35.46.[24] The formulas for the frequencies of methyl chloride lead to a quartic equation for the constants. Of the four sets of constants which result, only one is satisfactory: $G_{22}=3.61\times10^5$ dynes/cm. $G_{12}=0.560$, $G_{23}=-0.030$. The other sets have large values of G_{12}, and for them G_{22} does not even approximately equal the bond constant c of Sutherland

[15] See however W. Buchheim, Physik. Zeits. **36**, 694 (1935), who shows that a shift in the other direction is possible.

[16] Dr. Ginsburg kindly measured the infrared absorption of chloroform vapor, and obtained the value 3033 cm^{-1} for ν_1.

[17] Data for $HCCl_3$ from Kohlrausch, *Der Smekal-Raman Effekt* (1931), p. 116. CCl_4 ibid., p. 305. $DCCl_3$ R. W. Wood and D. H. Rank, Phys. Rev. **48**, 63 (1935); also Redlich and Pordes, Naturwiss. **22**, 808 (1934).

[18] K. W. F. Kohlrausch, Zeits. f. physik. Chemie **B28**, 340 (1935).

[19] Cf. Horiuchi, Zeits. f. Physik **84**, 380 (1933).

[20] Schaefer and Kern, Zeits. f. Physik **78**, 609 (1932).

[21] Cabannes and Rousset, Ann. de physique **19**, 229 (1933). L. Simons, Soc. Sci. Fennica, Comm. Phys. math. **6**, 1–58 (1932). Cf. also reference 18.

[22] L. Pauling and L. O. Brockway, J. Chem. Phys. **2**, 867 (1934); Cosslett and de Laszlo, Nature **134**, 73 (1934); reference 3.

[23] Mark, Zeits. f. Electrochemie **40**, 413 (1934); L. Pauling, Proc. Nat. Acad. Sci. **18**, 293 (1932); cf. also references 8 and 9.

[24] Use of this value for the mass of Cl is an approximation, but since the isotope shift for chlorine is very small, it is quite adequate for the present purposes.

TABLE II. *Potential energy constants.* The values given under the headings CCl_4 and CH_4 are the constants in the potential energy functions of these molecules when they are treated as though they were of the type XYZ_3. The numbers are given to the number of decimal places used in the calculations even though no significance can be attached to the last figure. All quantities are given in dynes$\times 10^5$/cm.

	CH_4	$ClCH_3$	$HCCl_3$	CCl_4
G_{11}	3.639	3.639	2.850	2.850
G_{22}	4.916	3.610	4.916	3.610
G_{33}	0.844	0.844	0.819	0.819
G_{12}	0.442	0.560	a −0.482 b 0	1.421
G_{13}	−1.295	−1.295	−1.110	−1.110
G_{23}	−0.250	−0.030	a 0.407 b 0	−0.661
G_{44}	2.876	2.876	1.357	1.357
G_{55}	0.657	c 0.628 d 0.892	c' 0.570 d' 0.555	0.563
G_{66}	0.657	0.657	0.563	0.563
G_{45}	−0.392	c −0.360 d −0.735	c' −0.155 d' 0.072	−0.161
G_{46}	−0.392	−0.392	−0.161	−0.161
G_{56}	0.657	c 0.013 d 0.367	c' 0 d' 0	0.563

and Dennison[1] ($c=3.44$ for $ClCH_3$) Furthermore, with these other sets it is not possible under the present assumption to correlate the frequencies of carbon tetrachloride and chloroform. The complete set of constants for $ClCH_3$ is given in Table II.

With the value $G_{22}=3.61$, the relationship between G_{22} and $\bar{A}$, $\bar{B}$, $\bar{D}$, $\bar{E}$ expressed in Eqs. (3), and the four known frequencies, it is possible to obtain the five constants in the general potential function of carbon tetrachloride. Thus the values $\bar{A}=3.619$, $\bar{B}=0.402$, $\bar{C}=0.256$, $\bar{D}=0.643$, $\bar{E}=0.283$ are found. Another possible set is $\bar{A}=2.53$, $\bar{B}=0.840$, $\bar{C}=0.256$, $\bar{D}=-1.04$, $\bar{E}=0.283$, but this has been rejected because it is incompatible with the data for chloroform. The potential function for CCl_4 determined in this manner shows certain interesting similarities to that for CH_4, as may be seen by comparing the values of A, B, C, D, E. Urey and Bradley[25] have given a special potential function for carbon tetrachloride. Their assumption requires[5] $\bar{D}=10\bar{B}-2\bar{C}-8\bar{E}$. This relation is not satisfied however, for $10\bar{B}-2\bar{C}-8\bar{E}=1.243$, while $\bar{D}=0.643$. The two potential functions seem, therefore, to give rather different descriptions of the molecule.

[25] H. C. Urey and C. A. Bradley, Phys. Rev. **38**, 1969 (1931).

The parallel frequencies of $HCCl_3$ may now be investigated. As three frequencies and only two unknown constants are involved, a test of the present assumption is possible. Substitution of the frequencies in Eqs. (4) (in this case barred and unbarred constants are interchanged) leads to equations with imaginary roots. However the real values $\bar{G}_{12}=-0.482$, $\bar{G}_{23}=0.407$ give a very close reproduction of the frequencies, as is evident on examination of the values under a in Table III. If, following Sutherland and Dennison's treatment of the parallel frequencies of methyl chloride, the further assumption that $\bar{G}_{12}$ and $\bar{G}_{23}$ are zero is made, the results shown under b in the table are obtained. These also agree very well with the experimental values, and there is in fact little to choose between the two alternatives. The results with the second are particularly gratifying, since they represent frequencies for chloroform which have been calculated entirely on the basis of data from methane, methyl chloride and carbon tetrachloride. The insensitivity of the frequencies to the values of $\bar{G}_{12}$ and $\bar{G}_{23}$ is due to a partial concelation of terms involving these constants in the equation, and to the fact that the constants themselves usually occur with smaller coefficients than do constants of type $\bar{G}_{22}$.

TABLE III. *Experimental and calculated frequencies for $HCCl_3$.*

	CALC. a $G_{12}=-0.482$, $G_{23}=0.407$	CALC. b G_{12}, $G_{23}=0$	OBS. (corr.)
ν_1	3034	3010	3033
ν_3	675	681	683
ν_5	380	388	376

THE PERPENDICULAR FREQUENCIES

Eqs. (5) for the three perpendicular frequencies of both $HCCl_3$ and $ClCH_3$ involve three undetermined constants and no further test of the major assumption is possible. However, the constants may be calculated and may then be used to compute the frequencies of the corresponding deuterium compounds. In each case algebraic elimination leads to an equation of the fourth degree, and in each case two of the four sets of constants can be rejected for physical reasons. However, there remain two alternates for G_{55}, G_{45}, G_{56} and two for $\bar{G}_{55}$, $\bar{G}_{45}$, $\bar{G}_{56}$. These are all listed in Table II, as there seems to be no way at present of rejecting any of them. It is to be noted

in this connection that, while all constants for the perpendicular frequencies should be moderately small (less than 1×10^5 dynes/cm), those for cross terms, such as G_{45}, need not be small compared to those for squared terms in the potential, such as G_{55}. This is simply a consequence of the way the potential function has been defined (cf. Eq. (8) I).

Frequencies of the Deuterium Derivatives

It is a simple matter to calculate the frequencies of deuterochloroform and deutyl chloride with the constants which have been determined. Substitution of the constants, with the mass of deuterium set equal to twice that of hydrogen, in Eqs. (4) or (5) leads to a cubic equation; the three roots are the desired parallel or perpendicular frequencies. The values thus computed are listed in Table IV. c and d and c' and d' correspond to the two alternate sets of constants in Table II. The frequencies computed for deuterochloroform agree very well with those observed by Wood and Rank,[17] and this agreement is a further substantiation of the major assumption. For the perpendicular frequencies the agreement is so much better with the set of constants d' that c' could be eliminated on this basis.

The frequencies of $ClCD_3$ have not yet been observed. The predicted values are given in Table IV. Here the two alternate solutions for the perpendicular constants also yield frequencies which differ considerably, and experimental observations should permit elimination of one of the sets.

Table IV. *Computed and observed frequencies of deuterium derivatives in* cm^{-1}.

		$ClCD_3$ Calc.		$DCCl_3$ Calc.		Obs. (corr. to gas)
				a	*b*	
∥	ν_1	2081		2254	2219	2267
∥	ν_3	1110		651	659	666
∥	ν_5	645		377	386	376
		c	*d*	*c'*	*d'*	
	ν_2	2253	2231	884	919	916
⊥	ν_4	1059	1135	774	745	753
	ν_6	765	720	269	269	271

Concluding Remarks

The assumption that potential functions within molecular groups are preserved has been validated insofar as it has been possible to test it. It has led to consistent results, and has enabled determination of the general quadratic potential functions for methyl chloride, chloroform and carbon tetrachloride. However, a word of caution is necessary with regard to the potential constants given. Because of anharmonicity, incomplete knowledge of all the gaseous frequencies and the limitations of the primary assumption, these constants cannot be exact. In particular those for cross terms in the potential function are to be considered uncertain, since they are quite sensitive to small changes in the frequencies. But in spite of these reservations it is felt that when the sets of constants are used to calculate frequencies for molecules containing CH_3 or CCl_3 groups they will yield good results.

LETTERS TO THE EDITOR

This section will accept reports of new work, provided these are terse and contain few figures, and especially few halftone cuts. The Editorial Board will not hold itself responsible for opinions expressed by the correspondents. Contributions to this section must reach the office of the Managing Editor not later than the 15th of the month preceding that of the issue in which the letter is to appear. No proof will be sent to the authors. The usual publication charge ($3.00 per page) will not be made and no reprints will be furnished free.

The Relative Values of the Four Butane-Butene-Hydrogen Equilibrium Constants[1]

Eidinoff and Aston[2] have given a very convenient method for calculating the rotational entropy of molecules with internal rotating groups. This method, after some further development, has been used to calculate the following values for the translational plus rotational entropies at 25°C.

n-butane	75.366	2-butene, *cis*	68.225
isobutane	71.249	2-butene, *trans*	67.800
1-butene	72.98	isobutene	68.215

The value given for 1-butene is an estimate which should be reliable, but which will subsequently be replaced by an exact value. An accurate calculation of vibrational entropies for these molecules is not yet possible. It is probably a good approximation to assume that the vibrational contributions for *n*- and isobutane are the same, and also that the contributions for the four butenes differ only in the part coming from torsion about the C=C bond. This part may be estimated by taking the fairly reliable figure of 790 cm^{-1} for the torsion frequency in ethylene to determine the force constant, and by using the ratio 21.5 : 1 for the moments of CH_3 and H about the C=C axis. A simple calculation gives 572 cm^{-1} for the torsion frequency in 1-butene and isobutene, 244 cm^{-1} in both 2-butenes. The entropies calculated in this way may be combined with heats of hydrogenation determined by Kistiakowsky, Ruhoff, Smith and Vaughan.[3] The most direct calculation is that of the *cis-trans* equilibrium, since here the torsion cancels out. The equilibrium constant is $[cis]/[trans]=\exp[-949/RT+0.425/R]$ or 0.61 at 400°C. The experimental value of Frey and Huppke[4] is 0.64. The 1-butene, transbutene calculation is more involved; the rotational entropy of 1-butene is 5.179 e.u. higher than that of transbutene; the torsion correction of 1.67 e.u. lowers this to 3.509 e.u. The heat content of 1-butene is 2720 cal. higher at 82°C; the torsion correction gives 2617 cal. at 400°C. Hence [1-butene]/[transbutene] =0.49, against the experimental value of 0.56. The ratio of the dissociation constant for isobutane to isobutene against that of *n*-butane to transbutene depends upon the rotational entropy differences between *n*- and isobutane, and between trans- and isobutene, the same calculated torsional entropy and heat content differences as in the preceding example, and the hydrogenation heats. The isobutane dissociation involves a 2.862 e.u. greater entropy increase and a 695 cal. greater heat input at 400°C. Hence $K_{iso}/K_{trans}=2.51$, in somewhat fortuitous agreement with 2.56, the experimental value of Frey and Huppke. The experimental determination of [1-butene]/[transbutene] varies less with temperature, and that of K_{iso}/K_{trans} varies more, than the theoretical values. Frey and Huppke have stated, however, that the accuracy of their data would not justify a calculation of ΔH from the temperature coefficient. The agreement of calculated and observed values is thus as good as could be expected.

It is of interest to note the extremely simple basis of these calculations. The bond distances and angles are semispectroscopic in origin, but might have been determined entirely from x-ray diffraction. The individual translation-rotation entropies depend upon the quantum constant h, but the entropy differences actually used are ratios of purely classical phase-space volumes. The treatment of the torsional vibration is the only part of the calculation that Gibbs or Boltzmann would have been unable to make.

A more complete account of this work is contained in two papers, of which one has been, and the other shortly will be, submitted to the *Journal of Chemical Physics*.

LOUIS S. KASSEL[5]

Physical Chemistry Section, Pittsburgh Experiment Station,
U. S. Bureau of Mines, Pittsburgh, Pennsylvania,
December 20, 1935.

[1] Published by permission of the Director, U. S. Bureau of Mines. (Not subject to copyright.)
[2] Eidinoff and Aston, J. Chem. Phys. **3**, 379 (1935).
[3] Kistiakowsky, Ruhoff, Smith and Vaughan, J. Am. Chem. Soc. **57**, 876 (1935).
[4] Frey and Huppke, Ind. Eng. Chem. **25**, 54 (1933).
[5] Physical chemist, Pittsburgh Experiment Station, U. S. Bureau of Mines, Pittsburgh, Pa.

The Mutarotation of Glucose in H_2O-D_2O Mixtures

In an earlier communication[1] it was shown that the dependence of the specific velocity constant for the mutarotation of α-*d*-glucose could be described satisfactorily by the equation

$$k_{obs}=k_{H_2O}C_{H_2O}+k_{HDO}C_{HDO}+k_{D_2O}C_{D_2O}. \quad (1)$$

Eq. (1) furnishes evidence for the kinetic influence of the decrease in basicity of the solvent with increase in D content but implicitly denies any influence of the isotopic exchange which takes place in the substrate.

TABLE I.

P_w	$k(10)^5$	(H_2O)	(HDO)	R_w	R_g	K	P_g
0.050	976	50.03	5.20	9.61	0.090	0.87	0.08
0.056	979	49.91	5.78	8.54	0.086	.73	0.09
0.112	925	43.82	10.76	4.07	0.174	.71	0.17
0.142	891	40.96	13.14	3.11	0.238	.74	0.21
0.145	869	40.69	13.36	3.05	0.284	.87	0.22
0.179	826	37.61	15.74	2.39	0.382	.91	0.26
0.190	829	36.64	16.46	2.23	0.375	.84	0.27
0.265	762	30.38	20.68	1.469	0.561	.82	0.36
0.369	677	22.70	24.52	0.925	0.885	.82	0.47
0.384	653	21.69	24.88	0.868	1.003	.87	0.49
0.404	654	20.35	25.34	0.803	0.987	.79	0.51
0.416	644	19.57	25.56	0.765	1.050	.80	0.52
0.507	560	14.17	26.23	0.540	1.638	.89	0.61
0.575	526	10.68	25.74	0.414	1.984	.82	0.67
0.624	496	8.50	24.66	0.345	2.38	.82	0.71
0.652	467	7.31	23.94	0.303	2.87	.87	0.73
0.663	452	6.88	23.58	0.292	3.18	.93	0.74
0.831	356	1.81	15.06	0.120	7.68	.92	0.87
0.890	324	0.79	10.62	0.073	12.1	.88	0.92
0.895	328	0.71	10.14	0.070	11.67	.82	0.92
0.960	293			0.025			0.97
0.960	293			0.025			0.97
						Av.	0.83

R_g (Col. 6) $= \frac{(P_g \text{ Eq. 2})}{1-P_g \text{ (Eq. 2)}}$; P_g (Eq. 2) $=(1040-k_{obs})/(1040-273)$; P_g (Col. 8) $= \frac{0.83/R_w}{1+0.83/R_w}$.

If one adopts as a working hypothesis the alternate view that the decrease in velocity is due only to replacement of H by D in that position in the glucose molecule which is involved in the mutarotation and does not depend kinetically upon the relative abundance of H_2O, HDO, and D_2O, we may write

$$k_{obs}=k_{H_2O}-(k_{H_2O}-k_{D_2O})P_g. \qquad (2)$$

P_g denotes the fraction of α-*d*-glucose in which the OH on the terminal carbon atom has become OD. This exchange may be assumed as more rapid than mutarotation. This hypothesis may be tested readily by calculating from Eq. (2), values of P_g over the range H_2O-D_2O, using the experimental values of the k's. P_g is readily converted into R_g, the ratio of the concentrations of heavy glucose and light glucose, which may be combined with $R_w=(HOH)/(HOD)$ to give the exchange constant

$$R_gR_w=\frac{(D-G)(HOH)}{(H-G)(HOD)}=K. \qquad (3)$$

The earlier data[1] together with more recent results have been combined in Table I. $P_w=\Delta s/0.1079$ is the excess specific gravity ratio. The K's are constant within experimental error. The average $K=0.83$ agrees exactly with that for tetramethyl glucose found directly from exchange experiments[2] but disagrees with the value for glucose (0.69). This is to be expected since the exchanging hydrogen atom in tetramethyl glucose is the only one which is involved in mutarotation catalyzed by bases while the constant reported for glucose is an averaged constant $(K_1K_2K_3K_4K_6)^{1/5}$, where subscripts refer to the positions of the five exchangeable hydrogens in the glucose molecule.

When k_{obs} is plotted against P_g as calculated from $K=0.83$, Eq. (2) is obeyed within the experimental error. The single experimental value for the isotopic exchange with tetramethyl glucose must be confirmed before the hypothesis advanced may be accepted as conclusive. The correct explanation may lie between the two extreme views.

W. H. HAMILL
V. K. LA MER

Fordham University,
New York City.

Columbia University,
New York City.

[1] Hamill and La Mer, J. Chem. Phys. **2**, 891 (1934).
[2] Hamill and Freudenberg, J. Am. Chem. Soc. **57**, 1427 (1935).